Poster Sessions

P001A

pH-Sensitive Thin Films Containing Carboxyl-terminated Poly(amido amine) Dendrimer

Shigeru Tomita, Katsuhiko Sato, Jun-ichi Anzai

Graduate School of Pharmaceutical Sciences,Tohoku University, Japan

A layer-by-layer (LbL) deposition of anionic and cationic polymers on a solid surface affords multilayer thin films. Recently, much attention has been devoted to the development of stimuli-sensitive LbL films which can be disintegrated by chemical and physical stimuli such as pH changes, binding of small molecules, and electrical signals. For example, hydrogen bonding LbL films composed of poly(methacrylic acid) (PMAA) and neutral polymers can be disintegrated upon being exposed to neutral media due to deprotonation from the carboxylic acid groups in PMAA, which results in the breakage of the hydrogen bonds.

We have found that PMAA/PAMAM-COOH multilayer films can be constructed when pH of the PAMAM-COOH and PMAA solutions from which the LbL films are deposited is pH 4 or more acidic, while, in neutral pHs, the LbL film does not form. This means that the PMAA/PAMAM-COOH films can be arbitrarily decomposed by regulating pH of the medium in which the LbL films are immersed (Fig 2) .

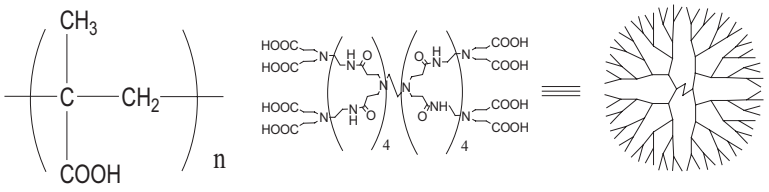

Fig 1 The chemical structures of PMAA and PAMAM-COOH

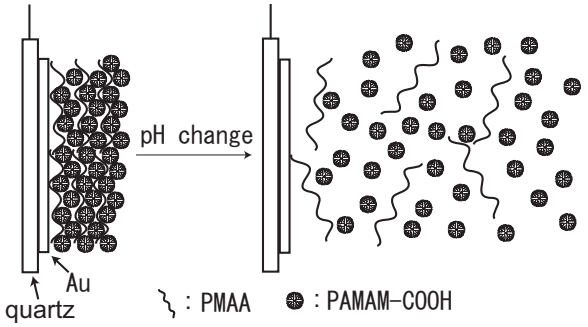

Fig 2 Aschematic illustration of disintegration of a (PMAA/PAMAM-COOH) LBL films induced by a pH change.

The PAMAM-COOH/PMAA films were deposited on a Au film-coated quartz resonator to monitor the resonance frequency using QCM. The quartz resonator was mounted in a flow cell and the surface was exposed to a PMAA and PAMAM-COOH solutions (0.5 mg mL^{-1}) for 15 min alternately (The solutions were allowed to stand without flow for this period). Between the deposition of PMAA and PAMAM-COOH layers, the surface of the resonator was rinsed with the working buffer for 5 min. The multilayer films were prepared by repeating the alternate deposition. The disintegration of the LbL films were studied by monitoring the frequency changes of the LbL film-coated quartz resonator upon exposing to buffer solutions of different pH.

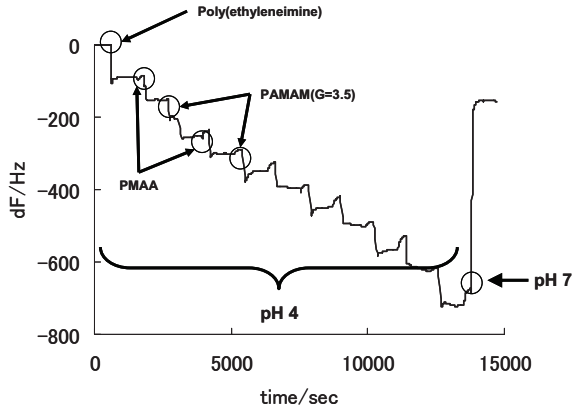

Fig 3 The deposition and disintegration of $(PMAA/PAMAM\text{-}COOH)_5$ films.

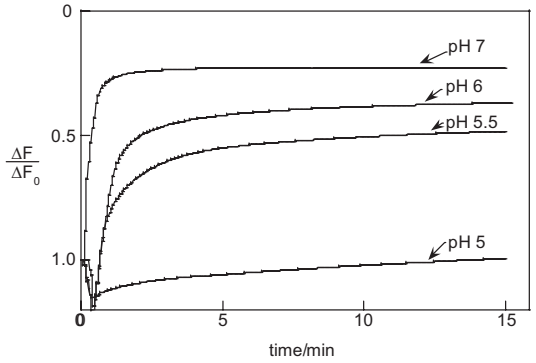

Fig 4 QCM frequency changes of the $(PMAA/PAMAM\text{-}COOH)_5$ films induced by pH changes.

Fig. 3 shows changes in the resonance frequency (dF) of QCM observed for the deposition of 5-bilayer $(PMAA/PAMAM\text{-}COOH)_5$ film on the quartz resonator and its disintegration induced by a pH change. From the QCM results, the loading of the $(PMAA/PAMAM\text{-}COOH)_5$ LbL film was calculated to be ca. 3.5 x 10^{-6} g cm^{-2} (1.7 x 10^{-6} g cm^{-2} for PMAA and 1.8 x 10^{-6} g cm^{-2} for PAMAM-COOH). Fig. 4 shows the effects of pH on the rate of decomposition of the $(PMAA/PAMAM\text{-}COOH)_5$ film which was prepared at pH 4.

We are now studying these effects on the formation and decomposition of the films. The present dendrimer films may find applications in the development of pH-sensitive biosensing and drug delivery systems because dendrimers are promising candidate for drug carriers.

P002B

Preparation of Layer-by-Layer Assemblies Containing Insulin

Shigehiro TAKAHASHI, Kentaro Yoshida, Hiroshi SATO, Jun-ichi ANZAI*

Graduate School of Pharmaceutical Sciences, TOHOKU UNIVERSITY

Abstract

Insulin (pI ~5.4) consists of 51 amino acids and has negative charges at neutral pH. Thus, we have prepared Layer-by-Layer (LBL) thin films composed of insulin and cationic polyelectrolytes, such as polyallylamine (PAA) and polyethyleneimine (PEI). The deposition of LBL thin films was confirmed by quarts crystal microbalance measurement (QCM). The resonance frequency increased depending on the number of layers of PAA/Insulin, but didn't when PEI was used. We also investigated the polyelectrolytes modified with phenylboronic acid (PBA), which can bind sugar specifically.

Introduction

Insulin is an essential hormone produced by pancreas. Diabetes develops when the pancreas does not produce and secrete enough of this hormone. People suffering from diabetes depend on exogenously administered insulin by twice-daily subcutaneous injection of it. The various commercial injectable insulin products, such as rapid-, short-, intermediate-, and long-acting forms, have been developed for individual patient need. However, frequent-injection remains and there isn't an ideal synchronization between time-action profile and glucose absorption from a meal. Thus, the development of alternatives to subcutaneous injection has been a focal subject in insulin drug delivery systems. For this purpose, LBL thin films containing insulin have been prepared for coating the surface of transducer. We report here results on the preparation of thin films composed of insulin and polymers modified with PBA.

Experimental

The Au-coated surface of a quartz resonator was thoroughly rinsed with distilled water before use. The cleaned Au surface was modified with multilayerfilms by immersing it alternately in 0.1 mg/mL PAA, 0.1 mg/mL PAA modified with PBA (PBA-PAA), 0.1 mg/mL PEI or 0.1 mg/ml PEI modified with PBA (PBA-PEI) and 0.5 mg/ml insulin (all solutions contained 10 mM HEPES pH 7 and 150 mM NaCl) (Fig.1). The thin films were deposited on the surface of the quartz resonator (i.e., the total area of the Au coated surface is 0.2 cm^2), and the film-deposited probe was wet after each deposition until the frequency showed a steady-state value with which to estimate the weight of the film.

PBA-PAA was prepared by modifying poly(allylamine hydrochloride) (PAH) with 4-carboxyphenylboronic acid in an aqueous solution (pH 4.9) using 1-ethyl-3-(3-dimethylaminopropyl)carbodiimide HCl as a coupling agent. The PAH-PBA was purified by dialysis

against water and the content of PBA in the polymer was determined to be 9.1% (or 9.1% of $-NH_2$ residues in the PAH was substituted with PBA through amide linkage) by UV-visible absorption spectrum. PBA-PEI was prepared in similar manner and the content of PBA was determined to be 5.0 %.

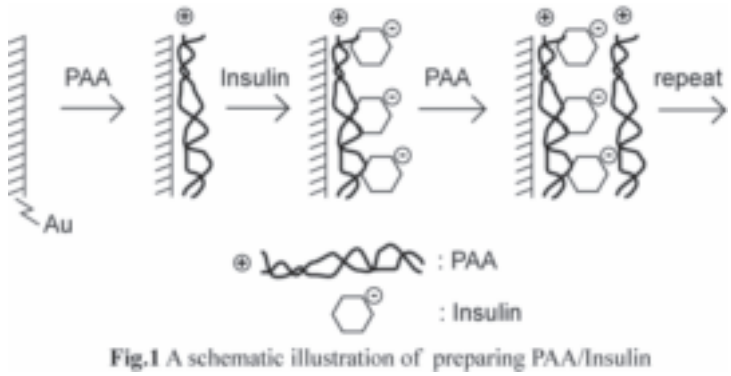

Fig.1 A schematic illustration of preparing PAA/Insulin

Result and Disscussion

Insulin consists of 51 amino acids, including four acidic amino acid residues. We evaluated the LBL thin films composed of two cationic polyelectrolytes and Insulin. The resonance frequency increased depending on the number of layers of PAA/Insulin, but didn't when PEI was used. The frequency changes of ca. 66 Hz per layer were measured for the deposition of insulin, showing that the molecular area occupied by a single insulin molecule was 2.6 x 10^{-14} cm^{-2} $layer^{-1}$. Judging from the fact that calculated molecular area of insulin is 1.3 x 10^{-13} cm^{-2}, this result indicated that five-times much amount of insulin was immobilized in PAA/insulin films. We prepared also LBL thin films composed of PBA-PAA or PBA-PEI and Insulin. Fig.2 shows the QCM frequency changes for the formation PBA-PAA/insulin (a) and PBA-PEI/insulin (b) multiplayer films. The resonance frequency increased depending on the number of layers of PBA-PAA/insulin, but didn't when PBA-PEI was used. Compared with PAA/insulin film, the frequency changes of ca. 54 Hz were almost equal to that of PAA/Insulin. A pH-response of the film was also tested. PBA is known to form a negative charge at basic pH. Consequently, it is expected that LBL thin films containing PBA and Insulin could be collapsed due to the electrostatic repulsion between PBA and insulin. The frequency changes of ca. 99 Hz was observed by the collapse of $(PBA\text{-}PAA/insulin)_5$ upon adding buffer (pH 9, 150 mM NaCl). This result suggested that increasing the concentration of sugar could control the collapse of LBL thin films containing insulin because PBA bound sugar to form negative charge at neutral pH.

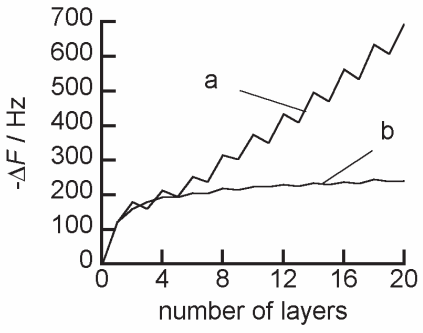

Fig 2. QCM frequency changes for the formation PBA-PAA/ insulin (a) and PBA-PEI/insulin multiplayer films (b). The odd layer numbers show the deposition of PBA-PAA or PBA-PEI, the even numbers correspond to the deposition insulin.

P003C

pH-Triggered Release of Insulin from Layer-by-Layer Assemblies

Kentaro Yoshida*, Jun-ichi Anzai
Graduate School of Pharmaceutical Sciences, Tohoku University
Aramaki, Aoba-ku, Sendai 980-8578, Japan
E-mail: k-yoshida@mail.tains.tohoku.ac.jp

Insulin is widely used to treat diabetic patients. In general, the hypodermic injection is adopted as a method of administering insulin. However, the development of new drug delivery system (DDS) is required for reducing problems such as patient's pains. Oral capsules of insulin have been researched with micro capsules for new DDS. There are still problems such as remaining and enclosing organic solvent used. If the layer-by-layer (LbL) deposition technique that can be operated in water solution is used, it becomes easy to enclose unstable polypeptides and proteins. We report here insulin containg LbL assemblies that are prepared considering the isoelectric point of insulin. The release of insulin from the LbL assemblies by pH changes are studied (Figure 1).

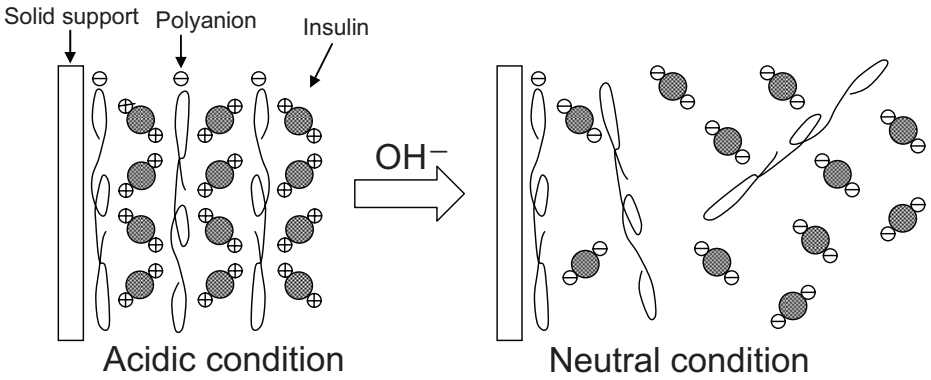

Fig.1 Insulin containing LbL assemblies can be prepared and insulin is released by pH change.

In more acidic side than the isoelectric point of insulin (pI=5.3), the content of positive electric charges of insulin increases. For this reason, LbL assemblies based on an electrostatic interaction of polyvinylsulfuric acid (PVS) and insulin were prepared under an acidic condition. The PVS/insulin LbL thin film was prepared by alternately dipping a solid support in the 0.5 mg/ml PVS solution for 15 min and in the 0.2 mM insulin solution for 15 min at pH 3. When the prepared thin film was dipped in a neutral or an alkaline solution, the content of the negative charges of insulin increases. As a result, insulin was released by an electrostatic repulsion of insulin and PVS (Fig.1).

Figure 2 shows the frequency change of formation and disintegration of PVS/insulin thin film monitored by a quartz crystal microbalance (QCM). The frequency has decreased about 150 Hz in average per an insulin layer, and the adsorbed amount of insulin can be calculated to be 640 ng/cm^2. Thus, when the thin film was dipped in the solution and the pH was increased stepwise, the disintegration of the PVS/insulin film was observed. The disintegration of the thin film was induced at pH 6 or higher.

Figure 3 shows time course of the disintegration of PVS/insulin film in the pH in the vicinity of the isoelectric point of insulin investigated by QCM. The film disintegrated gradually in pH 5.3, and the disintegration was quick at pH 5.6 and 6.0 though the disintegration was not induced at pH 5. This is because an electrostatic repulsion is caused between insulin and PVS, when PVS/insulin film was dipped in the solution in the vicinity of isoelectric point of insulin.

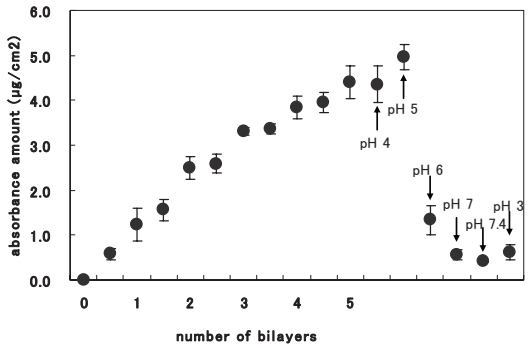

Fig.2 The formation and disintegration of PVS/insulin thin film.

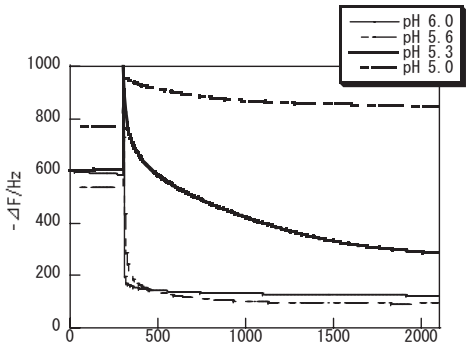

Fig.3 Time course of disintegration of the PVS/insulin film.

Figure 4 shows released amount of insulin from the PVS/insulin thin films with different number of layers. The released amount of insulin increased with the increase of the number of layers.

In conclusion, we have demonstrated that PVS/insulin thin film can be prepared at acidic pH and disintegrated at a neutral pH.

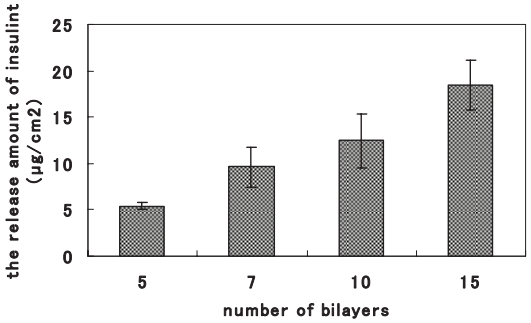

Fig.4 The released amount of insulin from PVS/insulin thin films with different thickness.

P004A

PREPARATION OF NOVEL SULFONATED BLOCK COPOLYIMIDES FOR PROTON CONDUCTIVITY MEMBRANES

Kouta Yamazaki, Shoji Nagaoka , Hiroyoshi Kawakami
Dept. of Applied Chemistry , Tokyo Metropolitan University
Hachioji , Tokyo 192-0397 , Japan
Phone. +81-426-77-1111, (ext) 4972 , Fax.+81-426-77-2821, E-mail:kawakami-hiroyoshi@c.metro-u.ac.jp

Introduction

The study of proton conducting polymers has attracted much attention due to their application in fuel cell systems. Although perfluorosulfonate ionomer membranes such as Nafion® have been the most widely used for such as high cost and low conductivity at high temperature. The proton conductivity of polymer electrolyte membranes is not only a function of the chemical structure of the polymers but is also determined by the morphology or the domain structure formed in the membrane. Particularly, in the case of a block copolymer, the proton conductivity may indicate a high value due to ionic channels formed by microphase or nanophase separation between the hydrophilic proton transport sites and the hydrophobic domain. There are several reports on the proton conductivity of block polymer electrolyte membranes based on sulfonated polyimide, sulfonated polysulfone, and sulfonated polystyrene. However, the difference in the proton conductivity or water uptake between random and block copolymers is small or negligible. To develop the block copolyimers, which can be used in fuel cell systems, the relationships between the proton conductivity and block copolymer properties, such as the domain size or block chain length, should be systematically investigated.

In this study, the proton conductivities of novel sulfonated block copolyimides synthesized by a two-pot procedure as functions of the relative humidity and temperature using four-point-probe electrochemical impedance spectroscopy were measured. Specifically, the influence of the block chain lengths on the proton conductivity and water uptake was focused on.

Experiments

The sulfonated block copolyimides were synthesized by the two-pot procedure. In one flask, the dianhydride-terminated poly(amic acid) oligomers were prepared by the reaction of BDSA and NTDA in *m*-cresol at 120℃. In another flask, the diamine-terminated poly(amic acid) oligomers were prepared from NTDA and 6FAP at 120℃. After 28hr, the two poly(amic acid) oligomers were compounded to synthesize the sulfonated block copoly(amic acid). After stirring for 24hr, the sulfonated block poly(amic acid) precursors were converted into the block copolyimide by chemical imidization with acetic anhydride and triethylamine at 180℃. After a 24hr conversion, the sulfonated block copolyimides were precipitated in ethyl acetate.

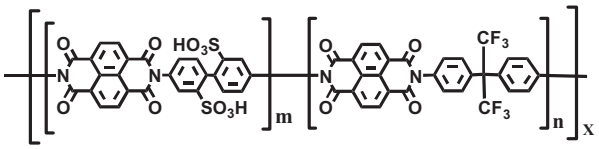

Fig. 1 Chemical structure of NTDA-BDSA-b-6FAP.

The sulfonated copolyimide membranes were prepared using a solvent-cast method. The dimethyl sulfoxide solution of the polyimide was cast on a glass plate, and then the plate was placed in a vacuum oven at 110℃ for 24hr. The membranes were immersed in ethanol and deionized water for 4hr each, then acidified with 0.1M HCl solution for 8hr, and finally washed with deionized water.

The ion exchange capacity (IEC) of the membranes was measured by classical titration using NaOH and HCl solutions. The water uptake of the sulfonated copolyimide was gravimetrically measured from the dried and humidified membranes. The dried sample weights were measured by drying the membrane samples of the polymer electrolytes in vacuum at 80℃ for 12h. The humidified sample weights were measured by immersing the membrane samples of the polymer electrolytes into water at room temperature for 24h. Proton conductivity was measured using a four-point-probe electrochemical impedance spectroscopy technique over the frequency range from 50Hz to 500kHz.

Results and Discussion

The degree of imidization of the sulfonated copolyimides was determined by ^{1}H-NMR spectroscopy. The results of the ^{1}H-NMR spectroscopy showed that the sulfonated polyimides synthesized by the chemical imidization were completely imidized. The IEC values determined by the titration for the random and block copolyimide membranes were similar to the theoretical values and were adjusted by the molar ratio (m/n) of the two diamines. The derivatives of the thermogravimetric curves for the sulfonated copolyimides showed no glass transition temperature (T_g) as observed for the other sulfonated polyimides. The decomposition temperature (>280℃) was almost as high as that of Nafion®.

Proton conductivity of the block copolyimide membranes indicated significantly higher values when compared with those of the random copolyimides, despite similar diamine compositions. The proton conductivities of the sulfonated block copolyimide membranes synthesized by the two-pot procedure increased with an increase in the lengths. However, the water uptake amounts did not depend on the block chain lengths and were almost constant. Figure 2 showed temperature dependence of the proton conductivity of the block copolyimide membranes at 98% relative humidity. It was found that the block copolyimide membrane, NTDA-BDSA-b-6FAP (70/30), showed a higher proton conductivity when compared with the random membrane, NTDA-BDSA-r-6FAP (70/30), at all temperatures. Additionally, it should be noted that the block copolyimide, NTDA-BDSA-b-6FAP (140/60), indicated a significantly high conductivity when compared with that determined for Nafion® at all temperatures. Figure 3 shows the relative humidity dependence of the proton conductivity for the block copolyimide membranes at 80℃. The conductivities of the block copolyimide membrane, NTDA-BDSA-b-6FAP(140/60), were similar to or higher than those of Nafion® from 70 to 100% humidity. In general, the proton conductivity for most polymer electrolyte membranes based on the sulfonated polyimide is well known to significantly decrease at low humidity. However, the conductivity of the block copolyimide membranes showed a humidity-dependence like Nafion®.

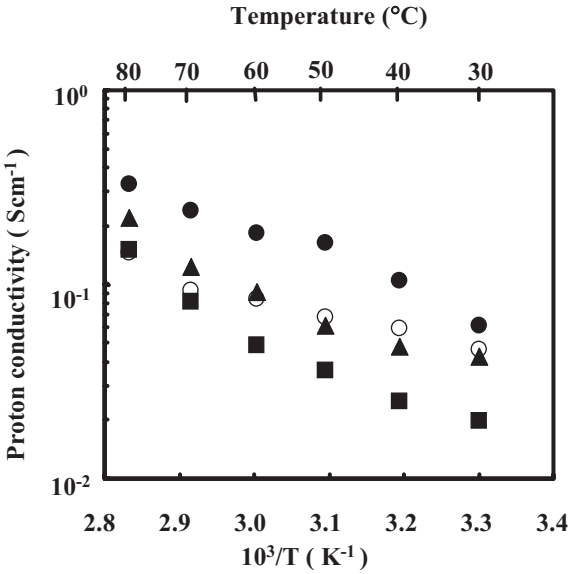

Fig.2 Temperature dependence of the proton conductivity for sulfonated copolyimide membranes at 98% RH.
●NTDA-BDSA-b-6FAP (140/60)
▲NTDA-BDSA-b-6FAP (70/30)
■NTDA-BDSA-r-6FAP (70/30)
○Nafion117

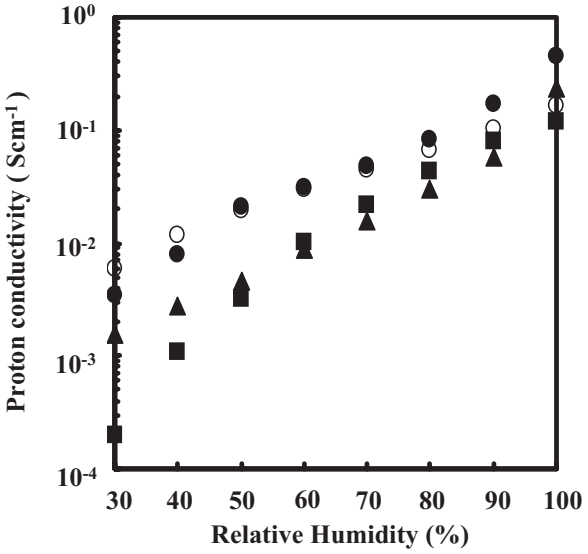

Fig.3 Relative humidity dependence of the proton conductivity for sulfonated copolyimide membranes at 80℃.
●NTDA-BDSA-b-6FAP (140/60)
▲NTDA-BDSA-b-6FAP (70/30)
■NTDA-BDSA-r-6FAP (70/30)
○Nafion117

Reference:
Takahiko Nakano, Shoji Nagaoka and Hiroyoshi Kawakami.Preparation of novel sulfonated block copolyimides for proton conductivity membranes. *Polym. Adv. Techol.*, **16**, 753-757 (2005).

P005B

GAS TRANSPORT PROPERTIES OF A NOVEL ORGANIC-INORGANIC HYBRID MEMBRANE BY PLASMA BASED ION IMPLANTATION

D.Muraoka[1)],T.Tezuka[1)],S.Nagaoka[1)],Y.Suzuki[2)],T.Kobayashi[2)],and H.Kawakami[1)]

1) Dept. of Applied Chemistry, Tokyo Metropolitan University, Hachioji, Tokyo 192-0397, Japan

2) The Institute of Physical and Chemical Research , 2-1 Hirosawa, Wako, Saitama 351-0198, Japan

Phone: +81-426-77-1111 (Ext) 4972, Fax: +81-426-77-2821, E-mail: kawakami-hiroyoshi @c.metro-u.ac.jp

Introduction

In this paper, we describe an organic-inorganic hybrid membrane, which exhibits an asymmetric structure consisting of a carbonized, an ultrathin and defect-free skin layer, used to synthesize a novel gas separation membrane combining high gas permeability and selectivity. In particular, we focused on the permeability of the gas through the partially carbonized skin layer prepared using low irradiation energy and fluence, because the partially carbonized membrane prepared by pyrolysis is reported to show a good balance between the gas permeability and selectivity when compared with the finally pyrolyzed membrane. Additionally, the skin layer thickness and the effect of the He^+-irradiated fluence on the gas permeability are also discussed in this study. It is well-known that plasma based ion implantation (PBII) can directly modify the surface of a membrane and that the polymer surface irradiated with low energy ion beam is carbonized (Figure 1). In this study, we fabricated novel organic-inorganic hybrid membranes using PBII and invesigated their gas permeability properties.

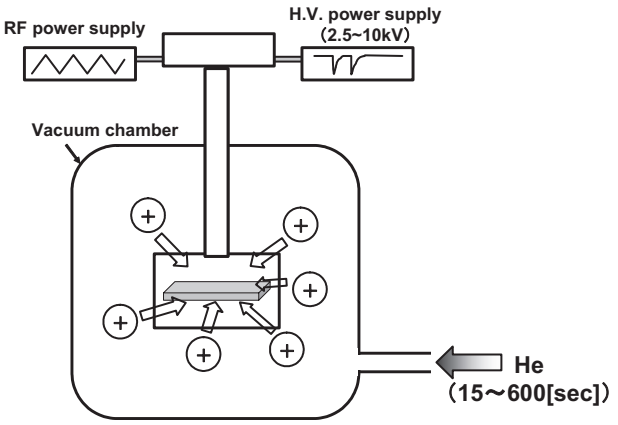

Fig.1 Schematic representation of PBII apparatus.

Experimental

The fluorinated polyimide, 6FDA-6FAP, was synthesized by chemical imidization of the poly (amic acid) precursors. Asymmetric polyimide membranes were prepared by a dry-wet phase inversion process with surface skin layer thickness 120nm. Finally, the membranes were dried in a vacuum oven at 150 ℃ for 15 h to remove all the residual solvents.

Gas permeability of CO_2, O_2, N_2, and CH_4 were measured with a high vacuum apparatus (Rika Seiki, Inc., K-315H, Tokyo, Japan). The gas permeation measurements of the membranes were carried out at 35 ℃ and 76 cmHg.

PBII on asymmetric membranes was carried out to modify surface using low energy ion beam (Riken ion implanter, Riken, Saitama, Japan). Ion irradiation was carried out on the polyimide surface at a pulse voltage of 2.5 kV He^+ for 15 to 600 sec at room temperature.

Surface characteristics of the asymmetric membranes were estimated by SEM, AFM, GATR-FTIR, contact angle, and laser Raman spectroscopy.

The depth profiles of the energy loss for He^+ in the asymmetric polyimide membranes were calculated using a well-established Monte Carlo simulation method (TRIM code). The mean projected range of the He^+ in the membrane was 116 nm.

Results and Discussion

In the Raman spectra of the asymmetric membranes irradiated by a 2.5 kV He^+ with control, 60, and 120 sec, the peaks at 1240, 1380, 1620, and 1780 cm^{-1} correspond to C-F_3, C-N, and C=C in the aromatic ring, and C=O respectively. After the irradiation of a 2.5 kV He^+ at PBII time of 600 sec, these peaks on the polyimide surface disappeared. However, two broad peaks on the polyimide surface irradiated at PBII time of 600 sec appeared at around 1360 and 1580 cm^{-1}. These peaks correspond, respectively, to the well-known D and G broad bands of disordered graphitic materials, indicating that the surface on the membrane changed to a carbon-enriched material.

The results of the gas permeability and selectivity of the asymmetric polyimide membranes for CO_2, O_2, N_2, and CH_4 at 35 ℃ and 76 cmHg are shown in Table 1. The PBII times were from 15 to 600 sec. The control asymmetric membrane indicated an O_2 permeability of 1.1×10^{-4} [cm^3 (STP)/(cm^2 s cmHg)], and the mean skin layer thickness calculated from the oxygen permeability coefficient was about 116 nm. The gas selectivities of the asymmetric membranes He^+-irradiated from 15 to 600 sec were similar to or greater than those (O_2/N_2 = 4.5 and CO_2/CH_4 = 29) of a dense membrane, which indicates that the permeability of the asymmetric membrane is predominantly carried out by a solution-diffusion mechanism and that the surface skin layer is essentially defect-free.

It is desirable to prepare a polymer membrane with both a high gas permeability and selectivity for gas separation. The ion-irradiated asymmetric polyimide membrane prepared in this study showed interesting gas permeation results, and we consider that the ion-irradiation would be one of the important membrane fabrication techniques for realizing a high gas permeability and selectivity.

Tab. 1 Effect of He^+-PBII on gas permeability and selectivity of asymmetric 6FDA-6FAP membranes at 35 ℃ and 76 cmHg.

PBII time [sec]	Q_{O2}	Q_{O2}/Q_{N2}	Q_{CO2}	Q_{CO2}/Q_{CH4}
control	110	5.3	420	43
15	49	6.4	220	53
30	24	7.3	110	76
60	13	8.2	62	79
90	4.4	6.3	19	33
120	2.9	4.4	12	18
150	1.2	3.1	4.5	9.7
300	1.9	2.3	6.4	7.0
600	14	1.2	25	1.8

Q：GPU ($\times10^{-6}$[cm^3(STP)/cm^2· sec· cmHg])

Apparent skin layer thickness was about 116 nm.

References

[1] H.Kawakami, M.Mikawa, S.Nagaoka, Gas permeability and selectivity through asymmetric polyimide membranes, *J. Appl. Polym. Sci.*, **62**, 965-971 (1996).

[2] H.Kawakami, M.Mikawa, S.Nagaoka, Gas transport properties of asymmetric polyimide membrane with an ultrathin surface skin layer, *Macromolecules*, **31**, 6636-6638 (1998).

[3] M.Iwase, A.Sannomiya, S.Nagaoka, Y.Suzuki, M.Iwaki, H.Kawakami, Gas permeation properties of asymmetric polyimide membranes with partially carbonized skin layer, *Macromolecules*, **37**, 6892-6897 (2004).

[4] A.Sannomiya, K.Fukui, S.Nagaoka, Y.Suzuki, M.Iwaki, H.Kawakami, Gas transport properties of asymmetric polyimide membranes prepared by ion-beam irradiation, *J. Polym. Sci., Polym. Phys.,* **45**, 262-269 (2007).

P006C

TOCOPHEROL TARGETED-HYBRID MOLECULARLY IMPRINTING APPLIED AS MEMBRANE ADSORBENTS

Che Ku Mohammad Faizal, Takaomi Kobayashi*

Department of Chemistry, Nagaoka University of Technology, 1603-1 Kamitomioaka, Nagaoka, Japan. 940-2188

Introduction

Molecular imprinting polymer (MIP) technique is well known for creating polymer materials with molecule selectivity in adsorption and separation. In the imprinted polymers, the cross-linked polymers retained the template volumetric space, which gave both molecule recognition and target-binding. This was due to that resultant imprinting polymers well memorized the target molecule in shape and functionality. In the present work, we had extended such technique on formation of membrane adsorbents using hybrid molecular imprinting membrane (HMIP). Namely, embedded the crosslinked imprint polymer was with commercial scaffold membrane in order to selectively separate tocopherol derivatives. α-Tocopherol was selected as target molecule due to its antioxidant ability and important roles in disease prevention, nutrient supplement and food preservation. Herein, the evidence included for advantage in HMIP membrane technique in their binding natures to tocopherol and phenol derivatives was studied on basis of selectivity of the HMIP membrane. We also focused and considered on the kinetic mechanism to target template in view point of hybridized imprinting.

Experimental

Functional monomer, α-tocopherol methacrylate (α-TMA), was copolymerized in covalent networks of divinyl benzene (DVB). For α-tocopherol (α-Toc) imprinting, esterification of α-Toc with methacryloyl chloride was carried out. The resulting α-TMA monomer was copolymerized with DVB (1:20, 1:10 and 1:4 mol ratios) in the presence of AIBN. The copolymer was hydrolyzed in 2M H_2SO_4 for 24 h to remove the template from the copolymer. The resulting MIP was hybridized in range of 10-50 wt% toward scaffold membranes polysulfone (PSf), nylon (Ny) and cellulose acetate (CA) by dissolving in appropriate solvent. The scaffold membrane solution contained the MIP powder was spread on glass plate at 50°C and then coagulated in water for phase inversion process. As the reference, each scaffold membrane without MIP powder also was prepared in the same manner. Uptake experiments of substrate for resultant HMIP were carried out in ethanol or hexane solvent (20 mL) containing each 100 μM of α-Toc, δ-Toc, pentamethyl-6-chromanol (PMC) and 4-chromanol by shaken at 30°C for 24 hours. The binding amounts of each substrate to HMIP membranes were calculated by concentration changes before and after the uptake experiments.

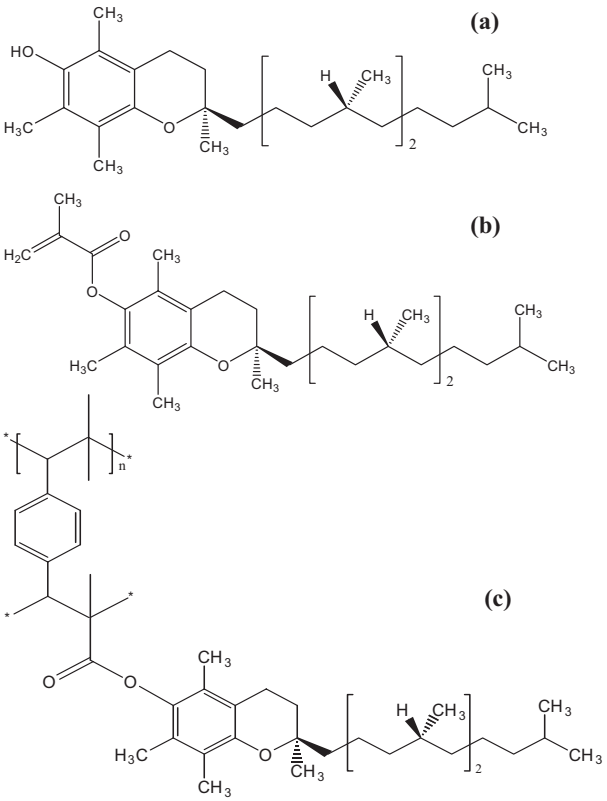

Scheme 1. Chemical structures of (a) α-Toc, (b) α-TMA and (c) α-TMA-MIP

Results and Discussion

Figure 1 shows SEM pictures of cross-section for HMIP membranes. The pictures demonstrated that hybridization was successfully performed in each case. In the SEM, presence of less void space between the powder and the scaffold membrane was observed. Results of uptake experiments for α-Toc analogs are listed in Table 1. For PMC and 4-chromanol, low binding was observed to the all imprinted systems. The binding amounts of α-Toc to each HMIP membranes were relatively higher than that of δ-Toc, although both MIP powder and scaffold used for the hybrid imprinting showed lower binding.

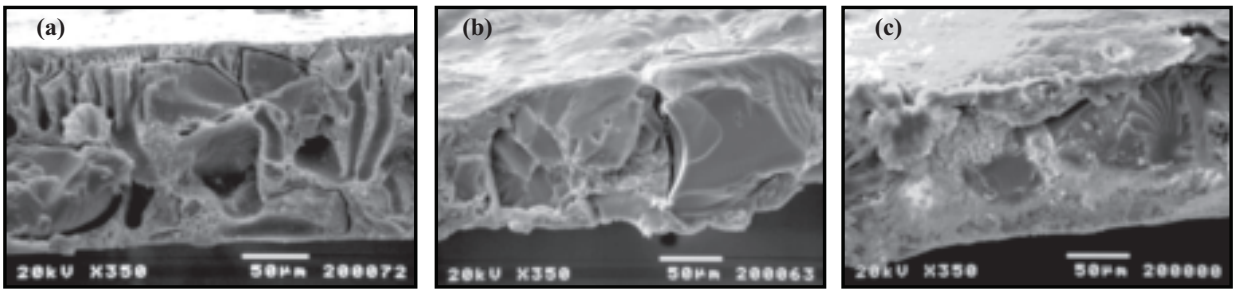

Fiqure 1. SEM pictures of (a) PSf, (b) CA and (c) Ny-HMIP

Table 2 lists the obtained value of imprint efficient, α_i, for the each HMIP membranes. Almost similarity to that of the α-TMA-MIP powder was observed in HMIP, while the binding capacity for HMIP membrane was about 2~4 folds higher than that of the α-TMA-MIP. Therefore, it was clear that the HMIP membrane exhibited effective binding ability to α-Toc relative to that of the α-TMA-MIP. This indicated that the covalent imprinting of α-Toc was able to recognize both chemical structures of tocopherol derivatives with or without methyl group in their chemical structures. Furthermore, the reason of high recognition ability for α-Toc in the HMIP membrane was considered that surrounding environment of the scaffold polymer changed the binding ability of the MIP powder.

Table 1 Binding amounts of substances

Sorbents	α-Toc	δ-Toc	PMC	4-Chromanol
	μmol/g			
α-TMA-MIP	11.8	5.8	3.7	0.5
NIP	2.7	1.0	0.9	0.7
CA	23.7	22.3	7.3	4.1
PSf	20.5	16.6	18.3	10.3
Ny	18.2	11.2	7.6	9.6
CA-HMIP	35.1	18.5	11.0	8.5
PSf-HMIP	42.7	25.8	21.6	21.1
Ny-HMIP	28.5	18.3	17.5	11.2

Table 2 Imprint efficient (α_i) of substances

Sorbents	α-Toc	δ-Toc	PMC	4-Chromanol
α-TMA-MIP	1	0.49	0.31	0.04
NIP	1	0.87	0.75	0.58
CA	1	0.94	0.31	0.17
PSf	1	0.81	0.89	0.50
Ny	1	0.62	0.42	0.53
CA-HMIP	1	0.53	0.31	0.24
PSf-HMIP	1	0.60	0.51	0.49
Ny-HMIP	1	0.64	0.61	0.39

Reference

1. K. Takeda, T. Kobayashi, *Sci. Technol. Adv. Mater*. 6 (2005) 165.
2. K. Takeda, T. Kobayashi, *J Membr. Sci*. 275 (2006) 61.

P007A

EFFECT OF SUPERCRITICAL CARBON DIOXIDE UPON PROPERTIES OF MOLECULARLY IMPRINTED MEMBRANES WITH SELECTIVE URACIL BINDING

Quanqiu Zhang, Takaomi Kobayashi *

Department of Chemistry, Nagaoka University of Technology, 1603-1Kamitomioka, Nagaoka, Jappan, 940-2188

INTRODUCTION

Molecularly imprinted is rapidly developing past decade, because of facile way encoding monomer by shapes and molecular functions into polymers. It has been attracted more interesting in molecularly recognized materials. On the other hand, it was recently found supercritical CO_2 was effect in preparing polymer architecture materials for microspheres, porous fibers and porous foams. In the present work, we selected supercritical CO_2 instead of water as non-solvent to prepare porous imprinted membrane for uracil (URA) recognition and binding. Molecularly imprinted membranes of poly(acrylonitrile-co-methylacrylic acid) targeted for uracil were prepared in supercritical CO_2. In order to increase the recognition ability of resultant membrane, supercritical CO_2 fluid was good solvent to reduce the lost of template uracil during the membrane formation.

EXPERIMENTS

Membrane materials poly(acrylonitrile-co-methacrylic acid) [P(AN-co-MAA)] was synthesized with AN and MAA monomers (mole ratio; AN/MAA=95/5) by radical copolymerization in DMSO solvent and azobisisobutyronitrile (AIBN) initiator for 8 hours at 60°C. Figure 1 shows illustration of preparation of URA imprinted membrane. Casting solution containing both 10 wt% of P(AN-co-MAA) and 1 wt% URA template was spread onto a glass plate (100×100 mm^2) at 50°C. The glass slide was immediately transferred into the supercritical reactor (150 mm diameter and 85 mm depth, Toyo Koatsu co.). The reactor was sealed as soon as possible after the sample was set. Then, CO_2 was introduced into inside from the cylinder by a high-pressure syringe pump at -5°C. When the system reached to the desired pressure (16MPa), the valve was closed immediately. The system was held for 2 hours at 35°C and then depressurized for 1 hour. By taking the glass slide from the reactor, the dry membrane was obtained.

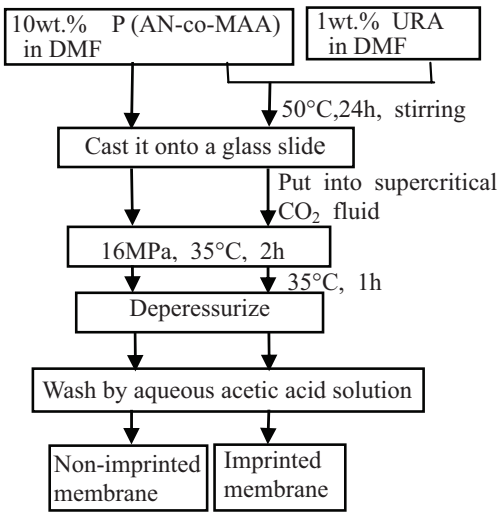

Figure 1 Scheme of preparation of URA imprinted and non-imprinted membranes in supercritical CO_2 fluid.

In order to measure binding ability of resultant membrane, batch binding experiment was carried out as followed. Imprinted membrane (15×15 mm^2) was emerged in 15mL URA solution with concentration 100μM at 30°C. It was confirmed that the binding was saturated within 6 hours. So, saturated binding amount of URA was measured by incubation at 30°C and 6 hours. The concentration of URA solution before and after binding equilibrium was measured by UV-Vis spectrometer (V-570, JASCO) at 258nm. The value of saturated binding amount [S] (μmol/g) of substrate was calculated by the following equation; $[S] = (C_o - C_t)\ V / W$, where C_o and C_t represent molar concentrations of substrates measured

at an initial time and the saturated binding time. V (L) and W (g) represented volume of substrate solution and weight of imprinted membrane, respectively.

RESULTS AND DISCUSSION

SEM photograph of cross-section of the imprinted membrane is shown in Figure 2. It is observed that the membrane had various size pores in micron and sub-micron range and a dense layer with about 15μm in the cross-section, especially on the top surface.

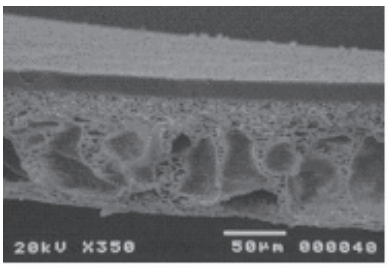

Figure 2 Cross-section of the imprinted membrane prepared in CO_2 fluid.

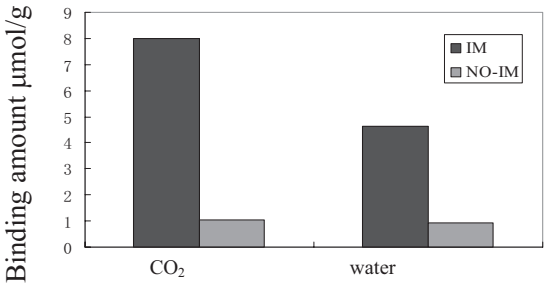

Figure 3 Saturated binding amounts of imprinted and non-imprinted membranes prepared in CO_2 fluid and water.

The saturated binding amounts of imprinted and non-imprinted membranes prepared in CO_2 fluid and water, respectively, are shown in Figure 3. For membranes prepared in the CO_2 fluid, the value of $[S]_{uracil}$ of the imprinted membrane was 8.0μmol/g, which was much higher than that of the non-imprinted membrane with the binding capacity of 1.0μmol/g. This meant that the imprinted membrane had binding ability for URA template. Although the resultant membrane prepared in water showed binding ability to URA, the binding amount with 4.6μmol/g was lower than the imprinted membrane prepared in the CO_2 fluid. This meant that the supercritical CO_2 was efficient for preparing imprinted membrane.

In order to confirm the recognition ability of resultant membrane, the binding amounts of the membrane was measured using dimethlyuracil (DMURA), cytosine solutions (Figure 4). Figure 5 shows the binding results of imprinted and non-imprinted membranes prepared in the CO_2 fluid in URA and its analog solutions. The binding amounts of imprinted membrane in DMURA and cytosine solutions were much lower than that in URA solution. This indicated that the resultant membrane had URA recognition sites, which showed selective binding ability to the URA template.

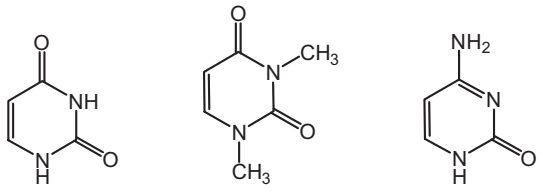

URA DMURA cytosine

Figure 4 Chemical structures of URA, dimethyluracil, and cytosine.

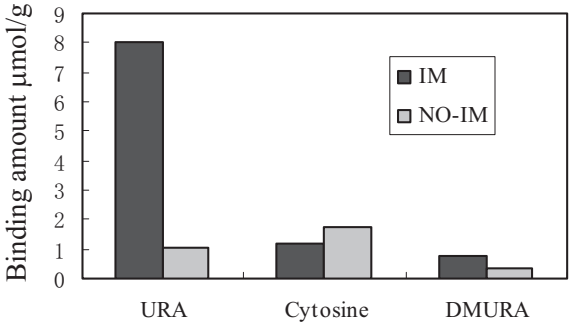

Figure 5 Binding amounts of imprinted and non-imprinted membranes in different solutions containing URA and its analogs.

REFERENCE

1. S. L. Xia, H. Y. Wang, T. Kobayashi, Mat. Res. Soc. Symp. Proc., 787(2004)103.
2. H. Matsuyama, H. Yano, T. Makia, M. Teramoto, K. Mishima, K. Matsuyama, J. Membr. Sci., 194 (2001)157.

P008B

Novel Membrane Adsorbents Made of Hybrid Molecularly Imprinted Polymer for Indole Derivatives

Kohei Takeda, Kohei Uemura and Takaomi Kobayashi*

Department of Chemistry, Nagaoka University of Technology

1603-1 Kamitomioka, Nagaoka, Niigata, Japan, 940-2188

Introduction

Indole is known as cause of various illnesses and the framework is contained in various key molecules which relate to biological systems. In addition, the molecules having the indole framework have been used in pharmacology. Therefore, it is interesting as selective recognition tool adsorbs selectively and separates from other substances in food and medical fields. For development of such adsorbents for indole, molecular imprinting has been very useful as alternative methods; the technique is an effective for preparation of advantageous functional polymers, which selectively recognize a target molecule in mixture solution. We have studied hybrid molecularly imprinted polymer (HMIP) membrane embedded with crosslinked imprinting polymer in order to develop new types of membrane materials having molecule selectivity[1]. In the present study, the technique was applied for targeted indole by using HMIP membranes with selective separation.

Experiments

Indole-3-ethyl methacrylate (IEMA) was used as functional monomer for imprinting indole-3-ethanol (IE) (Scheme 1) and synthesized by etherification of IE and methacrylic acid chloride. In the presence of AIBN, the resultant IEMA monomer was copolymerized with divinylbenzene (DVB) (1:10 mol ratio). In order to synthesize IE imprinted polymer, IE segments from the P(IEMA-*co*-DVB) (Scheme 1) were extracted as followed. The P(IEMA-*co*-DVB) was hydrolyzed in 2 M HCl aqueous solution with stirring for 12 hours at 60°C[2]. In order to prepare HMIP membrane, the resultant IE imprinted polymer was hybridized with polysulfone (PSf) membrane by phase inversion process[1]; The imprinted polymer (1.5 g) powder was mixed in PSf (1.5 g) *N*-methyl-2-pyrrolidone solution. The mixture solution was spread on glass plate at 50°C and then coagulated in water. As a reference, PSf membrane without MIP powder was also prepared.

Permeation experiments of substrates (Scheme 1) were followed; The IE imprinted HMIP membrane was mounted in 50 ml capacity ultrafiltration cell (UF-8050, Amicon Inc.). Aqueous solution (40 ml) containing each 25 μM of IE, indole, pyrrole and (HQ) was permeated thorough the membrane. The concentration of substrates in permeating solution was determined by using the HPLC measurement system and then separation factors (α_s) were estimated by following equation,

$$\alpha_s = (C_{sp} / C_{ip}) / (C_{sf} / C_{if}),$$

where C_{sp} and C_{ip} were the binding concentrations of a substrate

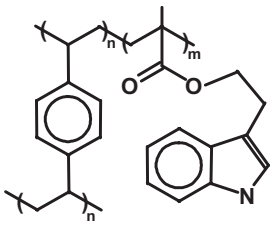

P(IEMA-co-DVB)

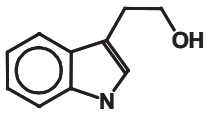

Indole-3-ethanol (IE)

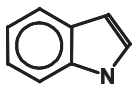

Indole

Pyrrole

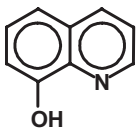

8-Hydroxyquinoline (HQ)

Scheme 1 Chemical structures of copolymer, IE and IE analogs.

and indole in the permeate solution and C_{sf} and C_{if} were the concentrations of substrate and indole in the feed solution, respectively[3].

Results and discussion

Figure 1 shows SEM images of cross-section of PSf and HMIP membranes. These pictures were for hybridization successfully performed in PSf scaffold polymer. This was because that void space between the imprinted polymer powder and the scaffold was absent in the cross-section of the resultant HMIP membrane.

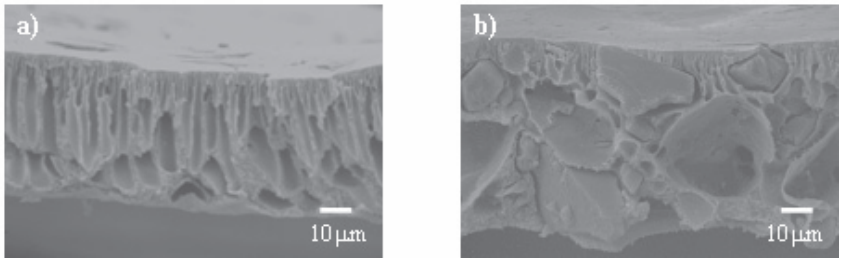

Figure 1 SEM pictures of cross-section of a) PSf and b) HMIP membranes.

Figure 2 shows HPLC chromatogram charts of the mixture solution containing pyrrole, HQ, IE and indole before and after the solution was permeated through the membranes. For the PSf membrane, un-significant changes in each peak intensity was found for four substrate peaks obtained before and after the permeation. On the other hand, for the HMIP membrane, the peak intensities of pyrrole and HQ were almost kept constant before and after the permeation. It was noted that the peak intensities of IE and indole remarkably decreased by the permeation. Especially, the decrease of the IE peak was larger than that of indole. The resultant HPLC data were used to estimate α_s, which expressed separation factor. As summarized in Table 1, the value of α_s of IE in the HMIP membrane was higher than that of indole, although PSf membrane showed lower α_s. The reason of high recognition ability for IE in the HMIP membrane was considered that the IE molecules were effectively absorbed by imprinting sites of the imprinted polymer powder in the PSf scaffold membrane. Accordingly, it was confirmed that the HMIP membranes effectively separated the IE molecule from mixture of indole and IE analogs by membrane permeation experiments[3].

Table 1 Separation factors of PSf and HMIP membranes in permeation experiments.

	Separation factor (α_s)			
	Pyrrole	HQ	IE	Indole
PSf membrane	-[a]	-[a]	0.80	1
HMIP membrane	-[a]	-[a]	1.11	1

[a] No binding of substrate for membrane.

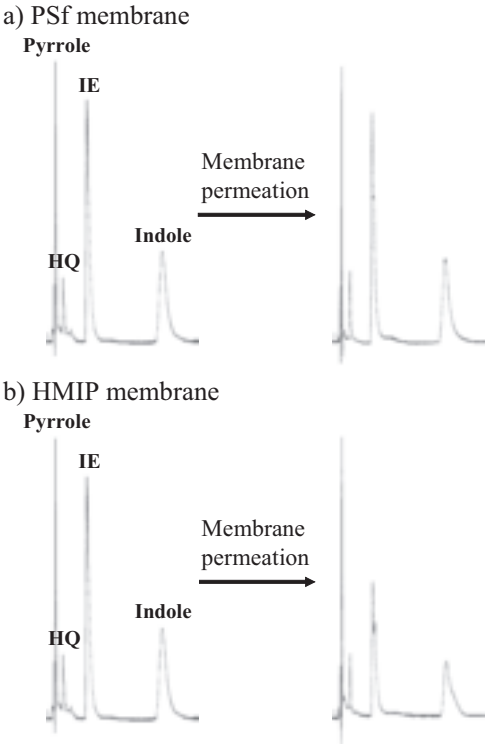

Figure 2 HPLC charts of aqueous solution containing pyrrole, HQ, IE and indole before and after permeation by the a) PSf and b) HMIP membrane.

References

1. K. Takeda and T. Kobayashi, *J. Memb. Sci.*, 275 (2006) 61-69.
2. K. Takeda and T. Kobayashi, *Sci. Tech. Adv. Mater.*, 6 (2005) 165-171.
3. K. Takeda, K. Uemura and T. Kobayashi, *Anal. Chim. Acta*, 591 (2007) 40-48.

P009C

MOLECULARLY IMPRINTED POLYMER SPHERES HAVING ADSORPTION SELECTIVITY OF BISPHENOL DERIVATIVES

Kaori Katagawa, Masaya Kozuka, Takaomi Kobayashi*

Department of Chemistry, Nagaoka University of Technology 1603-1 Kamitomioka, Nagaoka, Japan. 940-2188

Introduction

Molecular imprinting is template technique of producing polymeric materials with specific recognition sites tailored for targeted molecule. Such recognition materials would be utilized in adsorbent for separating the target from the analog mixture. In the present work, we reported preparation of imprinted polymer spheres having adsorption selectivity to bisphenol A (BPA) in order to separate it from bisphenol analog mixture.

Experiment

Imprinted copolymer with sphere shape was obtained by copolymerization using bisphenol A dimethacrylate (BADM) and ethylene glycol dimethacrylate (EGDM) crosslinker in the presence of α, α'-azobis(isobutylonitrile) in acetonitrile solvent. After the monomer solution was purged with nitrogen, a flask having the total amount of the mixture was kept at 55℃ in water bath for 24 h with shaking. Then, white sphere copolymers (Scheme 1) were deposited in the bottom and were washed by acetonitrile. Then hydrolysis of the BPA segments in the copolymer sphere was carried out in 1 M H_2SO_4 aqueous solution. After the hydrolysis was over, the imprinted spheres were dried under vacuum. When separation of BPA from other analogs was performed shaking in the mixed solution, containing each 2 μM of BPA, bisphenol E (BPE), bisphenol F (BPF) and 2-(4-hydoroxyphenylethyl) alcohol (HPA) was taken place for 24h at 30℃. Each substrate was analyzed using HPLC with UV detector at 210 nm.

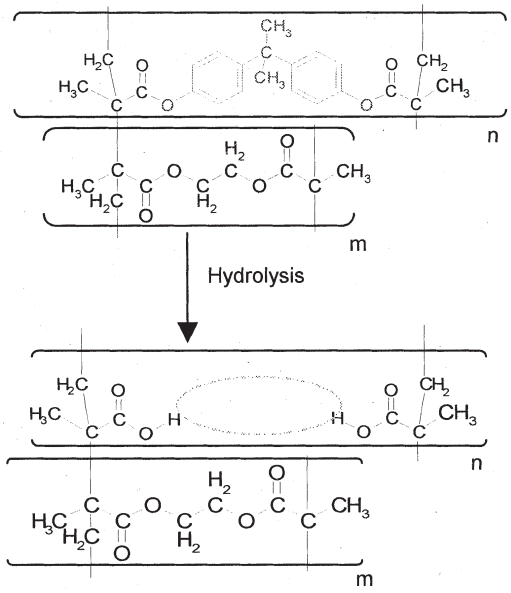

Scheme 1

Results and discussion

SEM Image (×20000) of P(BADM-co-EGDM) is shown in Fig.1. It was obvious that resulted sphere size was on homogeneity distribution in about 0.4 μm diameter. As shown in Fig.2, it was found that BADM imprinted polymers bond highly Bisphenol with 19.0 μ mol/g. Namely, in the obtained HPLC chart showing disappearance in the BPA peak, the BPA molecules were completely bound for after 24 h, when the binding experiment was finished.

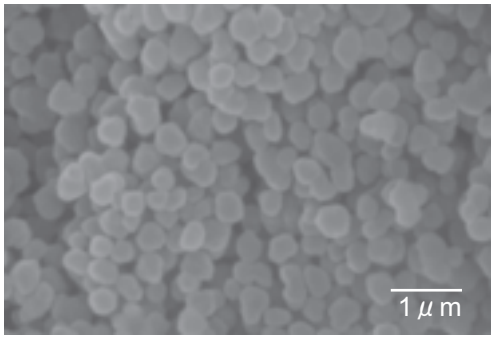

Fig.1 SEM image of P(BADM-co-EGDM) spheres obtained after the hydrolysis.

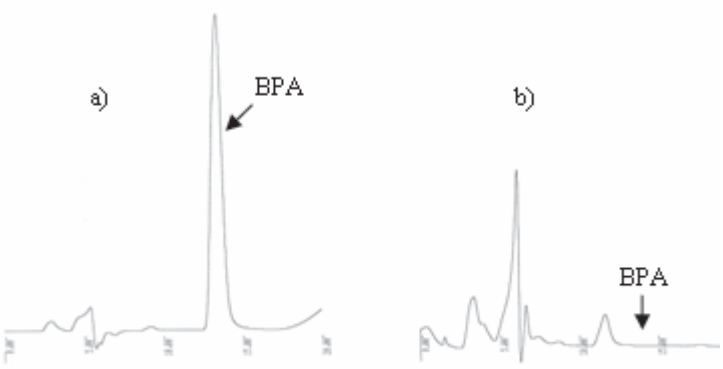

Fig.2 HPCL charts of 2 μ M BPA solution. Chart a) and b) were measured before and after 24 h binding experiment, respectively.

P010A

PREPARATION AND THERMOSENSITIVE PROPERTIES OF POLYNIPAM SPHERE MICROGELS CONTAINING ITACONIC ACID SEGMENTS

Takashi Onozuka and Takaomi Kobayashi*

Department of Chemistry, Nagaoka University of Technology,1603-1

Kamitomioka, Nagaoka, JAPAN. 940-2188

Introduction

In functional polymers, environmentally sensitive microgels have attracted much attention in recent years. For instance, poly*N-iso*propylacrylamide (PNIPAM) microgels were well known as thermosensitive microgels, because they exhibited a well-defined volume phase transition temperature (VPTT) in water around 31–34°C region. Since the temperature region is close to the body temperature, it is expected that such microgels would be applicable for drug delivery system. Therefore, to control their swelling/deswelling behaviors is important in scientific interesting. Hence, environmentally sensitive microgel is potentially useful for several fields. In the present study, the swelling/deswelling behavior was investigated by using novel polymeric microgels, P(*N-iso*propylacrylamide-co-Itaconic acid) (P(NIPAM-co-IA)), which contained two COOH groups in the itaconic acid (IA) segments.

Experimental

P(NIPAM-co-IA) microgel (Scheme 1) having 2 mol% IA segments and 6.7 mol% *N,N*-methylenebisacrylamide, which used as crosslinker, was synthesized by the surfactant-free emulsion according to previous report [1]. Aqueous pHs of the microgel solution were fixed at pH 3.0 and pH 7.0 by adjusting it with HCl/NaOH. Resultant diameter of the microgel particles observed at several temperatures was determined by a laser diffraction particle size analyzer (SALD-7000, Shimadzu) equipped with a small heater.

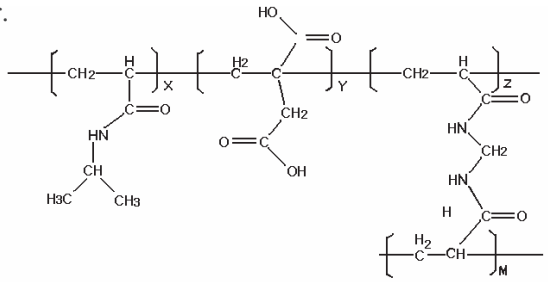

Scheme 1. Chemical structure of thermosensitive P(NIPAM-co-IA)

Results and Discussion

Figures 1 show results of laser diffraction phase transitions observed by laser diffraction particle size analyzer for P(NIPAM-co-IA). The temperature of the microgel solution was measured from 16˚C to 45˚C.It clearly exhibited influence of pH to the volume phase transition behaviors at different temperature. As the surrounding temperature became such from 16 to 45˚C, the observed diameter of the P(NIPAM-co-IA) microgel at pH5 was gradually changed to be smaller, especially at 37˚C to 45˚C. At the pH, the average diameters were 0.4 μm and 0.09 μm for 16 ˚C and 45˚C, respectively. On the other hand, at pH3, the temperature dependence of the particle size was complicate. Between 16 and 33 ˚C the tendency was to reduce the size, while the size was increased between 33˚C to 45˚C. Since two COOH groups of the IA segments showed less dissociation at pH3, actually, the difference in the temperature dependence was due to interaction of the –COOH groups in the IA segments.

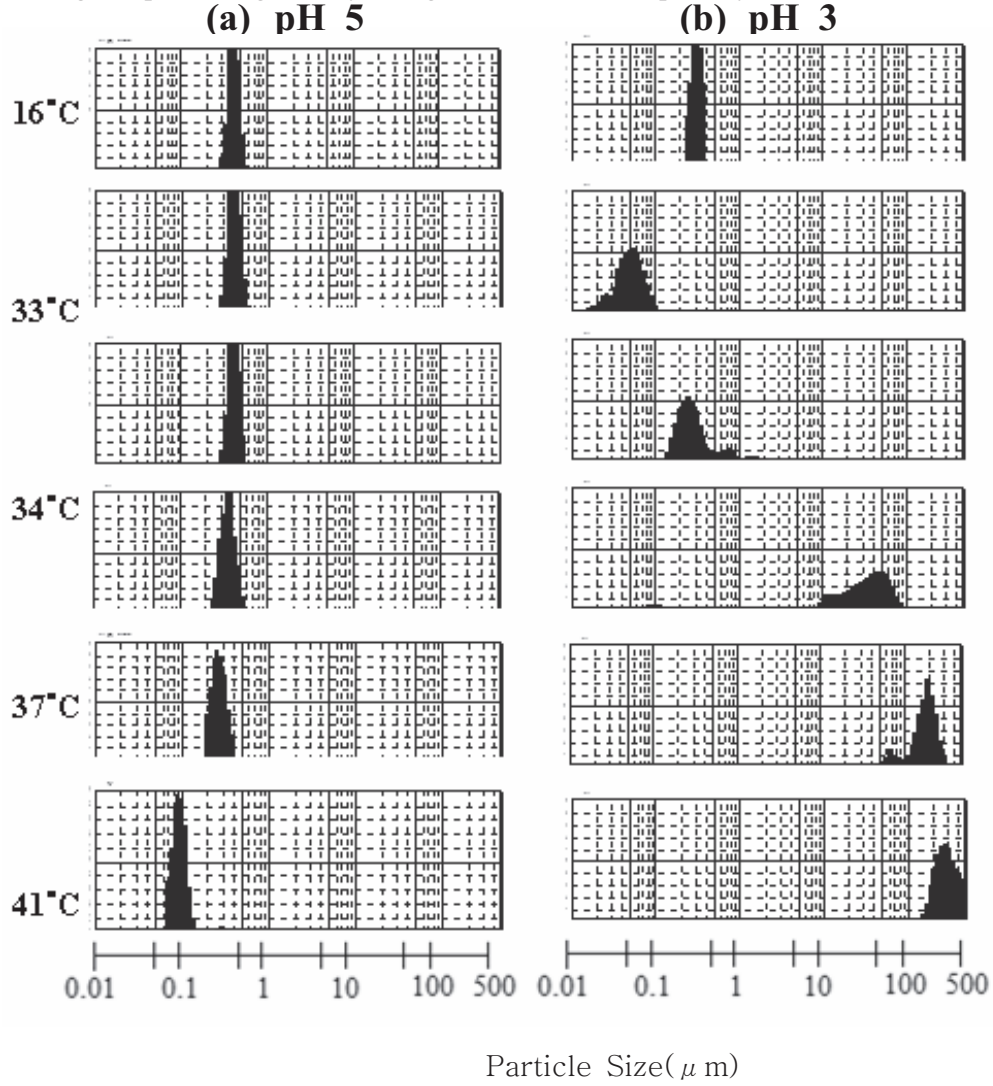

Figures 1 Influence of pH to the particle distribution of P(NIPAM-co-IA) in aqueous solution

References

[1]Dongxia, H; Yana, L; Takaomi, K. Advance Materials Research **2006,** 11 299-302

P011B

Preparation and Characterization of Environmentally Sensitive Microgel Particles with Fluorescence Probe

Yoshihiko Sato, Y. Xin, Takaomi Kobayashi*

Department of Chemistry, Nagaoka University of Technology, 1603-1 Kamitomioka, Nagaoka JAPAN 940-2188

Introduction

Intelligent microgel particles can respond to change surrounding in environmental conditions such as temperature, pH, ionic strength and solvency. Polymer microgels having *N-iso*propylacrylamide (NIPAM) are the most widely investigated as water-based and temperature-sensitive microgels. In the present work, to develop the investigation of NIPAM segment in the polymer microgels, fluorescence method was used. This was because of sensitivity and specificity to respond to the surrounding environment of NIPAM segments by the fluorescence probe. We prepared a new kind of environmentally sensitive microgels containing covalently attached with fluorescence proflavine probe. Novel proflavne methacrylamide was developed and introduced in the NIPAM segments of crosslinked microgels. In addition, the properties of prepared microgel were characterized at different pH and temperature.

Experiment

As shown in Scheme 1, poly NIPAM microgels containing proflavine segments used as fluorescencent probe were syn the sized. Surfactant free polymerization was applied to obtain such microgels. For example, P(NIPAM-MAPF-MBAAm) (PMN) was prepared by stirring a mixture of methacrylamide proflavine (MAPF), NIPAM and methylene bisacrylamide (MBAA) in the presence of potassium presulfate in 100ml of water for 6h at 70℃. Similarly, PAMN containing acrylic acid segments was prepared by stirring a mixture of MAPF, NIPAM, MBAAm and Acrylic acid (AA) similarly. Average particle diameter and fluorescence indensity of the proflavine segments were measured for PMN and PAMN at pH 3 and 5.

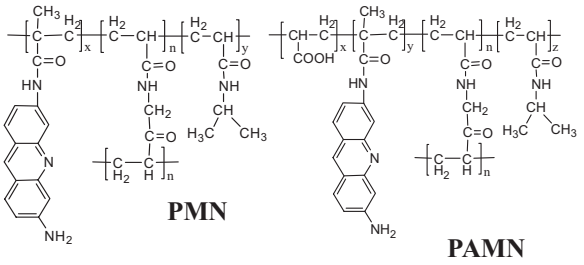

Scheme 1 Chemical structures of microgels

Results & Discussion

Figure 1 shows average particle diameter with pH 3 and 5 for PMN and PAMN by measuring with laser diffraction particle size analyzer. The microgel aqueous solution was prepared at pH 3 and 5.

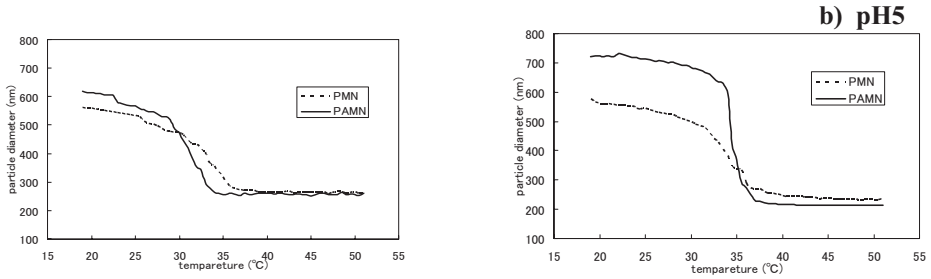

Figures 1 Average particle diameter measured with pH3 and 5 of PMN and PAMN

It was presented that Average particle diameter of PMN in aqueous solution was independent of pH, but when changed temperature, change in dramatical size was seen. In lower critical solution temperature (LCST) of NIPAM segment near about 33℃, it was presented that diameters decreased greatly. This behavior was almost same in that of PAMN. In addition, we measured fluorescence indensity of the probe segments at different pH and temperature. Figures 2 show fluorescence spectra of proflavine probe measured at various pHs and fluorescence indensity at 449nm for PMN and PAMN microgels (Fig 3). When the pH increased, fluorescence indensity for PMN decreased. In PAMN, such decrease of the fluorescence indensity was gradually observed between pH3 and 11. The relationship between fluorescence indenstiy and temperature for PMN and PAMN in the pH range from 3 to 9 indicated that, when the temperature increased, the fluorescence indensity gradually decreased in PMN about 35℃. But in PAMN increased fluorescence indensity was observed at about 35℃ in pH3. Therefore, the difference in Fig 1 and Fig 3 strongly indicated that the environmental condition of the probe change by introducing AA segment to the microgels.

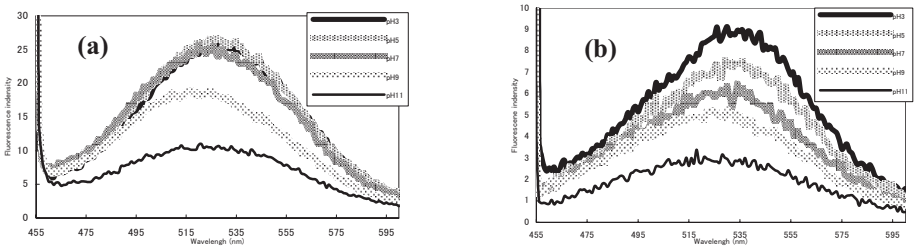

Fig.2 spectra of (a)PMN and (b)PAMN measured at different pHs in the range of pH 3～11. Excitation of the proflavine segments was performed at 449nm.

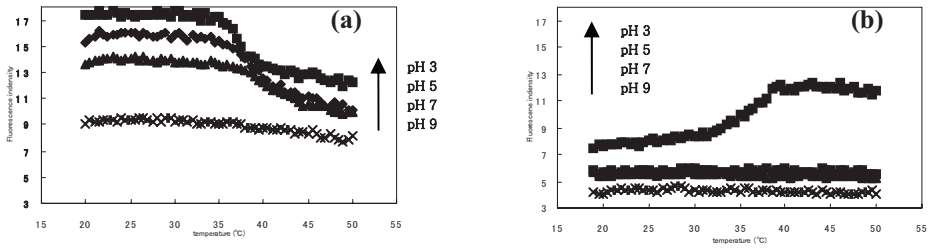

Fig.3 Relationships between fluorescence properties of intensity and temperature for (a)PMN and (b)PAMN.

P012C

MOLECULAR IMPRINTING MICROPARTICLES HAVING INOSINE RECOGNITION IN BINDING BEHAVIOR

Takayuki Kusunoki and Takaomi Kobayashi*

Department of Chemistry, Nagaoka University of Technology,1603-1 Kamitomioka, Nagaoka, JAPAN 940-2188

Introduction

Molecular imprinting provides a way to synthesize new materials containing artificial receptors that can be employed in a variety of applications, such as separation, sensor or catalysis. It is attractive to study nano-sized molecular imprinted polymers, which were expected to be with new function ability of molecule recognition and binding. Therefore, we focused in the present work on imprinted nano-sized polymers for inosine being one of the raw materials of DNA and RNA interests. Furthermore, there is another interest of the imprinted polymers in the causes of gout by the molecule; As a one of application, inosine imprinted polymer particles would be used in drug carrier for gout disease. So, we prepared and characterized inosine imprinted polymers having nano-sized particles.

Experiments

Polymer preparation. Methacrylic acid (15mmol), divinylbezene (15mmol), inosune (15mmol), LBSA (10mmol) and 2,2'-azobis-[*N*-(carboxyethyl)-2-methyl- propyonamidine] n-hydrate (0.9g) were dissolved in water/chloroform (30ml/270ml). The mixture was kept at 55 ^{o} C for 3h under ultrasound radiation (45kHz with 600W out put). After evaporating chloroform, the polymerized particles were washed with ethanol and then HCl aqueous solution to extract the template and LBSA. Using centrifugal separation (4000rpm), the extracted polymer powder was collected and finally lyophilized.

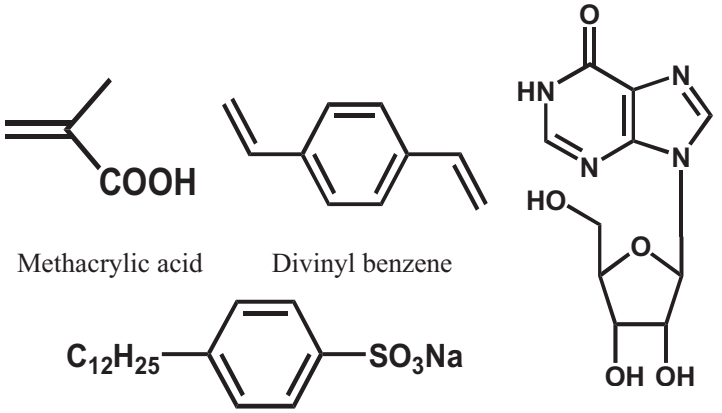

Morphology measurements. The morphology of the polymer particles was observed by scanning electron microscopy (SEM). Particle size distribution of the resultant was also measured by laser diffraction scattering method.

Binding experiments. Binding amounts assay of inosine to the polymer particles were performed by measuring substrate concentration of the water solution at various pHs. The inosine solution was shaken for 24h at 30°C and then the concentration was compared before and after binding. UV absorption spectra were also monitored for the solution (20ml) containing dialysis membrane with polymer particles (0.1g) and 20μM-inosine solution inside.

Results and discussion

Morphology of polymer particles. SEM image of inosine imprinted polymer particles is shown in Fig.1. It was clear that polymer particles of 100-400 nm were aggregated. Therefore, the emulsion polymerization used under ultrasound caused nano-sized morphology of resultant imprinted polymer. We also confirmed that non-imprinted polymer particles showed similar distribution of the particle size and shape with that of imprinted polymers.

Binding amounts of inosine. Binding amounts of inosine to the polymer particles list in Table. Both imprinted and non-imprinted polymers were highly adsorbed inosine at pH3; we compared them at other pHs for each system. The pH dependence of the binding experiments suggested that the divinylbenzene/methacrylic acid copolymers had binding ability to the inosine according to Fig.2, since the inosine substrate at pH 3 interacted through hydrogen bonds between the substrate and the polymer. However, when pH increased, the numbers of hydrogen bonding were reduced. This was due to dissociation of carboxylic acid groups of the methacrylic acid segments in the copolymer. In addition, inosine showed different chemical structures depending upon pH. It was found that the imprinted polymer adsorbed the substrate with 7.3 μmol/g, when the binding of inosine was carried out at pH3. Namely, the tailor-made binding sites were formed by the polymerization in the presence of inosine

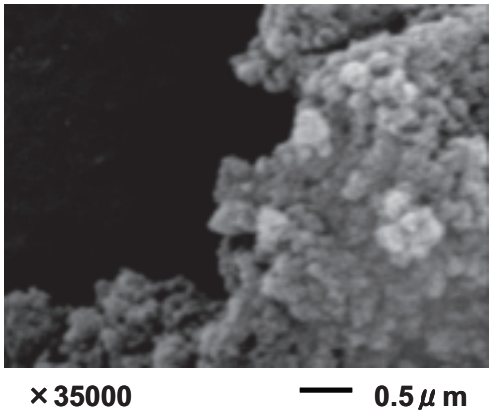

Fig.1 SEM image of imprinted polymer particles

Table Binding amounts of inosine at pH 3, 6 and 10.

	Binding amounts (μmol/g)		
	pH 3	pH 6	pH 10
Imprint	7.3	3.5	0.68
Non-imprint	0.76	0.52	0.19

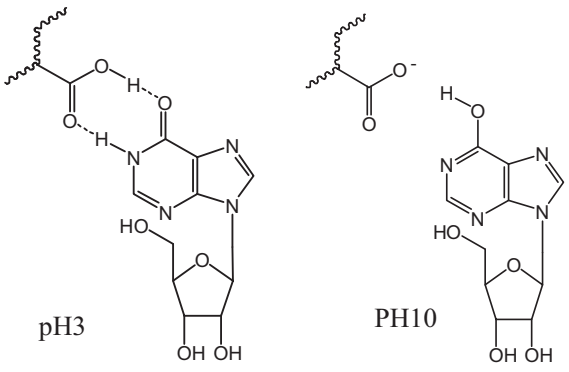

Fig.2 Binding illustration of inosine at both pHs.

References

1. N.Pérez-Moral, A.G.Mayes, Analytica Chimica Acta, 504 (2004) 15

2. N.Pérez-Moral, A.G.Mayes, Langmuir,20 (2004) 3775

P013A

SYNTHESIS AND GAS PERMEABILITY OF POLYPHENYLACETYLENE MEMBRANES HAVING AMINO GROUPS

Yuki Sato[1], Masahiro Teraguchi,[1,2,3] Takeshi Namikoshi,[3,4] Edy Marwanta,[3,4] Takashi Kaneko,[2,3] and Toshiki Aoki[1,2,3,4*]

[1] Graduate School of Science and Technology, [2]Center for Education and Research on Environmental Technology, Materials Engineering, and Nanochemistry, [3]Center for Transdisciplinary Research, [4]Venture Business Laboratory, Niigata University, Ikarashi 2-8050, Nishi-ku, Niigata 950-2181, Japan

In our laboratory poly(phenylacetylenes) having silyl groups were fabricated to good self-supporting membranes and exhibited high gas permeability[1)]. In this study, we synthesized and polymerized phenylacetylenes having amino groups, 3,5-bis(4-aminophenylethynyl)phenylacetylene (**BNDENPA**) and 4-{1-(2,2,5,5-tetramethyl-2,5-disilapirazolidinyl)}phenylacetylene (**BSNPA**) (Fig.1) and measured their permeabilities for CO_2(P_{CO2}) and N_2(P_{N2}).

A membrane from poly(**BNDENPA)** was prepared *in-situ* during polymerization of **BNDENPA**. We copolymerized **BSNPA** with trimethylsilylphenylacetylene(**SPA**) and its membranes were fabricated by solution casting method using toluene as a solvent. The value of P_{CO2}/P_{N2} of poly(**BNDENPA**) was 28.4. In case of copoly(**BSNPA/SPA**), P_{CO2}/P_{N2} increased with increasing the content of **BSNPA** unit while P_{CO2} decreased. And the values of P_{CO2} and P_{CO2}/P_{N2} were on or close to the Robeson's upper boundary line(Fig.2).

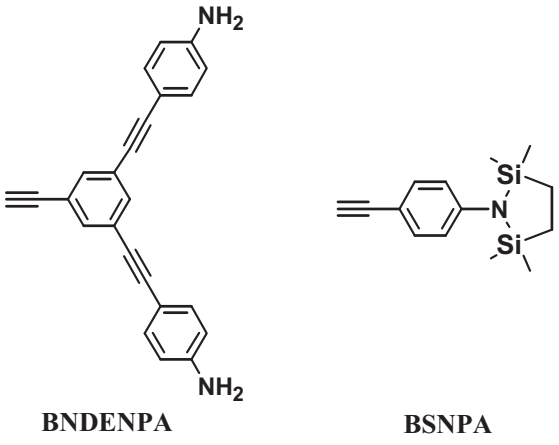

Fig. 1. Chemical structures of phenylacetylene containing amino groups.

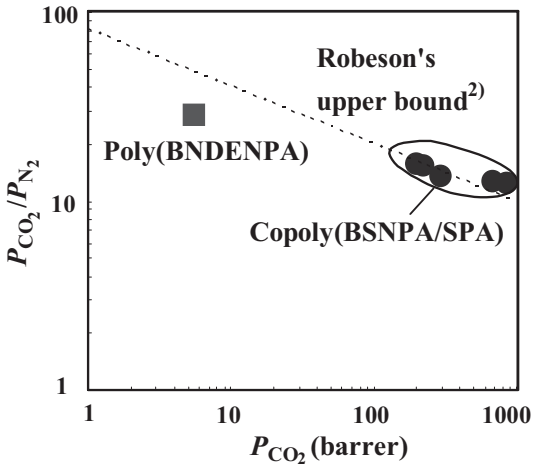

Fig. 2. The relationship between permeability and permselectivity for carbon dioxide of the polymer membranes.

References

1) T. Aoki and T. Kaneko, *Polym.J.*, **37**, 717(2005).

2) L. M. Robeson, *J. Membr. Sci.*, **62**, 165 (1991)

P014B

AIR HUMIDIFICATION BY TRIETHYLENE GLYCOL MEMBRANE SUPPORTED ON A HYDROPHOBIC MICROPOROUS MEMBRANE

Jinlong Li* and Akira Ito

Department of Chemistry and Chemical Engineering, Niigata University, Ikarashi 2, Niigata 950-2181, Japan

Abstract- The humidification performance of indoor air by separating water vapor from outdoor air with absorption liquid (TEG) supported on hydrophobic microporous membrane was investigated. Permeation rate of water vapor could reach 2-4.1 g-water/h when the attracting air flow rate was 6 L/min.

Introduction

Humidity control is important in many engineering applications, such as space air conditioning, storage warehouses and so on. Many researchers have reported the performance of air dehumidification by triethylene glycol (TEG) desiccant in a packed column [1]. Ito reported the dehumidification performance of air by surface-supported liquid membrane (TEG) for its nonvolatility and big surface tension [2]. The objective of this study is to characterize the performance of indoor air humidification by separating water vapor from outdoor air and make an economical and practical humidifier overcoming the risk of contamination of the air.

Humidification by separating water vapor from air

The humidifying apparatus was placed in outdoor and the permeate side pressure was decompressed to 30-60 kPa by a vacuum pump ($10\overline{W}$) as shown in Fig.1. Membrane cell was made up of three flat modules in parallel, the membrane area of two sides of one flat module is 0.13 m^2 and TEG liquid membrane thickness is about 30 um. The indoor air whose flow rate was controlled by a needle valve was attracted into the permeate side and along with the permeation water vapor coming from outdoor air was discharged to humidify indoor air. The point of this method is that the supplying water vapor to indoor comes from outdoor air but not using additional water. But the experiment was carried out in the same room.

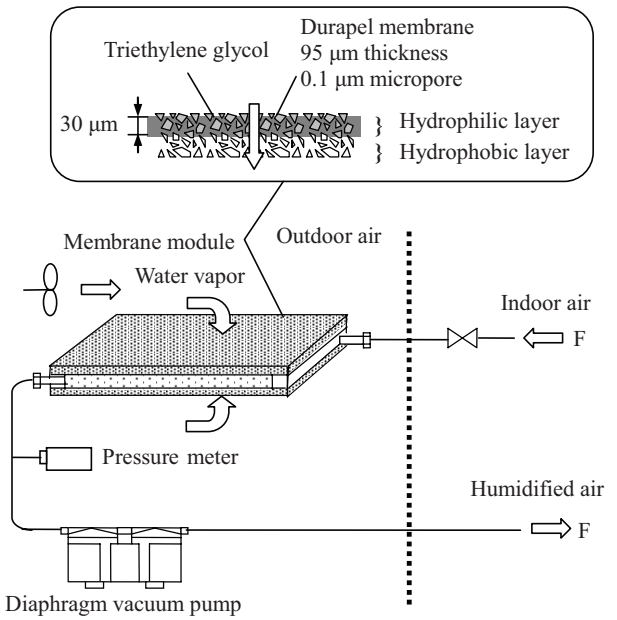

Fig.1 The set-up of indoor air humidification by a liquid membrane

The effect of outdoor air humidity on experiment was shown in Fig.2. Permeation rate was 2-4.1 g-water/h

when the attracting air flow rate was 6 L/min and humidity of attracting air and outdoor air was 20-48 %RH. Permeation rate increased with increasing of outdoor air humidity, because the driving force of water vapor partial pressure difference was increased. Fig.3 showed that permeation rate increased with increasing of attracting air flow rate but it decreased when the attracting air was to about 6 L/min. This is because the permeate side pressure was increased to decrease driving force by increasing of the attracting air flow rate. When the membrane area increased to 3 times the permeation rate increased to 1.5 times but not 3 times.

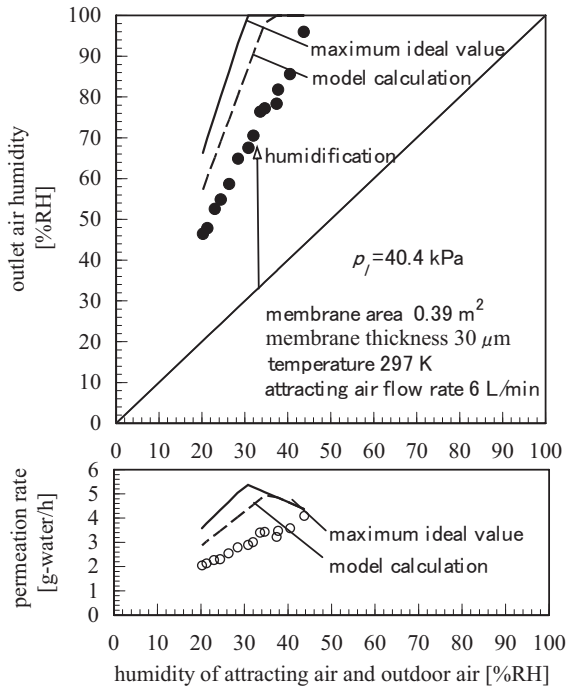

Fig.2 Effect of outdoor air humidity

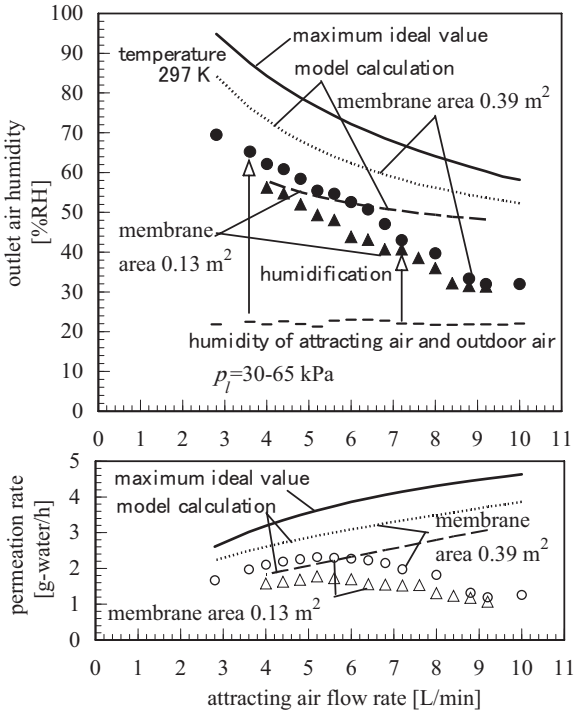

Fig.3 Effect of membrane area and attracting air flow rate

The maximum ideal value was calculated when water vapor pressure difference was zero. And model calculation was based on the vapor permeability Q_{water} [mol・㎡/(㎡・s・kPa)] as shown in followed equation.

$$\frac{dP_{water}}{dA} = \frac{Q_{water}}{\delta}\left(p_{h,water} - p_l \frac{P_{water}}{P_{air} + P_{water}}\right)$$

P_{water} [mol/s]: absorbed water vapor, P_{air} [mol/s]: attracting air flow rate, A [m^2]: membrane area, Q_{water} [mol・㎡/(㎡・s・kPa)]: water vapor permeability, δ [m]: liquid membrane thickness, $p_{h,water}$ [kPa]: outdoor water vapor partial pressure , p_l [kPa]: permeate side pressure.

References

[1] Y.H. Zurigat et al., Air dehumidification by triethylene glycol desiccant in a packed column, Energy Conversion and Management, 45, 141-155 (2004)

[2] Ito, A., Dehumidification of air by a hygroscopic liquid membrane supported on surface of a hydroscopic microporous membrane. J. Membrane Sci., 175, 35-42 (2000)

P015C

Preparation of hydroxyapatite composite gel by biomineralization and application to medical material

Sachiko OBARA[1], Hiroshi SAITO[2], Takeshi YAMAUCHI[1,3,4,]*,
and Norio TSUBOKAWA[2,3,4]

[1]Graduate School of Science and Technology, Niigata University, [2]Faculty of Engineering, Niigata University, [3]Center for Transdisciplinary Research, Niigata University, [4]The Center for Education and Research on Environmental Technology, Materials Engineering, and Nanochemistry

〔Introduction〕

Recently, osteoporotic patients are significantly increasing in this aging society. Bone filling materials made from hydroxyapatite are used for treating this disease. Even though a block and granules of hydroxyapatite are used as bone filling materials, there are several problems that mechanical strength of these materials is not enough to apply in large bone defect. Composite materials of hydroxyapatite and hydro-gels would be suitable to fill in such a large bone defect.

In this study, composite materials of hydroxyapatite and calcium alginate gel were prepared under room temperature and normal atmospheric pressure. Drug release behavior of the composite polymer gel was also investigated in order to utilize the composite gel for biomedical materials.

〔Experimental〕

Hydroxyapatite was prepared from $CaCl_2$ (100mM–1000mM) and $(NH_4)_2HPO_4$ (60mM–600mM) in calcium alginate gel under room temperature and normal atmospheric pressure. Surface structure of composite materials was investigated with optical microscope and scanning electron microscope (SEM). Content of hydroxyapatite in composite gels was calculated by the result of thermo gravimetric analysis and swelling ratio of composite gels was calculated. Composite gels containing $St\text{-}CH_2P^+(C_4H_9)_3Cl^-$ as antibacterial agent were evaluated for characteristic of drug release with UV-VIS spectroscopy.

〔Results and Discussion〕

The gels prepared with $CaCl_2$ and $(NH_4)_2HPO_4$ had white color and diameter of these composites gels was increased with concentration of $CaCl_2$ and $(NH_4)_2HPO_4$. Crystallization of white colored hydroxyapatite in the composite gel was identified by X-ray analysis. The amount of hydroxyapatite in the gel was significantly related with concentration and ratio of $CaCl_2$ and $(NH_4)_2HPO_4$. Surface structure of composite gel was also drastically changed at the concentration ratio of $CaCl_2$ and $(NH_4)_2HPO_4$ was 5: 3. This value was as same as composition ratio of hydroxyapatite ($Ca_{10}(PO_4)_6(OH)_2$). It was estimated that hydroxyapatite generation was superior to preparation of calcium alginate gel. Swelling ratio of composite gel was decreased with the content of hydroxyapatite, because large quantity of hydroxyapatite was interacted with crosskicking process. According to the SEM images, Composite gel was observed porous structure on its surface.

Drug release characteristic of composite material was measured using UV-VIS spectrometer. Antibacterial agent was effectively released from composite gels which have high porous structure.

P016A

Preparation of poly(*N*-isopropylacrylamide) gel containing polymer-grafted carbon micro-coils and its application to drug carrier

Shigenori SATO[1], Takeshi YAMAUCHI[1,3,4]*, Norio TSUBOKAWA[2,3,4], Kenji KAWABE, Yukio HISHIKAWA[5], and Seiji MOTOJIMA[6]

[1]Graduate School of Science and Technology, Niigata University; [2]Faculty of Engineering, Niigata University; [3]Center for Transdisciplinary Research, Niigata University; [4]Center for Education and Research on Environmental Technology, Materials Engineering, and Nanochemistry, Niigata University; [5]CMC Technology Development Co. Ltd.; [6]Faculty of Engineering, Gifu University

〔Introduction〕

Thermo-sensitive polymer gels have been actively studied for application to drug carriers in bio medical field. Shrinking by external thermo stimulus, these materials advantageously release drugs at affected areas in human body. Thermo distribution of human body sometimes interferes in controlling the shrinkage of the gel in human body. It has been reported that carbon micro-coils (CMCs) generate heat with electromagnetic irradiation. In this research, we prepared composite materials of poly(*N*-isopropylacrylamide) (PNIPAM) gels as thermo-sensitive polymer gels containing CMCs by photo-polymerization. It is expected that the material shrinks with heat which CMCs generate with electromagnetic irradiation. The properties of the material such as content of CMCs, swelling ratio, breaking strength, and thermo-sensitivity, and its function as drug carrier were evaluated.

〔Experimental〕

The composite gels were prepared by photo-polymerization with irradiation of ultraviolet light. *N*-isopropylacrylamide, monomer, *N,N'*-methylenebisacrylamide, crosslinker, 2,2'-Azobis(2-amidinopropane)dihydrochloride, and initiator were dissolved in water. Untreated CMCs, poly(vinyl ferrocene (VFE)-*co*-methyl methacrylate (MMA))-grafted CMCs, and PNIPAM-grafted CMCs were respectively added to this solution with stirring. The gelation was carried out by irradiating with ultraviolet light for several hours. Obtained gels were immersed in water until it reached an equilibrium condition. Content of CMCs was calculated with thermogravimetric analysis (TGA). Swelling ratio was calculated from weight of swollen gel and that of dry gel. Breaking strength was evaluated by compression test. Thermo-sensitivity and function as drug carrier were evaluated by relationship between temperature and volume alteration modulus**.**

〔Results and Discussion〕

The black colored composite gel membranes were prepared by this method, and polymer-grafted CMCs were uniformly dispersed in PNIPAM gels. It was estimated that grafted polymers augmented hydrophilic of CMCs, and CMCs were dispersed in the polymer network which contained water solution. Composite gels had slightly larger swelling ratio and smaller breaking strength than normal PNIPAM gel. Composite gels were changed their volume with temperature alternation as same as normal PNIPAM gel, and showed phase transition temperature at 35 ℃. During the shrinking process of composite gels, no CMC eluted off from the composite gels. These results suggested that CMCs were entrapped polymer matrix very well and the composite gels maintained their thermo-sensitivity to shrink with heat.

〔Acknowledgement〕

This study is supported by Grant for Promotion of Niigata University Research Projects.

P017B

LSPR for Applications to Biosensing Element

Yasutaka Anraku[1*], Hiromi Kitano[2]
1 The University of Tokyo, 2 University of Toyama

Introduction

Recently, the interaction between self-assembled monolayer (SAM) and various proteins has been examined by using various techniques so far. For example, SAMs of specific substrate and inhibitor for α-chymotrypsin and aspartyl proteases (pepsin and HIV-1 protease), were constructed on a gold electrode for the detection of the enzymes.[1]

In this research, the phenylboronic acid (PBA) derivatives-carrying copolymer was accumulated on a colloidal gold-immobilized glass substrate, and the usefulness of the polymer brush as a sensing element for glycoproteins (ovalbumin (OVA), avidin) was examined by using a UV-visible spectrophotometer with a help of localized surface plasmon resonance (LSPR).[2] Moreover, we tried to constructed the sensing element using the molecular imprinting technique, which recognizes OVA selectively.

Experimental Section

【Preparation of Sensing Element】 The glass substrates were immersed in 3-Aminopropyl triethoxysilane aqueous solution. The amine-terminated glass cover slips were subsequently immersed into a colloidal gold solution to form a SAM of colloidal gold. The colloidal gold-fixed glass substrates were modified with various disulfide-carrying polymers or monomers by immersion in a solution, and subsequent extensive rinsing with water (**Scheme 1**).

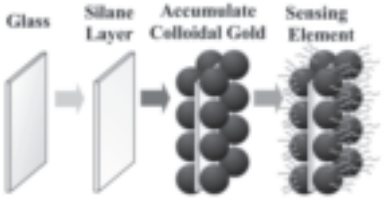

Scheme 1. Preparation of sensing element

【Polymerization of PBA-carrying Polymers】 The PBA-carrying polymers (Cys-Poly(APBA-*co*-DMAPMA) (**Scheme 2(A)**) were prepared by living radical polymerization using a disulfide-carrying iniferter (Cys-BDC). Cys-BDC, APBA and DMAPMA were dissolved in a mixture of THF and MeOH, and photo-irradiated at 35 °C for 6 h.

【Synthesis of DTPA-PBA (Scheme 2(B))】 DTPA was dissolved in water, and the pH value of the solution was adjusted to 4.8 (Solution A). APBA was dissolved in water, and the pH value of the solution was adjusted to 4.8. WSC (condensing agent) was added, and the solution mixture was stirred at 0 °C (Solution B). The Solution A was slowly added to the Solution B, and the reaction mixture was incubated for 1 h in ice, and afterwards overnight at 4 °C.

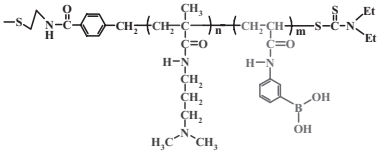

(A) Cys-Poly(APBA-*co*-DMAPMA)

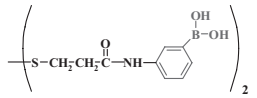

(B) DTPA-PBA

Scheme 2. Chemical Structures of PBA Derivatives. (A). Cys-Poly (APBA-*co*-DMAPMA); (B) DTPA-PBA.

【Construction of Molecular-Imprinted SAM on a Colloidal Gold】 Firstly, OVA and PBA derivatives were dissolved in carbonate buffer (pH 11.2). To prepare the OVA-PBA derivative complex, this mixture was incubated for 1 h at room temperature. The complex was purified by an ultra filter unit. The solution containing the complex on the filter was taken out from the ultra filter unit, and transfered to a sample vial. Then, the colloidal gold-fixed glass substrates were immersed in the solution of the complex for 1 h, and subsequently rinsed with a carbonate buffer extensively. Finally, the substrates were immersed in acetate buffer (pH 3.2) for 2 h to remove the OVA from the substrate.

Results and Discussion

Sensing Capabilities of Colloidal Gold Monolayer Modified with PBA-Carrying Polymer Brush

The characterization of SAM of colloidal gold on the glass and polymer-modified sensing element was pursued spectrophotometrically (**Figure 1**). From the previous study showed that the aggregation of colloidal gold would result in the coupling of plasmons of individual particles and a significant increase in the peak absorbance between 600 and 800 nm in the visible spectrum. Since such a feature in the visible spectra of the glass covered with colloidal gold and the subsequently prepared polymer-modified sensing element did not exist, the colloidal gold seemed to be immobilized as a monolayer on the glass surface and isolated from each other.

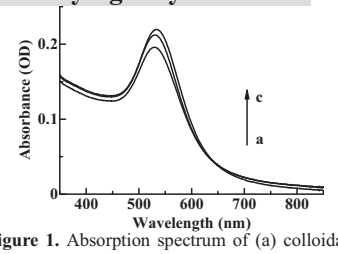

Figure 1. Absorption spectrum of (a) colloidal gold dispersion; (b) colloidal gold-fixed glass substrate; (c) Polymer-immobilized gold colloid on a glass surface.

The adsorption of four proteins (OVA, BSA, streptavidin and lysozyme) to brush was examined. **Figure 2** showed that, upon immersion in OVA solution, the absorbance at 550 nm for the polymer-modified colloidal gold on the glass chip gradually increased, and leveled off after ca. 40 min. In contrast with OVA, BSA, streptavidin and lysozyme showed only a very slight absorption change, indicating that non-specific adsorption of the protein had little or no effect on the sensing element.

Furthermore, we examined a similar evaluation by using other PBA-carrying polymer, and calculated the values of the association constant (K_{assoc}) and the detection limit for various proteins.

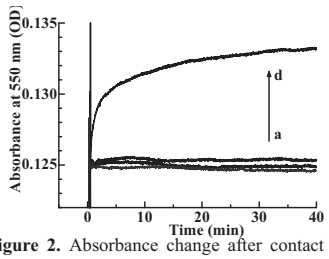

Figure 2. Absorbance change after contact of the Polymer-immobilized sensor chip with various proteins. The absorbance was monitored at 550 nm. (a) streptavidin (b) lysozyme (c) BSA and (d) OVA.

Molecular Imprinting at the Construction of Sensing Elements for a Glycoprotein

【Adsorption of OVA to Various Types of SAM】 We prepared the sensing element modified with various types of SAM. The objects of this experiment are the comparision between the affinity of OVA for the protein-imprinted SAM of PBA derivatives and that for the randomly deposited SAM of PBA derivatives. So far many chemists have mostly prepared SAM using randomly deposited method. However, the previous method could not distinguish any glycoproteins from other ones specifically. Therefore, the protein-imprinted SAM was prepared by using a characteristic of PBA.

At first, the DTPA-PBA was randomly self-assembled on colloidal gold on a glass substrate. After the sensing element modified with the randomly deposited SAM of DTPA-PBA was immersed in OVA and avidin solutions, a concomitant increase in the absorption at 550 nm appeared either (**Figure 3(A)**).

Next, OVA-imprinted SAM was prepared by using DTPA-PBA. When the sensing element modified with the OVA-imprinted SAM of DTPA-PBA was immersed in OVA and avidin solutions, a concomitant increase in the absorption at 550 nm was appeared, too (**Figure 3(B)**), though the change in absorbance was smaller than that in **Figure 3(A)**. However, the difference of the absorption upon immersion in two kinds of proteins appeared clearly compared with **Figure 3(A)**. These results indicated that the effect of OVA-imprinting was an important factor to construct the sensing element which recognizes OVA selectively. However, the absorption change was still observed for avidin (**Figure 3(B)**).

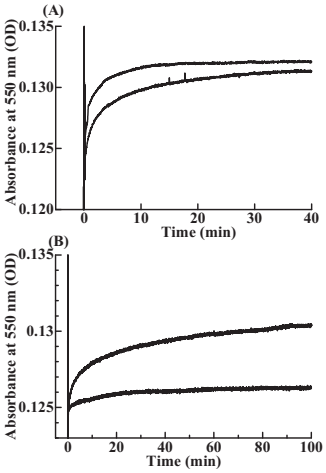

Figure 3. Absorbance change after contact of proteins with various types of SAM. (A) randomly deposited SAM of DTPA-PBA. (B) OVA-imprinted SAM. Upper curve is OVA. Lower one is avidin. [Protein] = 0.04 mM.

It is thought that, when the OVA-PBA complex was formed, all the PBA groups did not bind to sugar chains in OVA. Because of DTPA-PBA containing PBA groups in both end was used (**Scheme 2(B)**). As a result, the PBA groups without interaction with OVA molecule exist on the colloidal gold surface. To exclude such insufficiency, a similar experiment was done by using DTPA-PBA (-COOH) that had a PBA group at only one end.

【Kinetic of Adsorption of OVA and Avidin to Various Types of SAM】 The adsorption kinetics of OVA and avidin to various types of sensing elements were investigated by monitoring the absorbance change at 550 nm in real time. The K_{assoc} of OVA and avidin using a sensing element modified with the randomly deposited SAM of DTPA-PBA was determined to be 7.8×10^4 and 8.5×10^3 M^{-1}, respectively (**Table 1**). The ratio between K_{assoc} values for OVA and avidin was about 9. The K_{assoc} of OVA and avidin with the OVA-imprinted SAM of DTPA-PBA was determined to be 6.0×10^2 and 8.5 M^{-1}, respectively (**Table 1**). The ratio was about 70, which is much larger than that for the sensing element modified with the randomly-deposited SAM of DTPA-PBA. These result showed that the template effect occurred.

Table 1. Binding Constants for Glycoproteins with PBA Derivatives

DTPA-PBA	Protein	K_{assoc} (M^{-1})
Randomly deposited SAM	OVA	7.8×10^4
	Avidin	8.5×10^3
OVA-imprinted SAM	OVA	6.0×10^2
	Avidin	8.5

References

1. Kitano, H.; Makino, Y.; Sumi, Y. *Anal. Chem.* **2005**, *77*, 1588.
2. Kitano, H.; Anraku, Y.; Shinohara, H. *Biomacromolecules* **2006**, *7*, 1065.

P018C

EFFECT OF ZWITTERIONIC POLYMERS ON WOUND HEALING

Shigeto Fujishita[1,2], Chika Inaba[1], Susumu Tada[1], Makoto Gemmei-Ide[1], Hiromi Kitano[1]*,Yoshiyuki Saruwatari[3]

[1]*Department of Applied Chemistry, Graduate School of Science and Engineering, University of Toyama*

[2]*Teika Pharmaceutical Co., Ltd.* [3]*Osaka Organic Chemical Ind., Ltd.*

Wound healing is a complex process involving various cells, growth factors, a number of extracellular matrices and several proteases. Generally, it is well known that wound healing such as skin lesion is accelerated in a moist environment. Now, a variety of wound dressings have been used in wound healing. In this study, we prerared polymer films such as zwitterionic random copolymer of carboxybetaine, ［1-carboxy-N,N-dimethyl-N-(2'-methacryloyloxyethyl)methanaminium inner salt］ (CMB), and *n*-butyl methacrylate (BMA), Poly(CMB-*r*-BMA) (CMB, 30 mol%), on the poly(ethylene terephthalate) (PET) film, and studied the effect of the poly(CMB-*r*-BMA) film on the healing of a full-thickness excisional wound and a full-thickness incisional wound in hairless rats. The poly(CMB-*r*-BMA) film significantly enhanced a healing of a full-thickness excisional wound in rats when compared with PET and PBMA films. Both the amount of proteins adsorded and that of fibroblasts adhered onto the poly(CMB-*r*-BMA) film were significantly smaller than that onto the PBMA film. In this report, we discussed the relationship between the wound healing and the amount of proteins adsorded onto polymer films.

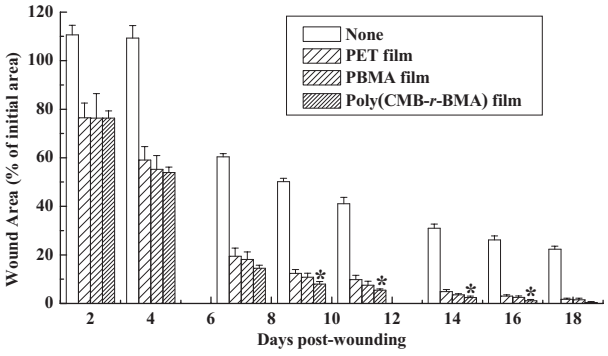

Effect of Poly(CMB-*r*-BMA) on Wound Closure in Rats.
Each column shows the mean±S.E. (n=5).
* p<0.05, compared with PET group (Student's *t*-test).

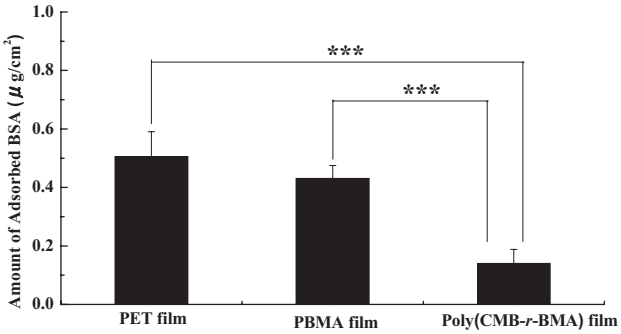

Total Amount of BSA Adsorbed onto Polymer Films.
Each column shows the mean±S.D. (n=4-5).
*** p<0.001, compared with PET and PBMA group (Student's *t*-test).

P019A

STUDY ON THE BIO-COMPATIBILITY OF POLYMERS WITH A CARBOXYBETAINE MOIETY

Makoto Gemmei-Ide[1], Chika Inaba[1], Susumu Tada[1], Hiromi Kitano[1]*,
Takayuki Matsunaga[2], Akira Mochizuki[3], Masaru Tanaka[4], Yoshiyuki Saruwatari[5]
[1]University of Toyama [2]Toyama Prefectural Institute for Pharmaceutical Research
[3]Tokai University [4]Tohoku University [5]Osaka Organic Chemical Industry Ltd.

The bio-compatibility of random copolymers of *n*-butyl methacrylate (BMA) and a carboxybetaine monomer, 1-carboxy-*N*,*N*-dimethyl-*N*-(2'-methacryloyloxyethyl)methanaminium inner salt (CMB), was evaluated. The bio-compatibility of nonionic polymers (poly(2-hydroxyethyl methacrylate) (PHEMA) and poly(*n*-butyl methacrylate) (PBMA)) and ordinary ionic copolymers was investigated as references. The total amount and the conformation of proteins adsorbed onto the polymers were examined by the micro-bicinchoninic acid protein assay and circular dichroism (CD) spectroscopy, respectively. On the CMB copolymers, the total amounts of absorbed proteins were decreased with increase in the content of CMB residues (Figure 1A). The amounts of proteins adsorbed onto the CMB copolymers were lower than those adsorbed onto other polymers and the conformation of proteins adsorbed onto the CMB copolymers differed little from the native one. Similarly, there was a dramatic decrease in the number of adhered cells (platelet and fibroblast) to the CMB copolymers compared with other polymers (Figure 1B and C). In addition, CMB copolymers were found to be inert to the complement and coagulation systems. These results suggest that the zwitterionic moieties seem to be markedly effective to give polymer materials bio-compatibility in general.

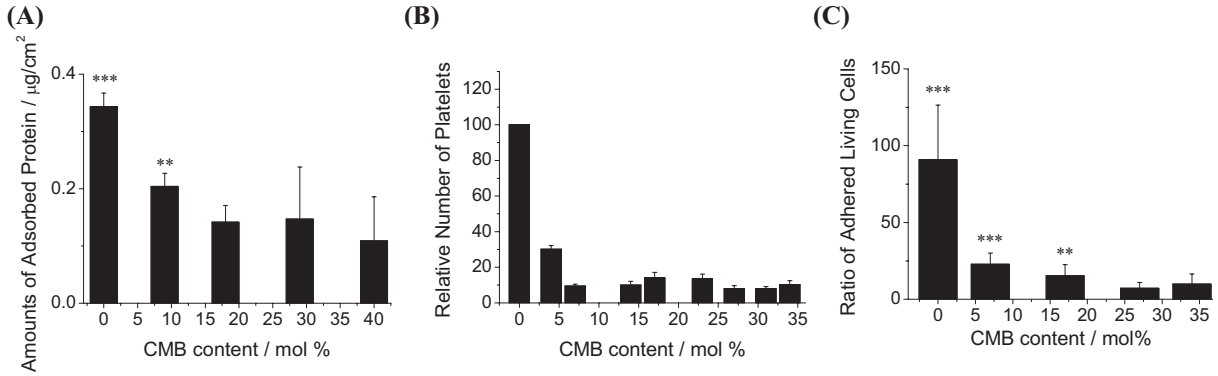

Figure 1. Effect of the content of CMB residue in the carboxybetaine polymer films on the amount of adsorbed protein (BSA) (A) and relative number of adhered cells (platelet (B) and fibroblast (C)).

P020B

GLUCOSE FUEL CELL WITH AN ANODE OF POLYTHIOPHENE DERIVATIVE BEARING GLUCOSE OXIDASE

Takashi Kuwahara, Mizuki Kondo, Rie Yamazaki and Masato Shimomura*

Department of Bioengineering, Nagaoka University of Technology

In recent years, biofuel cells have been expected as a compact electric power supply for the next generation. Enzyme electrodes can generate current from biomass such as sugars and alcohols and, therefore, have been considered to be potential components of biofuel cells. In the present study, glucose oxidase (GOx) was immobilized on a conducting polymer electrode, and the GOx-immobilized electrode (GOx-electrode) was applied to glucose fuel cells as an anode. The performance of cells was investigated by use of various cathodes (Pt and enzyme-immobilized cathodes).

The GOx-electrode was fabricated by immobilizing GOx on the film of conducting polymer, which was synthesized from 3-methylthiophene and thiophene-3-acetic acid by electrochemical copolymerization on Au-electrode. GOx was covalently immobilized on the surface of the polymer film by condensation reaction [1]. The GOx-electrode showed oxidation current in the presence of glucose and electron transfer mediator (Figure 1). The glucose fuel cell equipped with GOx-electrode and Pt-plate as an anode and a cathode, respectively, gave a maximum power output of 9.7 μW/cm^2 when cell voltage was 0.10 V. This result demonstrates that the GOx-electrode has an ability to function as an anode of the fuel cell. The power output of the glucose fuel cell was found to be limited by the nature of the cathode. The glucose fuel cells constructed with the cathodes bearing laccase (Lac) and bilirubin oxidase (BOx) gave larger power output than that constructed with the Pt-cathode (Table 1). As for the cell constructed with BOx-cathode, a maximum power output of 50 μW/cm^2 was obtained at pH 7.0, which was 5 times as large as the value obtained with Pt-cathode.

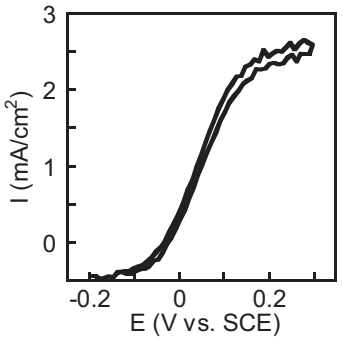

Figure 1. glucose oxidation current obtained by using GOx-electrode in the presence of 0.50 M glucose and 1 mM electron transfer mediator at a potential scan rate of 20 mV/s.

Table 1. Power outputs of fuel cells.

Anode	Cathode	Power output (μW/cm^2)
GOx	Pt	9.7
GOx	Lac	25.2
GOx	BOx	50.4

References

[1] T. Kuwahara, K. Oshima, M. Shimomura, S. Miyauchi, *Journal of Applied Polymer Science*, **104**, 2947-2953（2007）

P021C

DNA sensing with a quartz crystal microbalance for determination of *Esherichia coli*

K. Kon[1], M.Shimomura[1], K.Kaneko[2]

[1]*Department of Bioengineering, Faculty of Engineering, Nagaoka University of Technology, 1603-1 Kamitomioka-machi, Nagaoka 940-2188, Japan*

[2]*Niigata Environment Hygiene Central Laboratory Co., 2-12-7 shinsan, Nagaoka 940-2127, Japan*

A quartz crystal device was used for measuring a very small mass-change on its surface based on the change in its oscillation frequency and, therefore, called a quartz crystal microbalance (QCM).

In this study, a single-stranded DNA (target DNA) is detected with the QCM bearing complementary DNA (probe DNA) on its surface, based on a decrease in the oscillation frequency due to increased mass resulting from DNA hybridization. The probe DNA immobilized on the gold electrodes of QCM (21MHz) was adopted as a model of the fragment originating from 16S rDNA of *Esherichia coli* which is a synthesized DNA-disulfide probe consisting of 25 bases. The target DNA, which is the fragment of the oligonucleotide consisting of 36 bases, was prepared from the real cell body of *E. coli* as following procedures. Firstly, the DNA extraction from *E.coli* was treated by polymerase chain reaction (PCR) to obtain an enriched DNA portion of 527 base pairs from the 5th to 531th of the 16S rDNA. Then, the obtained DNA was treated with a restriction enzyme NlaIII to give an oligonucleotide including of 36 base pairs, which have 25-base sequence from the 3'-end complementary to the probe DNA immobilized on the QCM surfaces. The DNA fragment of 36 base pairs was extracted from gel after separated by electrophoresis, and finally treated by thermal denaturation to afford the target DNA with the single-strand of 36 bases. The solution including the prepared target DNA was employed as the analyte for the QCM determination.

The immobilization of the probe DNA on the surface of quartz crystal and the hybridization of the probe DNA with the target DNA was successful confirmed by the frequency change of the quartz crystal (Fig.1). A frequency decrease about 155 Hz was determined after immersed the quartz crystal in the probe DNA solution for 18 hours, which was corresponding to 1.05 pmol mass increase of probe DNA. Moreover, the frequency decrease about 213 Hz was obtained after immersed the probe DNA immobilized quartz crystal in a target DNA solution for another 18 hours, which was corresponding to 1.02 pmol mass increase of target DNA. The about result demonstrated that a considerable high hybridization efficiency (about 97 %) can be obtained by the present QCM system.

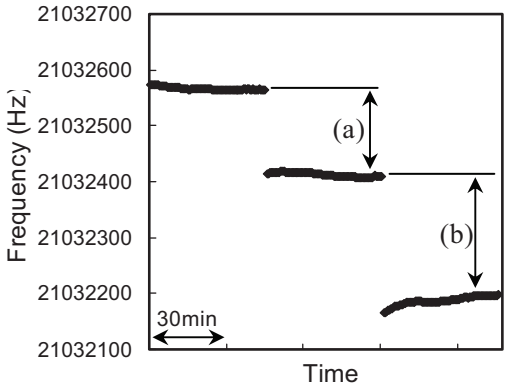

Fig.1 Frequency change after the immobilization of probe DNA (a) and the hybridization of target DNA prepared from 16S rDNA of *E.coli* (b).

P022A

SEPARATION OF SERINE PROTEASES USING A THERMORESPONSIVE POLYMER BEARING DIPHENYL 1-AMINO-2-PHENYLETHYLPHOSPHONATE

Shin Ono[1,*], Shigenori Yoshikawa[1], Atsushi Yamamoto[1], Kazuki Yasue[1], Fumie Manzaki[1], Takeshi Terashima[1], Hirofumi Kuroda[2]

[1]*Graduate School of Science and Engineering, University of Toyama, Toyama 930-8555, Japan,*
[2]*Department of Chemical and Biochemical Engineering, Toyama National College of Technology, Toyama 939-8630, Japan*

Diphenyl 1-aminoalkylphosphonate derivatives are known to irreversibly and specifically inactivate serine proteses [1]. We have tried to develop effective separation systems for serine proteases using polymers bearing such phosphonate irreversible inhibitors. A Phe-type phosphonate derivative (dipheny 1-amino-2-phenylethylphosphonate) was prepared and immobilized on Separose gel, and we demonstrated that chymotrypsin could be separated from a solution containing chymotrypsin and trypsin [2]. In our another study, the Phe-type phosphonate was introduced to poly(ethylene glycol)s (PEGs) to prepare PEG-inhibitor conjugates. The PEG-inhibitor conjugates were also shown to be useful for separation of chymotrypsin [3].

In this study, the Phe-type phosphonate was coupled with methacrylic acid and the obtained derivative was copolymerized with acrylamide to give the corresponding thermoresponsive inhibitor-acrylamide copolymer. Then, the usefulness of thermoresponsive property of the prepared inhibitor-acrylamide polymer for separation of serine proteases was examined. In addition, glycine oligomers (Gly, Gly-Gly, and Gly-Gly-Gly) were introduced between the Phe-type phosphonate moiety and methacryloyl group in the inhibitor-acrylamide polymers, and the effect of spacer between the inhibitor moiety and polymer main chain on the selective binding abilities of these inhibitor-acrylamide copolymers toward chymotrypsin was also evaluated.

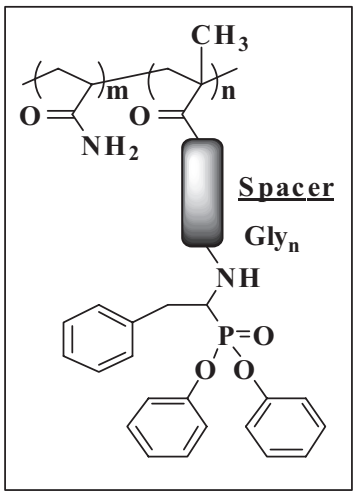

All prepared inhibitor-acrylamide polymers with different Gly oligomers were found to have upper critical solution temperature (UCST) of about 0℃ in 30% ethanol aqueous solution (data not shown). This phase separation system could be applied to easily separate chymotrypsin from other components. The inhibitory activities of the inhibitor-acrylamide polymers with different Gly oligomers toward chymotrypsin were evaluated. The result indicated that the Gly-Gly-Gly was the best spacer for the separation of chymotrypsin using the inhibitor-acrylamide copolymer system. Furthermore, a method of recovery of chymotrypsin which bound to the inhibitor-acrylamide copolymers have been also investigated. We will discuss the application of our separation system for serine proteases.

References

1. Oleksyszyn, J. and Powers, J.C., (1994) *Method in Enzymology,* **244**
2. Ono, S., Umezaki, M., Nabari, H., Nakayama, R., Hasegawa, K., Sako, S., Fujii, T., Yamazaki, I., and Yoshimura, T., (2002) *Biosci. Biotechnol. Biochem.,* **66** (5), 1111-1115.
3. Umezaki, M., Fujii, T., Yoshimura, T., Yamazaki, I., and Ono, S., (2003) *Biosci. Biotechnol. Biochem.*, *67,* 2273-2276.

P023B

Isolation of Microorganisms that Preferentially Degrade Crystal and Amorphous Region of Biodegradable Polymers

Naoya Kitamura, Satoshi Osawa

Kanazawa Institute of Technology, Material Design Engineering

1. Introduction

The study of degradation of polymer is important to understanding their usability and recycling. The common methods of polymer degradation are biodegradation, pyrolysis, oxidative degradation, photo degradation, and catalytic degradation[1)-4)].In our study, we investigated that degradation behavior of biodegradable polymers by isolated microorganisms that preferentially degrade crystal and amorphous region of biodegradable polymers.

2. Materials and methods

2.1 Materials

Biodegradable polymers used in this study were poly (ε-caprolactone) (PCL; DAICEL CHEMICAL INDUSTRIES Co.,Ltd., Celgreen pH-7) and poly(butylene succinate･adipate) (PBSA; SHOWA HIGHPOLYMER Co.,Ltd., BIONOLLE GRADE 3001). PCL and PBSA these films were made by the hot-press method at 20MPa, 100℃ and 120℃. The films with different crystallinity were made by quench and slow cooling after their melt molding. For preparing highly crystalline films, PCL and PBSA were kept for 24 hours at the melting point followed by the slowly cooling.

2.2 Methods

Test samples of two different types of crystallinity buried in soil, and microorganisms which degraded each sample were screened. Afterward, the degradation examination by the isolated microorganism was carried out in YPD medium. Concentration of microorganism was adjusted to a concentration of 10^7 microorganisms per milliliter. The liquid cultures were incubated

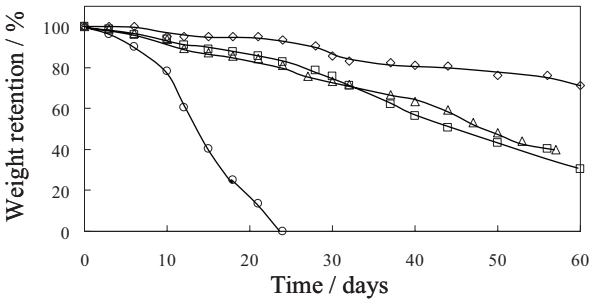

Figure 1. Weight retention of quenched PCL (○), slowly cooled PCL(△), quenched PBSA (□), slowly cooled PBSA(◇) in soil

for one month at 30℃. Afterward, each sample was analyzed by X-ray diffraction (XRD) and differential scanning calorimetry (DSC).

3. Results and discussion

Figure 1 shows weight retention of PCL and PBSA with different crystallinity in the soil. Quenched PCL and PBSA degraded faster than those of cooled ones.

There were many types of microorganisms that have degradation ability of PCL and PBSA in the soil. Two types of fungus (F-1 and F-2) were isolated from the soil. F-1 and F-2 were assigned to *Mucor circinelloides* and *Penicillium citrinum* (see Figure 2).

Figure 3 and Figure 4 show degradation tests of PCL and PBSA which controlled crystallinity by these fungi. *P.citrinum* degraded quenched PCL and PBSA, but *M.circinelloides* did not degrade them. On the other side, *P. citrinum* did not degrade slowly cooled PCL and PBSA, but *M.circinelloides* degraded them.

The enzymes produced by F-1 and F-2 strains recognized crystal and amorphous region of PCL and PBSA.

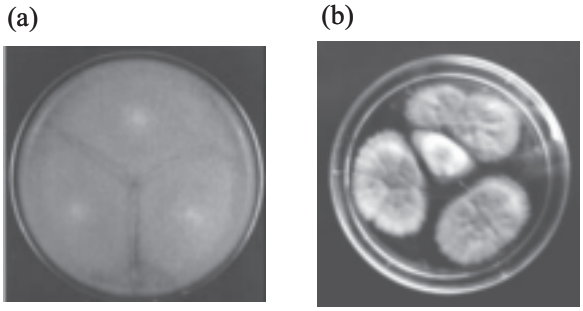

Figure 2. Photographs of F-1(a) and F-2(b) on PDA medium

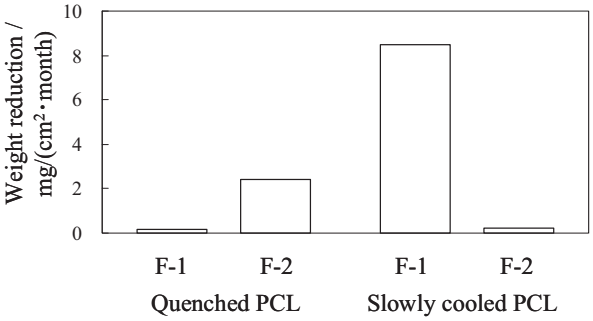

Figure3 Weight reduction of quenched and slowly cooled PCL biodegraded by F-1 and F-2

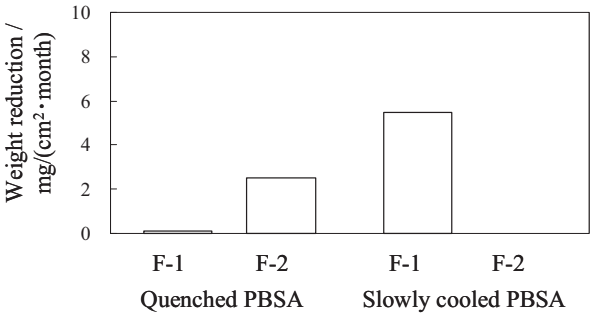

Figure 4 Weight reduction of quenched and slowly cooled PBSA biodegraded by F-1 and F-2

Reference(s)

1) Reich L, Stivala SS. Elements of Polymer Degradation. New York: McGraw Hill; 1971
2) Jellinek HHG. Degradation and Stabilization of Polymer. Smsterdam: Elsevier; 1983
3) Jellinek HHG. Degradation of Vinyl Polymer. New York: Academic Press; 1955
4) G.Sivalingam, Giridnar Madras. Polymer Degradation and Stability 80 (2003) 11-16

P024C

Gelation Behavior and Aggregate Morphology of Cholesterol Derivatives

Rie Yamazaki*, Mizuki Kondo, Masato Shimomura, and Noritaka Kimura

Department of BioEngineering, Nagaoka University of Technology

Nowadays, low-molecular-weight-gelators have been of interest not only for their gelation ability, but also for their aggregate morphology formed in the gels.

Twin-head type cholesterol derivatives as "gelators", including two cholesteryl moieties, an alkylene spacer (carbon number, n = 2-12), and two amide groups, were synthesized and their gelation behavior for organic fluids was studied. Furthermore, the aggregate morphology in the gel was investigated by POM and SEM.

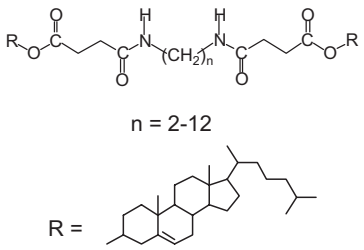

Figure 1 Illustration of "gelators".

The gelators were insoluble in some alcohol, but soluble and gelatinized benzene, toluene, nitrobenzene, DCM, and THF. It is noteworthy that the odd-numbered gelators does not give gels for THF, whereas the even-numbered gelatinizes one. For benzene, the gelation temperatures (T_{gel}s) depended on the carbon numbers of the alkylene spacer and showed an odd-even effect. The POM studies showed that the even-numbered gelators form three-dimensional networks with micro fibrils in benzene, while the odd-numbered gel specimens with benzene displayed a spherulitic texture.

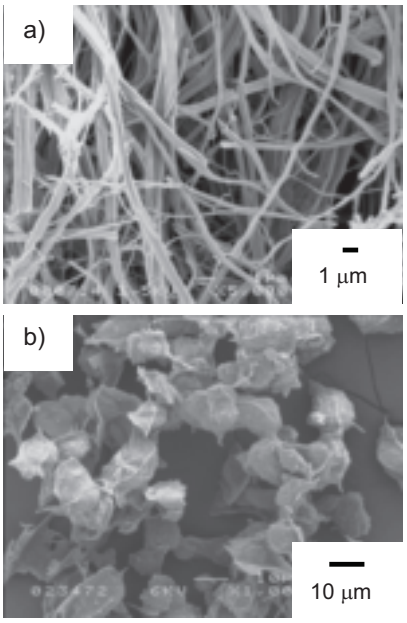

Figure 2 SEM images of freeze-dried specimens of 3wt% benzene gel samples. a) n = 6, b) n = 7.

Figure 2 shows typical SEM images of freeze-dried specimens of 3wt% gelator / benzene gel samples. In **Figure 2a**, in the case of n = 6, it is observed that a number of fibrous bundles are gathered up some fibrils each. The width of a fibrous bundle is approximately 2 μm. On the other hand, as shown in **Figure 2b**, the gelator (n = 7) did not show the fibrous morphology but rather featured particle-like aggregates with 10-20 μm diameter. The odd-even effects in the gelation behavior and the aggregate morphology may be induced by not only the hydrogen bonding arrangement between the amide groups, but also the spatial orientation of two cholesterol rings which differs between odd- and even-numbered gelators.

P025A

STRUCTURE AND SHRINKING KINETICS OF POLYMER HYDROGELS

Hiroshi Sasaki, Keita Tamura, Masamitsu Miya, Hiroki Takeshita*,
Katsuhiko Takenaka and Tomoo Shiomi

Dept. of Materials Sci. and Technol., Nagaoka Univ. of Technol.,
1603-1 Kamitomioka, Nagaoka, Niigata 940-2188, Japan
Tel: +81-258-47-9335, Fax: +81-258-47-9300 e-mail: takeshita@mst.nagaokaut.ac.jp

Introduction

Volume phase transition of polymer hydrogels have raised special interest due to the potentiality of the use for various applications such as a drug release system and an artifical muscle. However, for the application of volume phase transition as functional materials, it is necessary to overcome the remarkably slow shrinking kinetics and the low mechanical strength. In this study, poly(*N*-isopropyl acrylamide) (PNIPA) having a high shrinking rate was synthesized by the adding a kind of surfactants in the polymerization process. In addition, the relationship between the mechanical strength and the gelation condition was discussed from the viewpoint of the spacial heterogeneity, which is unavoidably induced in gelation.

Experimental

0-28 wt% of a surfactant, $HO(CH_2CH_2O)_{10}C_6H_4C_9H_{19}$, was dissolved to aqueous solutions of 9.3 wt% of NIPA and *N*,*N*'-methylene bisacrylamide (BIS) (NIPA/BIS = 1/0.03 w/w). Polymerization was carried out by adding potassium persulfate (KPS) an initiator under the existence of 20 μL of *N*,*N*,*N*',*N*'-tetramethyl-ethylenediamine (TMEDA) at 4 °C. The shrinking rate after a temperature jump from 24 °C to 40 °C was measured using cylindrical PNIPA gels with a diameter of 1 mm. The structure change in the shrinking process of the gels were observed by optical microscopy and a small-angle x-ray scattering technique (SAXS).

For the investigation of the formation of heterogeneity, poly(acrylamide) gels with various monomer concentrations and monomer/cross-linker ratio were used. The heterogeneity of the gels was estimated by a light scattering technique.

Results and discussion

Fig. 1 shows the shrinking rate of PNIPA gels with various concentration of the surfactant when temperature-jumped from 24 °C to 40 °C. PNIPA gels with more than 6 wt% of the surfactant shrunk within several minutes, while those without the surfactant needed about 200 hour to be completely shrunk state. This means that the addition of the surfactant accelerated the shrinking kinetics about a thousand times. SAXS measurements were performed to elucidate the origin of the fast shrinking kinetics. In the SAXS profiles of PNIPA gels showing the fast shrinking rate had a Porod's region in low q region (q is the magnitude of scattering vector), which is attributed to the surface structure of phase separation with submicron order. The exponent of the Porod's region was also plotted in Fig. 1. The gels with accelerated shrinking rate, showed a Porod's exponent about -4, which means comparatively smooth interface of phase separation. Consequently, the fast shrinking kinetics is considered to originate from the phase separation structure introduced by the addition of the surfactant.

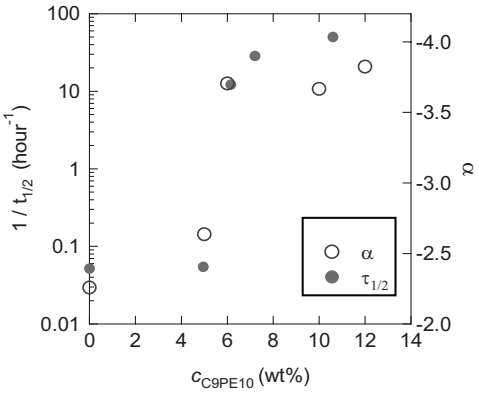

Fig .1. Surfactant concentration dependence of shrinking rate $1/t_{1/2}$ and the Porod's exponent *a*.

Relationship between gelation condition and the mechanical strength of the poly(acrylamide) gels will be discussed in the poster presentation.

P026B

PREPARATION AND CHARACTERIZATION OF INTERPENETRATING POLYMER NETWORKS (IPNS) WITH GOOD OPTICAL TRANSPARENCY AND FLEXIBILTY FOR SUBSTRATES OF FLEXIBLE DISPLAYS

Myeon-Cheon Choi and Chang-Sik Ha*

Department of Polymer Science and Engineering, Pusan National University, Busan 609-735, Korea

Polymer substrate with good transparency and flexibility has been attracted many scientists' attention to apply to flexible displays which are known as one of the prospective industries in the future. There are many polymer candidates including polyethylene terephthalate (PET), polyethylene naphthalate (PEN), polyesteretherketone (PEEK), polycarbonate (PC), polyether sulphone (PES), polyarylate (PAR), polycyclic olefin (PCO) as well as colorless polyimide. However there have not been so many reports on cross-linked polymers, especially interpenetrating polymer networks (IPNs) which are known to have a good thermal and mechanical properties as well as a good flexibility. On the other hand, polyacrylates are brittle and difficult to apply to the flexible substrates though they have many attractive optical properties including optical transparency.

In this work, we prepared IPNs of polyacrylate and polyurethane to use as a substrate of flexible displays and characterized their thermal, optical, and physical properties. We also report the electrical, optical, and structural properties of the ITO thin films deposited onto this transparent substrate.

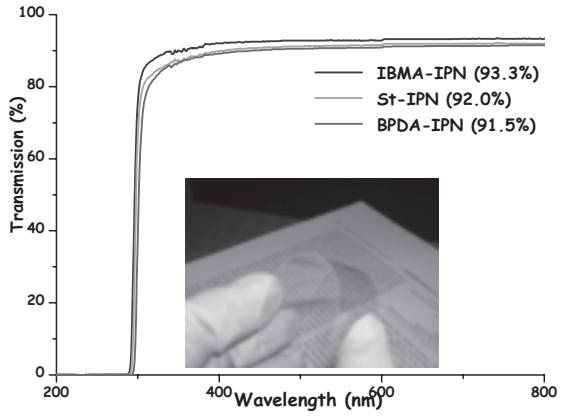

Figure 1. Optical transmission of the polymer films

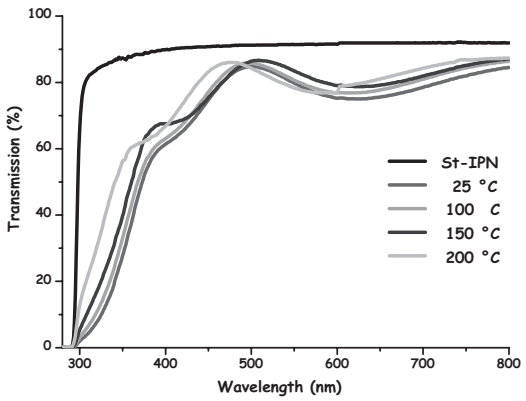

Figure 2. Optical properties of the ITO-grown films

Reference(s)

1. H.Lim, C. M. Bae, Y.K. Kim, C. H. Park, W. J. Cho, C. S. Ha, Preparation and characteration of ITO-coated colorless polyimide substrates, Syn. Met., 2003;135-136:49-50.

2. S.B. Pandit and V.M. Nadkarni, Sequential interconnected interpenetrating polymer networks of polyurethane and polystyrene. 1. Synthesis and chemical structure elucidation, Macromolecules, 1994, 27, 4583-4594.

P027C

COMPATIBILITY AND IONIC CONDUCTIVITY OF NITRILE RUBBER/IONIC LIQUID COMPOSITES

Edy Marwanta,[1,2] Tomonobu Mizumo,[3] and Hiroyuki Ohno[3]

[1]Venture Business Laboratory, [2]Center for Transdisciplinary Research, Niigata University, Ikarashi 2-8050, Nishi-ku, Niigata 950-2181, Japan
[3]Department of Biotechnology, Tokyo University of Agriculture and Technology, Naka-cho 2-24-16, Koganei-shi, Tokyo 184-8588, Japan

Polymer electrolytes with high ionic conductivity and good elasticity were prepared by mixing nitrile rubber (poly(acrylonitrile-co-butadiene) rubber; NBR) with ionic liquid, *N*-ethylimidazolium bis(trifluoromethane-sulfonyl)imide (EImTFSI). The NBR/EImTFSI composites were obtained as homogeneous and transparent films which showed single glass transition temperature (T_g) indicating good compatibility between NBR and EImTFSI. Raman spectroscopy suggested the interaction between nitrile group of NBR and $TFSI^-$ anion of the ionic liquid. Sample with ionic liquid content of 50 wt% showed an ionic conductivity of 1.2×10^{-5} S cm^{-1} at 30 °C. Addition of lithium salt to this NBR/EImTFSI composite further enhanced the ionic conductivity to about 10^{-4} S cm^{-1} without spoiling mechanical properties. DSC studies showed two T_gs for NBR/EImTFSI/LiTFSI composites indicating micro-phase separation into NBR-rich phase and ionic liquid-rich phase after addition of lithium salt. It is suggested that formation of micro-phase separation induced the improvement of ionic conductivity, in which ionic liquid-rich phase provides high ion mobility.

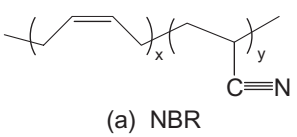

(a) NBR

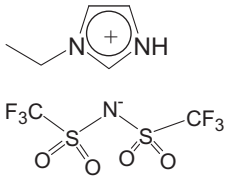

(b) EImTFSI

Fig. 1 Structures of NBR and EImTFSI

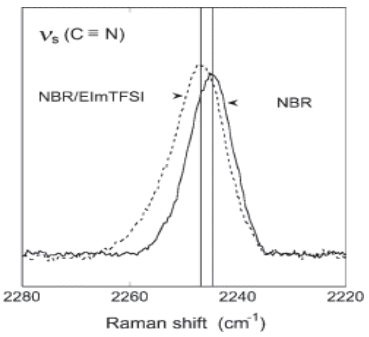

Fig. 2 Raman spectra of the C≡N bond stretching in NBR bulk and NBR/EImTFSI composite

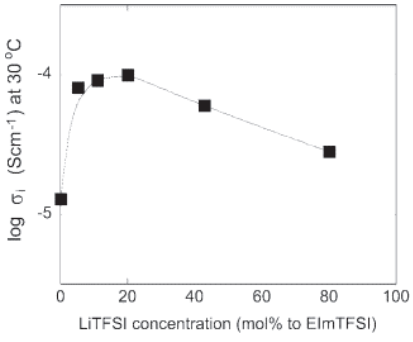

Fig. 3 The ionic conductivity of NBR/EImTFSI /LiTFSI composites as the function of LiTFSI concentration

P028A

REACTIVE MIXING OF EPOXIDIZED NATURAL RUBBER WITH POLY (L-LACTIDE)

Takayuki Saito, Warunee Klinklai, Niti Sripitakchai, Seiichi Kawahara*
Nagaoka University of Technology, Faculty of Engineering,
Department of Materials Science and Technology

Introduction

High resolution nuclear magnetic resonance (NMR) spectroscopy is recognized to be indispensable for characterization of primary structure of polymers. For example, conversion of polymer-reaction may be estimated from intensity ratio of signals in ^{1}H-NMR spectrum, in which an un-reacted polymer fraction is removed by extraction. In the previous work[1)], reaction of liquid deproteinized natural rubber having epoxy group (LEDPNR) with PLA was carried out, and chemical linkages between PLA and LEDPNR were confirmed through ^{13}C-NMR spectroscopy. To investigate the reaction quantitatively, it is necessary to estimate the conversion of LEDPNR through ^{1}H-NMR spectroscopy. However, the signals of PLA and LEDPNR in ^{1}H-NMR spectrum were overlapped with each other and some of the signals in aliphatic region of ^{1}H-NMR spectrum for epoxidized natural rubber were not assigned. Recently, we assigned the signals in the aliphatic region of ^{1}H-NMR spectrum for epoxidized natural rubber through 2D-NMR spectroscopy. Thus, in the present study, an attempt to estimate the conversion of the reaction between LEDPNR and PLA was carried out through ^{1}H-NMR spectroscopy.

Experiment

Natural rubber latex used in this study is commercial high ammonia natural rubber (HA-NR) latex. Deproteinization of HA-NR was carried out by incubation of the latex with 0.1w/w% urea for 1hr followed by centrifugation. The resulting deproteinized natural rubber (DPNR) latex, pre-cooled at 278 K, was subjected to epoxidation with peracetic acid for 3 hours at 278-283 K followed by depolymerization with 0.1w/w% ammonium persulfate for 10 hours at 333 K to prepare LEDPNR. Reaction of LEDPNR with PLA was carried out by heating at 473 K for 20 min. Un-reacted LEDPNR fraction was extracted with toluene. Characterization of samples was performed through ^{1}H-NMR spectroscopy.

Results and discussion

Figure 1 shows ^{1}H-NMR spectra for PLA, DPNR, LEDPNR and LEDPNR/PLA. In the spectrum for PLA, two signals appeared at 1.6 and 5.2 ppm, which were assigned to methyl and methine protons of PLA, respectively. As for DPNR, signals characteristic of methyl, methylene and un-saturated methine protons of *cis*-1,4-isoprene unit appeared at 1.68, 2.05 and 5.1 ppm, respectively. In contrast, for LEDPNR, new signals appeared at 1.28, 1.55, 2.15 and 2.7 ppm, which were assigned, according to previous our work[2)]. Thus, the epoxy group content of LEDPNR was estimated from intensity ratio of the signals at 2.7 and 5.1 ppm. The

estimated epoxy group content of LEDPNR was 43.1%. After reaction of LEDPNR with PLA, the signals of PLA were overlapped with that of LEDPNR. The conversion of LEDPNR may be estimated from intensity ratio of the signals of LEDPNR and PLA after extraction of un-reacted LEDPNR fraction, as in the following equation:

$$\text{Conv.}(\%) = \frac{I_{LEDPNR,after\ extraction}\ /I_{PLA}}{I_{LEDPNR,before\ extraction}\ /I_{PLA}} \cdots (1)$$

where I is intensity of the signals. Due to the overlapping of the signals, I_{LEDPNR} and I_{PLA} were estimated from the intensity ratio of the signals at around 1.5-1.7 and 2.1 ppm, as in the following equation:

$$I_{LEDPNR} = I_e + I_h = I_e + \frac{1 - X_{epoxy}}{X_{epoxy}} \times I_e$$

$$I_{PLA} = I_b = I_{b,c,h} - I_c - I_h$$

$$= I_{b,c,h} - \frac{3}{4} I_e - \frac{1 - X_{epoxy}}{X_{epoxy}} \times I_e$$

where X_{epoxy} is the epoxy group content of LEDPNR and subscripts represent the assignment of signals marked in Figure 1. Since the un-reacted LEDPNR fraction has to be removed before estimate the conversion, the molar ratio of LEDPNR to PLA was plotted against the extraction time to confirm the removal of the un-reacted LEDPNR fraction.

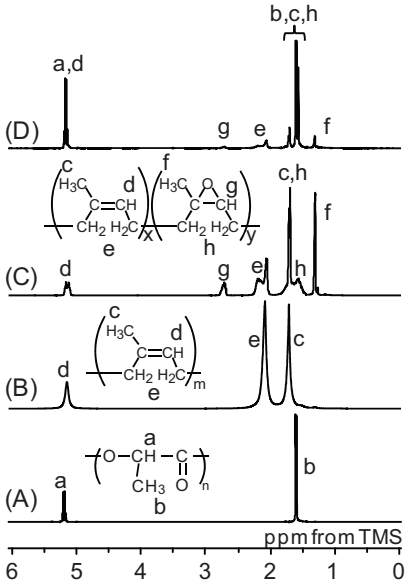

Figure 1 ^{1}H-NMR spectra for (A) PLA, (B) DPNR, (C) LEDPNR and (D) LEDPNR/PLA.

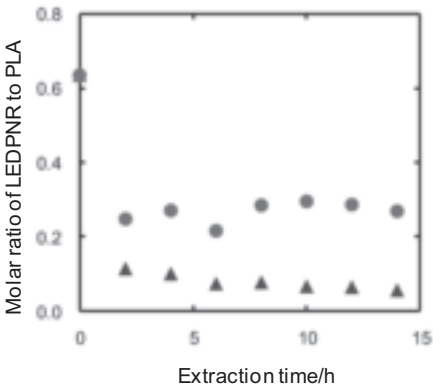

Figure 2 Molar ratio for (●) reacted LEDPNR/PLA and (▲) un-reacted LEDPNR/PLA *versus* extraction time.

Figure 2 shows extraction curves for reacted LEDPNR/PLA and un-reacted LEDPNR/PLA. For the reacted sample, the molar ratio of LEDPNR to PLA was about 0.3, reflecting the presence of grafted LEDPNR onto PLA. In contrast, for the un-reacted sample, the molar ratio decreased as the extraction time increased. Based on the extraction curve for the un-reacted sample, it is possible to think that the most of the un-reacted LEDPNR fraction is removed after extraction for 14 hours.Thus, the conversion of LEDPNR in the reaction was estimated from the molar ratio after extraction and that of before, according to equation (1). The estimated conversion of LEDPNR in LEDPNR/PLA was 38.1%. Consequently, quantitative analysis for the reaction between LEDPNR and PLA was achieved by ^{1}H-NMR spectroscopy.

References

1) Phan TN, Kawahara S, Yamamoto Y, Siripitakchai N. J Appl Polym Sci in press.

2) Saito T, Klinklai W, Kawahara S. Polymer 2007;48:750.

P029B

REMOVAL OF PROTEINS FROM NATURAL RUBBER WITH UREA AND ITS APPLICATION TO CONTINUOUS PROCESS

Yoshimasa Yamamoto, Warunee Klinklai, Takayuki Saito, Seiichi Kawahara*

Nagaoka University of Technology, Department of Materials and Science

1603-1, Kamitomioka-cho, Nagaoka, Niigata, JAPAN

1. introduction

Removal of proteins from natural rubber (NR) with urea through continuous process is conducted in order to prepare large amount of deproteinized natural rubber (DPNR). The proteins present at the surface of NR particle in the latex stage may bring about latex allergy and side reactions on chemical modification of NR. In the previous work,[1)] the removal of proteins present at the surface of the rubber particle as a dispersoid was mainly made in the latex stage by using proteolytic enzyme. After the enzymatic deproteinization, total nitrogen content of NR was reduced to less than 0.02 wt%, which was about 1/20 of that of the untreated NR.[2)] However, the enzymatic deproteinization must be carried out in a batch system because of long incubation time and strict temperature control. On the other hand, urea is known to change conformation of proteins through interactions.[3)] If the proteins are attached to the rubber particle with physical interaction but not chemical interaction, it may be possible to remove the proteins from NR in the latex stage after denaturation of the proteins with urea, rapidly and efficiently. In this study, the removal of proteins from NR latex with urea as denaturant in the presence of surfactant was investigated through batch process. Furthermore, the present method was applied to continuous process in order to prepare huge amount of deproteinized natural rubber (DPNR).

2. Experiment

NR latexes used in this study were commercial high ammonia NR (HANR) latex and fresh NR latex. In the batch process, the incubation of the latex was made with 0.1 wt% urea in the presence of 1 wt% sodium dodecyl sulfate (SDS, Kishida Co. Ltd., Japan) at 303 K. After centrifugation of the latex, the cream fraction was redispersed in 1 wt% SDS solution to make 30 wt% dry rubber content (DRC) latex and washed twice by centrifugation (fresh U-DPNR and U-DPNR). The NR latex was also deproteinized by incubation of the latex with 0.04 wt% proteolytic enzyme (Kao, KP-3939, Japan) in the presence of 1 wt% SDS for 12 h at 305 K followed by centrifugation. The cream fraction was redispersed in 1 wt% SDS solution to make 30 wt% DRC latex and was washed twice by centrifugation to prepare deproteinized NR (fresh E-DPNR and E-DPNR) latex. The rubber was recovered by centrifugation followed by coagulation with methanol and dried under reduced pressure at ambient temperature until a definite weight was achieved.

As a model plant for the continuous incubation, one end of a semicircular channel, which was 50.4 m in length and 150 mm in diameter, was lifted to a height of 4.8 m to spontaneously flow the latex. HANR latex containing 1.0 wt% of SDS and 0.1 wt% of urea was flowed from the lifted end of a semicircular channel, and was recovered at lower end of the channel. The recovered latex was centrifuged three times with batch type centrifugator to produce U-DPNR latex which was coagulated with methanol and dried under reduced pressure at ambient temperature.

Measurement of total nitrogen content of the rubbers was achieved by Kjeldahl method as described in RRIM Test.[4)]

3. Result and Discussion

A plot between total nitrogen content, which is proportional to the amount of proteins present in the rubber, *versus* time required for the deproteinization of HANR with urea at 303 K is shown in Figure 1. The total nitrogen content of HANR decreased suddenly from 0.380 wt% to 0.022 wt% after incubation for 10 min, which was similar to that prepared by incubation with proteolytic enzyme for 12 hours. Gradual decrease in the total nitrogen content of HANR was observed to 0.020 wt% after incubation for 1 hour. This indicates that almost all proteins are removed by incubation with urea within 10 min.

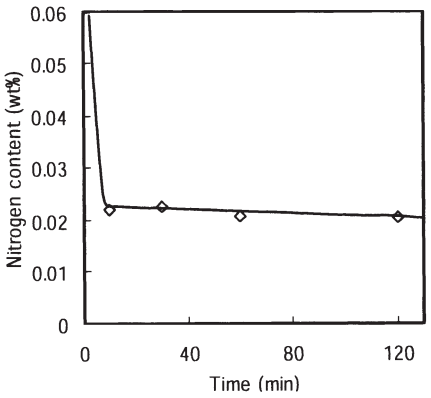

Figure 1. Total nitrogen content of DPNR at 303 K versus time for incubation

It is necessary to design a continuous process for the incubation of NR latex with urea in order to prepare huge amount of DPNR. In the continuous process, incubation of HANR latex may be performed by flowing the mixture of the latex and urea in the presence of SDS for 10 min through semicircular channel of 50.4 m in length and 150 mm in diameter. The most important thing in the continuous process is to take place efficient mixing for incubation of NR with urea. The total nitrogen content of HANR was reduced to 0.023 wt% after continuous incubation of NR with urea followed by batch centrifugation, which was quite similar to that prepared by batch incubation, as described above. This indicates that the flow of the mixture of HANR latex and urea through semicircular channel can bring about complete mixing for the incubation, which will apply to continuous process of deproteinization to prepare huge amount of DPNR, rapidly and efficiently.

References

1) Eng, A. H.; Tanaka, Y.; Gan, S. N. *J. Nat. Rubber Res.* 1992, 7, 152.
2) Eng, A. H.; Kawahara, S.; Tanaka, Y. *J. Nat. Rubber Res.* 1993, 8 , 109.
3) Creighton, T. E. Proteins; W. H. Freeman and Co.: New York, 1984; p. 514.
4) Rubber Research Institute of Malaysia. SMR Bulletin No. 17; (1973).

P030C

MOLECULAR WEIGHT OF GRAFTED POLYSTYRENE OF PS-g-DPNR COPOLYMER

Nanthaporn Pukkate and Seiichi Kawahara*

Department of Materials Science and Technology, Faculty of Engineering, Nagaoka University of Technology, Nagaoka, Niigata 940-2188, Japan

Tel.:81-258-47-9301; fax: 81-258-47-9300

**E-mail: kawahara@mst.nagaokaut.ac.jp*

Introduction Mechanism of graft-copolymerization of monomer onto natural rubber is very important for clarifying the effect of factors affecting conversion and grafting efficiency of the monomer. However, less information of the mechanism for the graft-copolymerization has been provided in the previous work. Thus, an attempt to propose the mechanism of the graft-copolymerization was carried out by determining molecular weight of grafted polystyrene linked with natural rubber, using ozonolysis-gel permeation chromatography technique. Effects of initiator and monomer concentration on the molecular weight of the grafted polystyrene were investigated.

Experimental Graft-copolymerizations of urea-deproteinized natural rubber (U-DPNR) latex was carried out with styrene as a monomer, using *tert*-butyl hydroperoxide with tetraethylenepentamine as an initiator under various conditions at 30ºC. The acetone/2-butanone solution was used in the ratio of 3:1 for extracting gross polymer in a Soxhlet apparatus to remove all homopolystyrene. The conversion and grafting efficiency of styrene was determined by gravimetric method. The ozonolysis-gel permeation chromatography technique was applied to characterize the graft copolymers.

Results and discussion Molecular weight of grafted polystyrene decreased with increasing initiator concentration, as a definite feed of styrene was fixed, as shown in Figure 1. On the other hand, molecular weight of grafted PS increased with increasing monomer concentration, as shown in Figure 2.

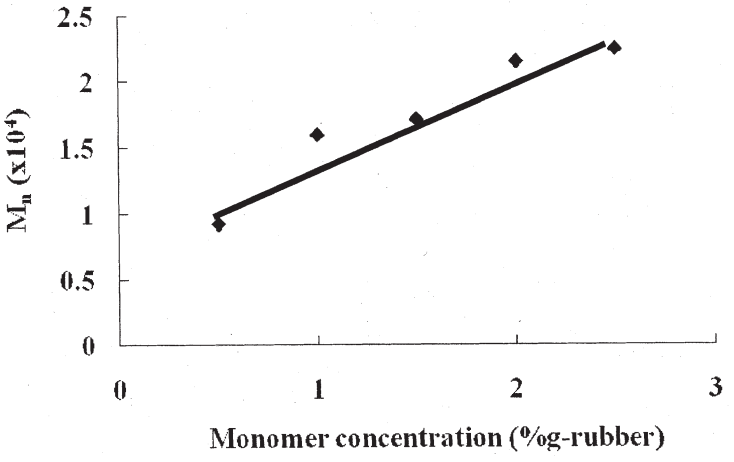

Figure 1 Initiator concentration dependence of molecular weight of grafted PS

This may be explained to be due to the ratio of monomer concentration and initiator concentration at the definite monomer concentration. The low conversion and low grafting efficiency at low monomer feed may be attributed to the deactivation of number of active site, as shown in Figure 3. In contrast, at high monomer feed, low conversion and low grafting efficiency may be explained to be due to chain transfer. Based on the results, the mechanism of the effects of initiator and monomer concentration on graft-copolymerization of styrene onto U-DPNR in latex stage can be proposed by measuring molecular weight of polystyrene linked natural rubber.

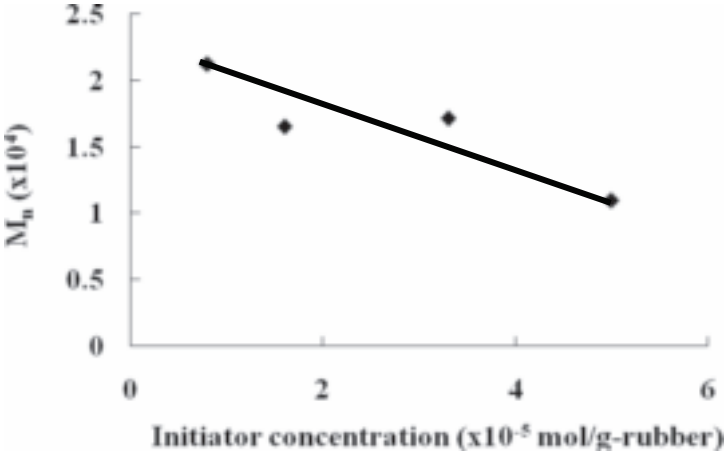

Figure 2 Monomer concentration dependence of molecular weight of grafted PS

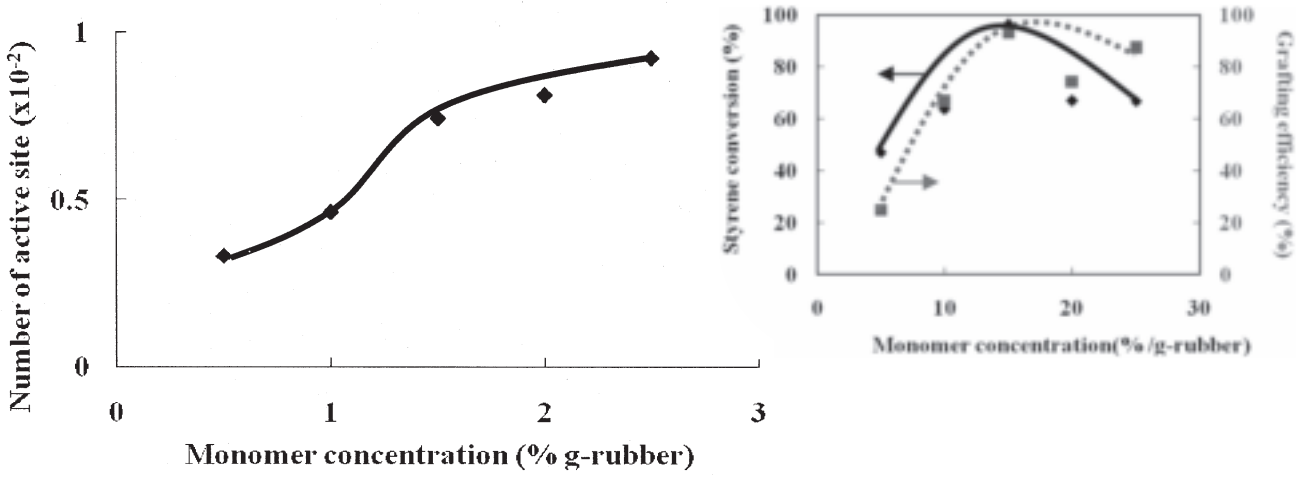

Figure 3 Monomer concentration dependence of number of active site

References

- Kawahara S, Kawazura T, Sawada T and Isono Y. *Polymer* **2003**;44(16):4527-4531.
- Fukushima Y, Kawahara S and Tanaka Y. *J Rubb Res* **1998**;1(3):154-166.
- Pukkate N, Kitai T, Yamamoto Y, Kawazura T, Sakdapipanich J and Kawahara S *Eur Polym J* **2007**, *article in press*.

P031A

PREPARATION AND CHARACTERIZATION OF POLY(STYRENE-*g*-NATURAL RUBBER) COPOLYMER

Patjaree Suksawad, Seiichi Kawahara*

Department of Materials Science and Technology, Faculty of Engineering, Nagaoka University of Technology, Nagaoka, Niigata 940-2188, Japan

Tel.:81-258-47-9301; fax: 81-258-47-9300

**E-mail: kawahara@mst.nagaokaut.ac.jp*

Introduction

Graft-copolymerization of vinyl monomer onto natural rubber is one of the important methods to improve properties of the rubber. It is required to achieve high conversion and high grafting efficiency of the monomer. In the last five decades, the conversion and grafting efficiency of the graft-copolymer was reported to be less than 60% for unpurified natural rubber, due to side reactions of proteins present in the rubber. Thus, in the previous work, we performed the graft-copolymerization of styrene on deproteinized natural rubber, which was prepared with proteolytic enzyme by long incubation at a suitable temperature of the enzymatic reaction. We proved more than 90% of both conversion and grafting efficiency attained for deproteinized natural rubber. However, problem still exist, that is, both a long incubation time necessary for the enzymatic deproteinization (i.e., more than 24 h), and remaining proteins, peptides, or amino acid sequence. Recently, we proposed novel method to remove the proteins from natural rubber with urea taking incubation-time about only 60 min. It was found that the nitrogen content of natural rubber was reduced to less than 0.02 w/w%. Therefore, urea-deproteinization may have more potential applications as a source to prepare organic materials. In the present work, to prove the advantage of U-DPNR, experiment was carried out by graft-copolymerization of U-DPNR latex with styrene monomer. The results obtained from graft-copolymerization of U-DPNR latex was compared with those from E-DPNR.

Experimental

Graft-copolymerization of E-DPNR and U-DPNR latices was carried out with styrene as a monomer, using *tert*-butyl hydroperoxide/tetraethylenepentamine as an initiator. U-DPNR or E-DPNR latex was charged with N_2 gas for 1 hr at 303K. The initiator of 3.3×10^{-5} mol/g-rubber and monomer were added to the latex, respectively. The reaction was carried out by stirring the latex at about 400 rpm for 2 hr at 303K. The gross polymer was extracted with acetone/2-butanone 3:1 mixture in a Soxhlet apparatus under nitrogen atmosphere. The obtained polymer from graft-copolymerization was subjected to analyze by FT-IR, ^{1}H-NMR, and

transmission electron microscope (TEM).

Results and discussion

Products after graft-copolymerization of styrene onto the rubber were characterized by gravimetric method, FT-IR and ^{1}H-NMR spectroscopies. The highest conversion and grafting efficiency of styrene for U-DPNR-*g*-PS was achieved at styrene feed of 1.5 mol/kg-rubber to be about 90 w/w% styrene conversion and 90 w/w% grafting efficiency, respectively, as shown in Figure 1 and 2. In addition, the nitrogen content of U-DPNR was about 0.02 w/w% as well as E-DPNR, as shown in Table1. Therefore, it could be suggested that the content of styrene units and conversion of styrene for U-DPNR-*g*-PS copolymer were dependent upon the feed of styrene. Theses were similar to the content of styrene units and conversion of styrene for E-DPNR-*g*-PS copolymer. Thus, it is possible to expect that the graft-copolymerization for U-DPNR may proceed in a similar way to E-DPNR. This may be explained to be due to the removal proteins from natural rubber.

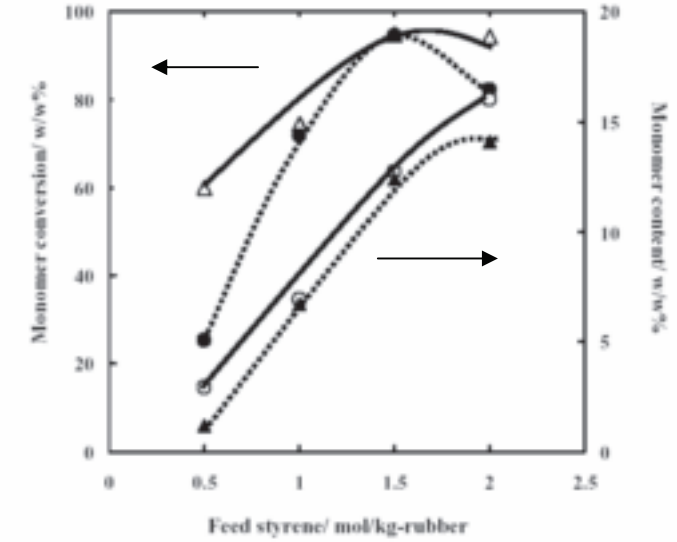

Figure 1 Content of styrene units and conversion of styrene for U-DPNR-*g*-PS and E-DPNR-*g*-PS copolymers; (△),conversion of styrene for U-DPNR-*g*-PS copolymer; (●), conversion of styrene for E-DPNR-*g*-PS copolymer; (○), content of styrene for U-DPNR-*g*-PS copolymer; (▲), content of styrene for E-DPNR-*g*-PS copolymer.

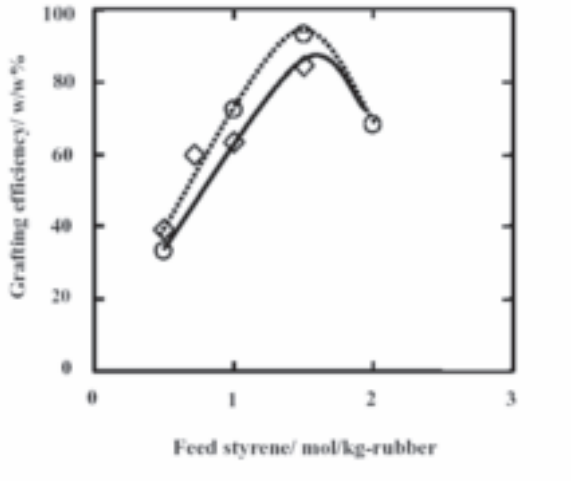

Figure 2 Value of grafting efficiency of styrene for U-DPNR-*g*-PS and E-DPNE-*g*-PS; ( ), U-DPNR-*g*-PS; (○), E-DPNR-*g*-PS copolymers.

Table 1 Total nitrogen content of HANR, E-DPNR, and U-DPNR.

Sample	Nitrogen content/ w/w%
HANR	0.35
E-DPNR	0.02
U-DPNR	0.02

References

1. Kawahara S, Kawazura T, Sawada T, Isono Y. Preparation and characterization of natural rubber dispersed in nano-matrix. Polymer 2003;44(16): 4527-4531.

P032B

HYDROGENATION OF NATURAL RUBBER HAVING EPOXY GROUP

Phan Trung Nghia, Agata Oshio, Yoshimasa Yamamoto, Seiichi Kawahara*

Faculty of Materials Science and Technology, Nagaoka University of Techbnology

Introduction

Natural Rubber is well known to be superior in tensile strength, tear strength and so forth. However, it is inferior in gas impermeability, weather resistance and ozone resistance. Thus, NR does not withstand for long term in use under severe environment. To improve the weather resistance, hydrogenation has been used to obtained ethylene propylene alternative copolymer, which is crystalline polymer. To accomplish not only the high weather resistance and ozone resistance but also the rubber elasticity, it is necessary to disorder the structure through chemical method. In this work, we take a notice of epoxidized natural rubber, since its epoxy group is randomly distributed into isoprene units and it may be converted to a hydroxyl group by hydrogenation [1]. After expoxidation of natural rubber followed by hydrogenation, the functional polymer which possesses the hydroxyl group may be prepared as shown in Fig. 1. In the present study, an attempt to prepare the functional polymer was performed.

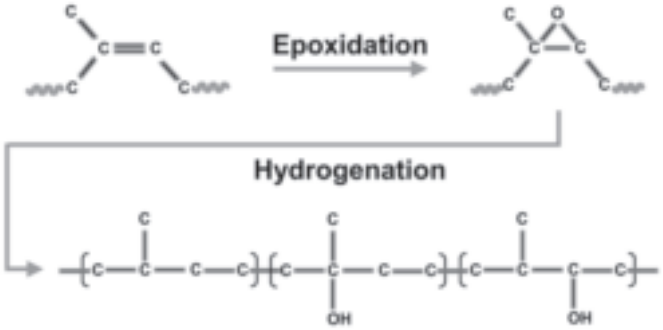

Fig.1. Possible reaction of hydrogenation of epoxidized natural rubber

Experimental

Natural rubber latex used in this work was commercial high ammonia latex. Deproteinization of natural rubber latex was made by incubation of the high ammonia latex with urea in the presence of surfactant. The cream fraction was re-dispersed in surfactant and it was washed twice by centrifugation to prepare deproteinized natural rubber (DPNR) latex [2]. Preparation of peracetic acid was performed by acetic anhydride with hydrogen peroxide at 40^{o}C for 90 min. The epoxidized natural rubber was prepared by epoxidation of deproteinized natural rubber with peracetic acid in latex stage. After completion the reaction, pH of the resulting latex was adjusted to 8 followed by coagulation with an excess amount of methanol, and the resulting rubber was dried under reduced pressure at 303K for a week. Before hydrogenation, the epoxidized natural rubber was dissolved in to *p*-xylene for a night. Hydrogenation of deproteinized natural rubber with epoxy group (HEDPNR) was carried out with presence of *p*-toluenesulfonyl hydrazide (PTSH) at 408K for 6 hours. The resulting polymer was purified by precipitation of toluene solution into excess methanol

and it was dried under reduced pressure at room temperature for a week. Characterization of the product was carried out by ^{1}H-NMR, ^{13}C-NMR, Correlation Spectroscopy (COSY) and Heteronuclear Chemical Shift Correlation (HETCOR) measurements.

Results and discussion

A typical ^{13}C-NMR spectrum for HEDPNR is shown in Fig. 2. Signals characteristic of methyl, methylene and methine appeared at 19.7, 24.5 and 32.8 ppm, respectively. Furthermore, small signals appeared at 75 and 75.5 ppm. To assign these signals, 2D NMR measurement was performed. Fig. 3 shows HETCOR spectra for HEDPNR. The ^{13}C signal at 75.5 ppm was correlated to the ^{1}H signal at 3.4 ppm. Thus, the signal at 75.5 ppm was assigned to the –CHOH. On the other hand, the 75 ppm was assigned to quaternary carbon which is connected with the hydroxyl group. The hydroxyl group content, $X_{hydroxyl}$ (mol %), was, thus, estimated from intensity ratio of the signals, as follows equation;

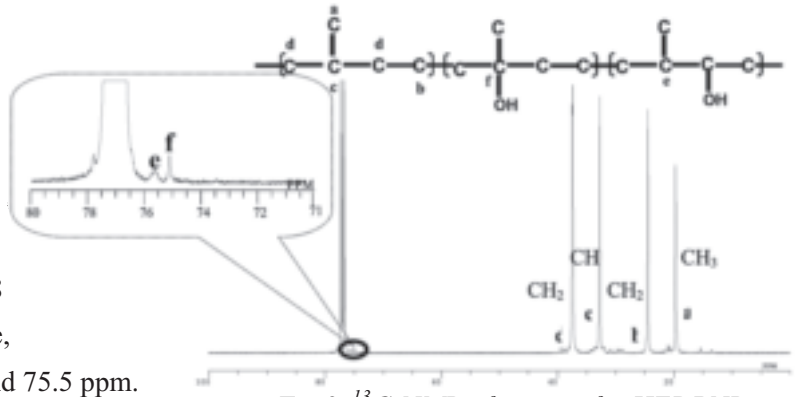

Fig.2. ^{13}C-NMR of spectra for HEDPNR

$$\text{The hydroxyl group content (mol \%)} = \frac{A_{75\text{-}76\text{ppm}}}{A_{33\text{ppm}} + A_{75\text{-}76\text{ppm}}} \times 100 = 4.6$$

The estimated hydroxyl group content was 4.6 %.

In conclusion, hydrogenation of EDPNR was carried out with 4 times molar quantity of PTSH 4 for 6 hours to prepare HEDPNR. The signals at 75 and 75.5 ppm were assigned to quaternary and tertiary carbons, respectively, linking up to hydroxyl group.

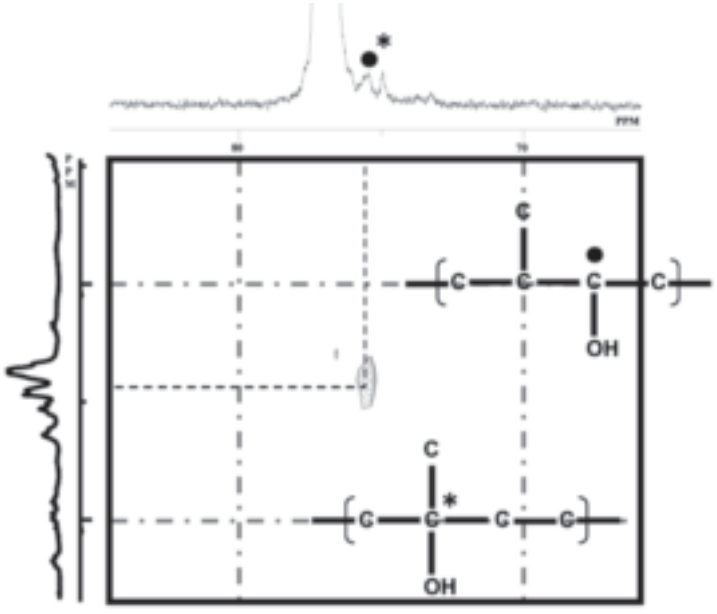

Fig.3. HETCOR spectra for HEDPNR

References:

[1] S. Bhattacharjee, A. Bhowmick, B. Nath Avasthi, Polymer, 1993, 34(24), 5168

[2] Klinklai, W., Kawahara, S., Mizumo, Isono, Y., Ohno, H., Euro. Polym. J., 2003, 39(8), 1707

P033C

Half width and relaxation time of latex state NMR spectroscopy for polyalkylacrylate

Jun Minowa, Seiichi Kawahara*, Yoshimasa Yamamoto

Department of chemistry, Faculty of Engineering,Nagaoka University of Technology

INTRODUCTION

Latex state NMR spectroscopy may have a potential to create a novel characterization method for polymeric materials; for instance, crosslinking junction of vulcanized rubbers and gels may be analyzed by the latex state NMR spectroscopy, even though they are heterogeneous systems[1]. To achieve high resolution latex state NMR spectroscopy, it is necessary to eliminate dipole-dipole interaction term in Hamiltonian for the nuclear magnetic resonance. This may be attained by motions of dispersoid and mobility of polymer present in the dispersoid. In the previous work, we reported a suitable condition for the high resolution latex state NMR spectroscopy; that is, 10 w/w % in dry rubber content, less than 1 w/w % in surfactant concentration and glass transition temperature, T_g + 70 K in experimental temperature[2]. In this work under the best condition, the effect of the mobility of polymer on the resolution was investigated for latex state NMR spectroscopy.

EXPERIMENT

The latex of poly *n*-butylacrylate, PBA, was prepared by emulsion polymerization of 0.56 mol/L *n*-butylacrylate, BA, with 1.5×10^{-3}mol/L anmmonium proxodisulfate aqueous solution in the presence of 0.2 w/w % SDS under nitrogen atmosphere at 333 K for 30 min. The total solid content of the resulting latex was adjusted to 10 w/w % with deionized water. ^{13}C-NMR spectra for the latex sample were obtained at 100.4 MHz with a JEOL EX-400 at 275–353K. Measurement of spin-spin relaxation time, T_2, were carried out under nitrogen atmosphere. The measurement was made with LOOP ranging from 10 to 5000 and 128 scans. The glass transition temperature, T_g, were measured by differential scanning calorimetry, DSC, with a SII DSC220.

RESULTS AND DISCUSSION

Fig.1 shows ^{13}C-NMR spectra for PBA latex at 295, 333, 353 K. The assignments of signals in the spectra were

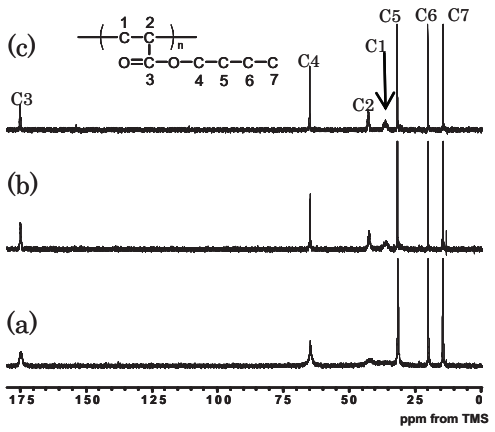

Fig.1 Latex state ^{13}C-NMR spectra for latex of PBA at (a)295 K, (b)333 K and (c)353 K.

performed as shown in Fig.1, according to Peter and co-workers[3]. The signals for the pendant group appeared clearly in the spectra, whereas the signals for main chain of PBA, i.e. C1 and C2 were small level comparable to the noise at 295 K. Fig.2 shows the half width of the signals at various temperatures. Half width decreased with increasing temperature; especially, for C1 and C2, remarkable temperature dependency was shown. Fig.3 shows T_2 for carbon atoms of PBA at various temperatures. T_2 of PBA latex was extensively dependent upon temperature; the higher the temperature, the longer was T_2.

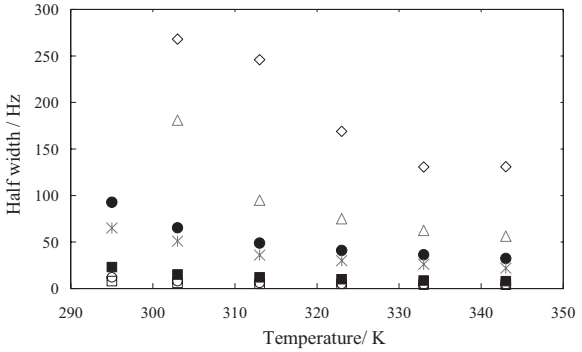

Fig.2 Dependence of half width on temperature for (□)C7, (○)C6, (■)C5, (＊)C4, (●)C3, (△)C2 and (◇)C1.

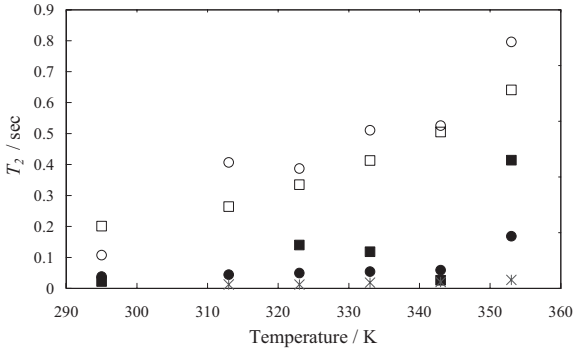

Fig. 3 Dependence of T_2 on temperature for (□)C7, (○)C6, (■)C5, (＊)C4 and (●)C3.

A plot of T_2 *versus* $(T\text{-}T_x)^{-1}$ is shown in Fig.4, where T is temperature , T_x is T_α, T_β and T_γ which are temperatures for α, β, and γ relaxation of PBA; that is T_α, T_β, and T_γ are 221 K, 154.5 K, 134 K[4]、[5], respectively. T_2's for C7, C6, C4 and C3 were superposed to a master curve, whereas T_2 for C5 was not. Consequently, the mobility of polymer expressed with T_α, T_β and T_γ was proved to associate to the resolution of NMR spectrum.

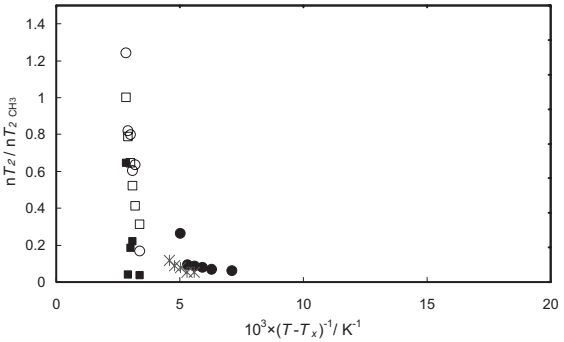

Fig.4 T_2 versus $(T\text{-}T_x)^{-1}$ for (□)C7, (○)C6, (■)C5, (＊)C4 and (●)C3.

Reference

1) Kawahara, S., Bushimata, S., Sugiyama, T., Hashimoto, C., Tanaka, T.:*Rubber chem.. Technol*., **72**, 844(1999)

2)Jinta Ukawa, Seiichi Kawahara, Junichiro Sakai, *J.Polym.Sci:PartB:Polym.Physics*, **45**, 1003 (2007)

3) Peter A.Lovell, Tahir H.S., Frank, H., *polymer communications*, **4**, 32, (1991)

4) J.Gomez R., J. M. Meseguet, D., M.Monleon, P., *J. Appl. Polym.Sci*., **70**, 1391 (1998).)

5) Hiroaki Kikuchi,et.al., *Macromoleculels.*, **26**, 7326 (1993)

P034A

Filler Network Characterization by Differential Dynamic Modulus in Reversing Double-Step Large Compression

Yukitoshi Yamaguchi, Kohji Suda, Shuji Fujii, and Yoshinobu Isono*

Nagaoka University of Technology, Nagaoka, Niigata 940-2188

INTRODUCTION

Rubber materials are made of two networks, one is a chemical network which consists of cross-linked polymer chains and the other is a physical network which consists of contacted filler network. Rubber materials are normally used in nonlinear condition, where the network, especially filler network, must change from the ones at equilibrium. Generally speaking, filler network is considered to be much weaker than chemical one. Thus, it is important to discuss the filler network density in a large deformation. For the evaluation of filler network, the possible method may be observation of differential dynamic modulus (DDM) measured by small oscillatory deformation superposed on large compressible and recovery. During the recovery process of deformation, the chemical network should immediately recover to the original states, but the filler network ruptured by deformation will take a long time to recover. Hence the change in DDM observed after cyclic compression and recovery may arise from the decrease in filler network density. The purpose of this work is to test the new idea for evaluation of filler network strength.

EXPERIMENT

The rubber used is styrene-butadiene copolymer (Nipol SBR1502, Zeon Co.). Three types of carbon-blacks (CB) are used in the compounds: N110, N330, and N660, (Mitsubishi Chemical Co.). Their average primary particle sizes are 19, 31, and 80nm, respectively. Other additives are Zinc Oxide (Shodo Chemical), Antioxidant (SANTOFLEX 6PPD, Flexsys), and Stearic Acid (Stearic Acid N for industrial use, Asahi-Denka). The compounds are cured for 30 minutes at 433K under a pressure of 400kg/cm^2. A specimen used in this work is a solid circular block (10mm in diameter and 2mm in thickness). Both ends of the specimen are fixed plates with cyanoacrylate glue. Simple compression can be given by their relative displacement along axis.

Before compression and recovery tests, the dynamic modulus, $G^*(\omega,0)$, where 0 denotes the zero static strain, were measured to record its original state. To obtain differential dynamic modulus, $G^*(\omega,\varepsilon_L;t)$ in large compression and recovery processes, a step-like compression λ_L (=0.9) started at time zero, and small compressive oscillations are imposed along axis. After 30 minutes elapsed, the compressive deformation was removed to zero strain, followed by intermittent measurements of DDM, $G^*(\omega,\varepsilon_L;t)$. Strain amplitude of the small oscillations was 0.005 corresponds to the linear viscoelasticity. All measurements are made at 293K.

RESULT & DISCUSSION

Figure 1 a-d show the results in compression and recovery experiments for unfilled and CB filled SBRs. In each panels, the broken lines denote the initial value of dynamic modulus measured before imposition of compressive strain. For unfilled SBRs (Fig.1a), G' shows subtle increase from the initial one in compressive deformation. After the recovery of deformation G' recovers to the initial value. Thus, chain conformation of the chemical network completely recovers to the original state by eliminating the deformation. For CB filled SBRs, (Fig.1 b-d), the increase in G' is observed in compression deformation process which is similar to that for unfilled SBR. After the elimination of compressive deformation, however, G' show initial drop followed by recovery to the original state. The drop becomes larger with decrease in the primary particle size of CB. The results for all the samples are summarized in Figure 2 where the difference between the values in the recovery process and the initial states, $G'_{//}(\omega,\varepsilon;t)-G'_{//}(\omega,0)$, are taken in ordinate. Complete recovery in $G'_{//}(\omega,\varepsilon;t)-G'_{//}(\omega,0)$ for unfilled SBR means no chemical network scission. Therefore, the difference in $G'_{//}(\omega,\varepsilon;t)-G'_{//}(\omega,0)$ between unfilled and filled SBRs comes from the rupture of the filler network. The drop in $G'_{//}(\omega,\varepsilon;t)-G'_{//}(\omega,0)$ becomes larger with decrease in the primary particle size of CB. This means that filler network strength depends on primary particle size of CB. In addition to the filler network strength, the slopes in the recovery curve also depend on the primary particle size of CB. This obviously means that the recovery rate depends on CB grade.

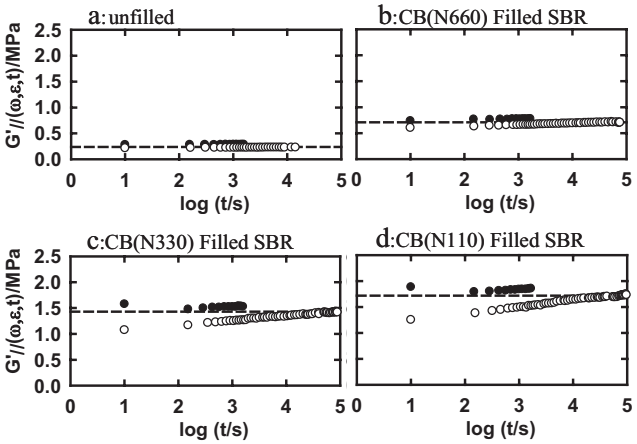

Figure 1 Differential dynamic modulus for the unfilld, cured Sample a and the CB filled, cured Samples b-d, respectively. Filled and open symbols denote the values at compressed and recovered states, respectively.

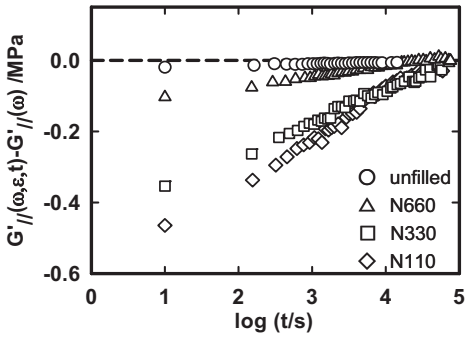

Figure 2 Differences in differential storage modulus between the values of recovered and initial states as a function of time after elimination of compression. Broken line shows the initial value.

We conclude that 1) differential dynamic modulus in compression and recovery process is useful for the characterization of filler network, 2) CB makes dense but weak filler network, and 3) the recovery rate of the filler network depend on the kind of CB, that is, the primary particle size of CB.

P035B

RECOVERY OF FILLER NETWORK RUPTURED IN CARBON BLACK FILLED RUBBER

Yoshitomo SATO, Shuji FUJII and Yoshinobu ISONO*

Department of Chemistry, Nagaoka University of Technology, Nagaoka, Niigata 940-2188, Japan

1. Introduction

Most of rubber products are made through processing of filled, uncured rubbers to which large deformation are given. Under the large deformation, rubber materials show significant nonlinear viscoelasticity, which originates with strain-induced chain anisotropy, chain entanglement, and rupture of filler networks. In order to manufacture high-quality and high-performance rubber products, therefore, it is very important to understand recovery process of uncured, filled rubbers. However, the recovery process of filled rubber is quite complicated because these effects occur simultaneously. In nonlinear viscoealsticity of rubber materials, the change in filler network structure will be main factor rather than other effects. Therefore, it is necessary to extract in formation on the change in filler network structure. We combine mechanical measurement with electrical resistivity measurement by using carbon black (CB) which is typical filler having high conductivity. The purpose of this work is to discuss recovery process of CB filled, uncured SBRs suffered large deformation .

2. Experimental

The rubber used was Styrene-Butadiene copolymer (SBR) (Nipol SBR-1502, ZEON Co., Japan). The CB used as a conductive filler was N330 (Mitsubishi Chemical Co., Japan) having average primary particle size of 31nm. CB component was 50 phr. Other additives were Antioxidant (Suntoflex 13), Stearic Acid, and Zinc Oxide. Their components were 1, 2, and 3 phr, respectively. Dynamic modulus and electrical resistance were measured simultaneously by using rotational rheometer RDA-3 (Rheometric Scientific) and digital electrometer R8340 (ADVANTEST), respectively. For the electrical contact, the sample specimen, molded into disk shape (19.8mm diameter and 2mm thickness), was fixed to directly steel plates. Figure 1 shows experimental procedure to detect recovery process after reversing double-step deformation. First, the step shear deformation (γ=0.1) was imposed at t=0. At t=10^3s, the shear deformation was removed and filler network recovery process was followed by measuring dynamic modulus and volume resistivity simultaneously. All measurements were carried out at 353K.

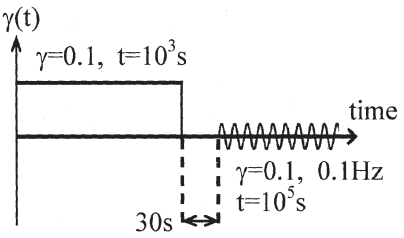

Figure 1 Schematic illustration of reversing double-step deformation procedure.

3. Result and Discussion

Figure 2 shows recovery curves of G' and ρ after the reversing double-step shear deformation. Broken lines denote the original values of G' and ρ. Immediately after the reversing double-step shear deformation, G' shows initial drop accompanying significant increase in ρ. Since the step shear deformation (γ=0.1) corresponds to nonlinear region, their deviations from original value indicate that CB filler network is ruptured. After the reversing double-step deformation, G' and ρ recover into their original states. In CB filled SBR system, the electric path is formed by CB-CB contacts only. Therefore, the recovery in ρ indicates the reformation of the filler network. As time elapses, they show excessive recovery over their original ones. Figure 3 shows time development in G' after temperature jump from 298K to 353K at quiescent state. G' increases with almost the same slope as that observed in the recovery process. Similar behavior was observed for ρ too. In temperature jump test, there should be no rupture in filler network by shear deformation. Thus, it may be suggested that the uncured, filled rubber always keeps on developing into new state at quiescent state. Such anomalous development in G' is also observed in physical aging of polymer glass. Glass-like polymer phase may exist in CB filled rubber as a filler gel. Thus, slow development in G' may be due to physical aging effect of filler gel around CB. Under this assumption, the physical aging curve obtained in Figure 3 is subtracted from recovery curve to extract pure recovery process (Figure 4). By subtracting the physical aging curves from G' and ρ, recovery times are estimated to be $t=1.27\times10^4$s and $t=1.25\times10^4$s, respectively. This agreement of the recovery times for ΔG' and Δρ indicates that the reformation of filler network plays main role for the recovery of uncured rubber materials.

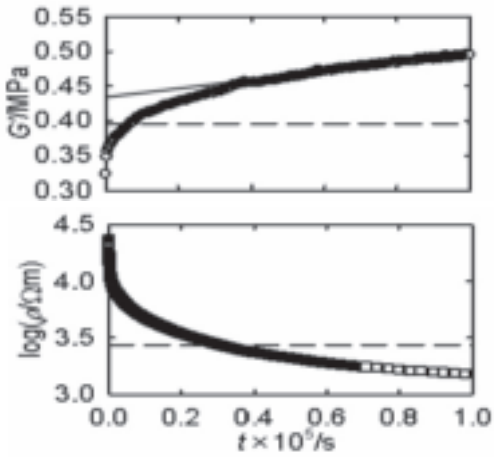

Figure 2 Recovery behavior of storage modulus and volume resistivity measured after reversing double-step deformation. The solid line is slope of increase in G' and the broken line denotes initial value in each panel.

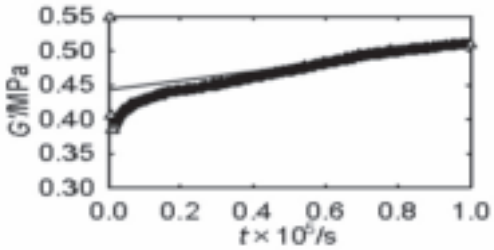

Figure 3 Recovery behavior of storage modulus measured no deformation. The solid line is slope of increase in G'

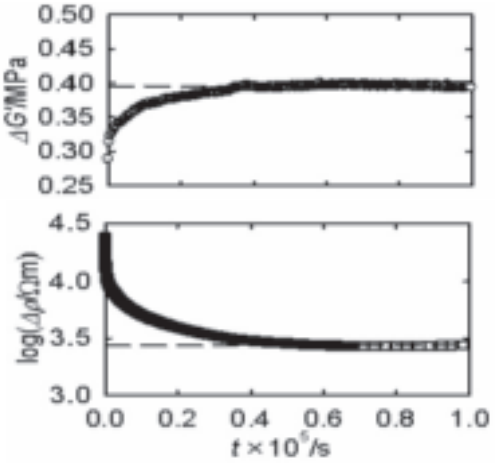

Figure 4 Recovery behavior of storage modulus and volume resistivity eliminated physical aging effect. The broken line denotes initial value in each panel.

P036C

Nonlinear Viscoelasticity and Change in Filler Network of Filled Rubber

H. Kondo, Y. Satoh, S. Fujii, and Y. Isono

Nagaoka University of Technology, 1603-1 Nagaoka, Niigata 940-2188, Japan

1. Introduction

Rubber materials show remarkable nonlinear viscoelasticity. It is very important to understand nonlinear viscoelastic properties and relaxation mechanisms of filled rubbers in order to design and to manufacture high-quality and high-performance rubber products. However, viscoelasticity of filled rubbers are complicated due to many interactions, e.g. polymer-filler and filler-filler interactions in addition to polymer-polymer one. In order to distinguish these effects separately, we propose the complementary use of volume resistivity and differential dynamic modulus (DDM) measured by small oscillatory strains superimposed on a large strain in addition to relaxation modulus measurement. Rubber is a non-conductive material. Carbon black (CB) has high conductivity. Thus, its separating these effects could be possible by measuring the volume resisitivity, DDM, simultaneously during the stress relaxation. The purpose of this work is to discuss nonlinear viscoelastic properties of carbon black filled, uncured SBRs from the viewpoints of change in various networks by simultaneous measurements of relaxation modulus, DDM, and volume resistivity with the use of SBRs having no filler and carbon black fillers of wide range of concentration.

2. Experiments

The samples used was uncured, CB filled styrene-butadiene rubber (Nipol SBR-1502, Zeon Corporation). Details on compound formulation are shown in table 1. The sample specimen was fixed to steel plates by fusion to keep the electrical contact (20 mm in diameter and 3mm in thickness). Electric resistance was measured by R8340A (ADVANTEST). Stress relaxation and differential dynamic modulus (DDM) was measured by biaxial rheometer (BAR) made by ourselves. Static shear strains ranged from 0.001 to 1 were applied to axial rotational direction. The frequency and the strain amplitude of the small oscillations were 0.2Hz and 0.003, respectively. All measurements were performed at 313K.

Table 1 Sample formulation (unit in phr)

sample No.	CB00	CB20	CB35	CB50	CB65	CB80	CB95
SBR(1502)	100	100	100	100	100	100	100
CB(N330)		20	35	50	65	80	95
Anti Oxidant	1	1	1	1	1	1	1
Stearic Acid	2	2	2	2	2	2	2
ZnO	3	3	3	3	3	3	3

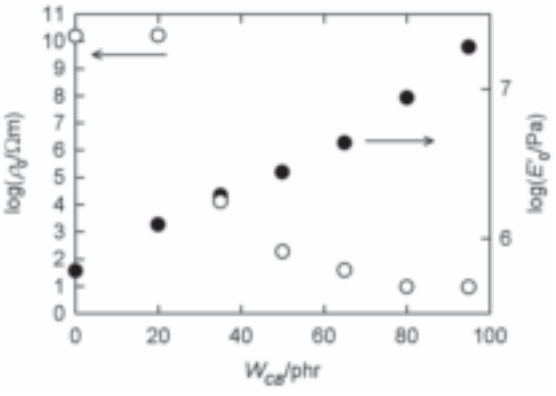

Figure 1. CB content dependence of volume resistivity (open symbol) and storage modulus (filled symbol).

3. Result and Discussion

Figure 1 shows CB content dependence of E'_0 and ρ_0. As CB content is increased from 20phr to 35phr, ρ_0 drastically decreases by around 6 orders of magnitude. This data indicates percolation threshold for filler network formation dynamic modulus exists between 20 and 35phr. Figure 2 shows typical results of time dependence of $E'(\omega,\gamma,t)$ and $\rho(\gamma,t)$ observed simultaneously with relaxation modulus at several shear strains for CB(50phr) filled SBR. Here the filler network is already formed at 50phr of CB content. In the panels for $E'(\omega,\gamma,t)$ and $\rho(\gamma,t)$, broken lines denote the initial value before shearing. In relaxation modulus, linear or quasi-linear behavior is observed at small strains. But nonlinear behavior is clearly observed at large strains. $\rho(\gamma,t)$ did not change at small strains where linear or quasi-linear behaviors in $G(\gamma,t)$ were found, but increase with increase in shear strains corresponding to the nonlinear behavior. Similar behaviors were observed for $E'(\omega,\gamma,t)$, although the change from the initial value were not so large. Deviations from initial value observed in nonlinear region will be due to rupture of the filler network. Thus, small decrease in $E'(\omega,r,t)$ from initial value will be due to the rupture of the filler network. In the figure 3, the deviations from initial value in $\rho(\gamma,t=5)$ and $E'(\gamma,t=5)$ obtained for various CB contents are collected as a function of shear strains. In unfilled or low filled samples (CB00, CB20), change in $\rho(\gamma,t=5)$ is not found with increase in shear strain, while the strain dependence of the deviation is observed for high CB loaded samples (CB35-CB95). Especially, large increase in $\rho(\gamma,t=5)$ was observed near the percolation threshold. Differential dynamic modulus also shows similar behavior. In high CB filled samples, the amount of deviation is decreased, despite of large the shear strain.

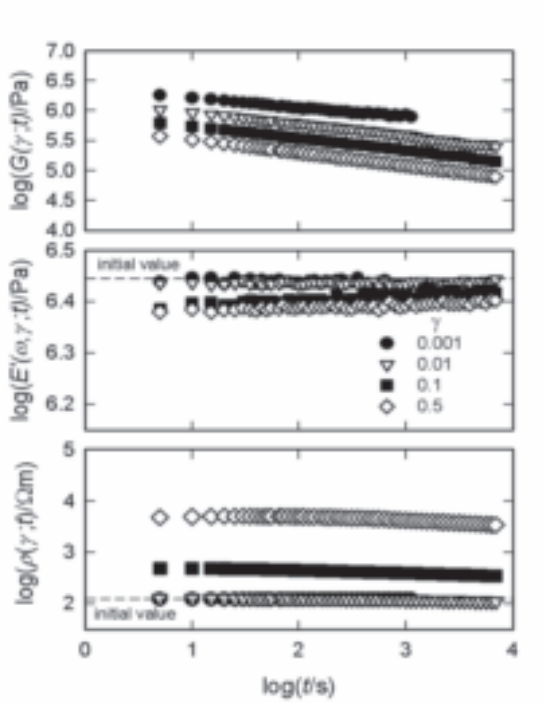

Figure 2. Relaxation modulus G, differential dynamic modulus E' and volume resistivity ρ for CB(50phr) filled SBR.

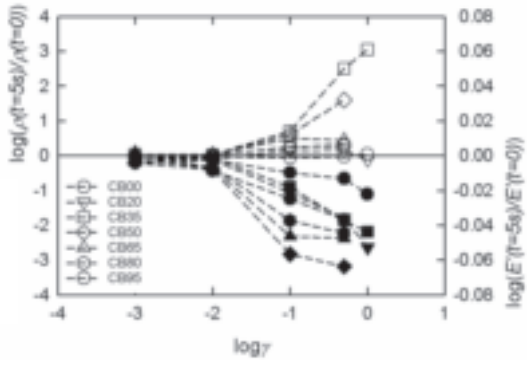

Figure 3. Increment in volume resistivity (open symbols) and decrement in E'(filled symbols) vs. shear strain.

This means that it is hard to rupture the filler network in high CB loaded samples. We found that i t is possible to observe the change in the filler network structure by simultaneous measurements of DDM a nd volume resistivity during the stress relaxation.

P037A

Viscoelastic Properties of Spatially Confined Multilamellar Vesicles

S. Fujii* and Y. Isono

Department of Chemistry, Nagaoka University of Technology,

Nagaoka, Niigata, 940-2188, Japan

Multilamellar vesicle (MLV) phase is obtained by shearing the lamellar phase. Detailed investigations by combining scattering experiments with rheometry yielded an "orientation diagram" on the development of the MLV structure [1]. Interestingly the orientation diagram suggested that the MLV radius is a decreasing function of the shear rate, while this process consists of a shear-thickening and shear-thinning regime. In addition, the orientation diagram is effectively modified by the sample thickness. Thus, the sample thickness seems to be a significant parameter for the dynamics of MLVs. In this study, we focus on the viscoelasticity of MLVs with the development of MLV radius as a function of the sample thickness as well as the shear force.

Non-ionic surfactant, tri-ethylene glycol mono-decylether($C_{10}E_3$) purchased from Nikko chemicals Co.,Ltd., was dissolved into deutrium oxide, D_2O, with a weight fraction of 40%. MLV was prepared by following previous report [2]. Microscopy under shear was performed by using a plate-plate shear cell. MLV radius was estimated from the intensity profile of the 2D-FFT images. Viscoelastic functions were measured using Bohlin CVO-120 rheometer with a plate-plate shear cell.

Figure 1 shows the gap size dependence of R_{MLV}. At the large gap sizes, R_{MLV} is independent of D, while the MLVs start to grow when D is reduced smaller than a threshold gap size, Dc. In figure 1, our results were by re-plotted as a function of the inverse of shear stress. MLV radius, R_{MLV}, is expressed as follows.

$$R_{MLV} \propto \sigma_{eff} / \eta\dot{\gamma} \qquad (1)$$

Where σ_{eff} is an effective surface tension and defined by bending modulus K and compression modulus B of bilayer membranes, $\sigma_{eff} = (KB)^{1/2}$ [3]. The evolution of R_{MLV} with $1/\eta\dot{\gamma}$ at high shear rates and large gap sizes ($>Dc$) shows a master curve which passes through the origin, while the data corresponding to the small gap sizes ($<Dc$) get off the master curve. The slope, $\sigma_{eff} = (KB)^{1/2}$, was $2.1 \pm 0.15 \times 10^{-4}$ (Nm^{-1}). The same parameter, $(KB)^{1/2}$, can be extracted from a Caille parameter estimated from the structural

factor of SAXS and SANS data. Our estimated value is quite similar to that obtained for the other surfactant systems. This result shows that the MLV structure at small gap size is affected by a confinement effect.

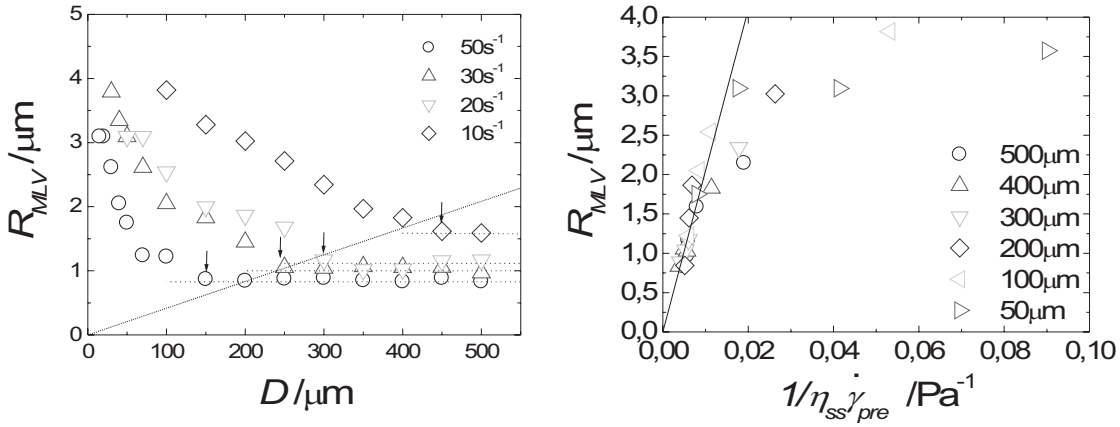

Figure 1: (a) R_{MLV} as a function of gap size, D, and (b) R_{MLV} as a function of the inverse of the shear stress, $1/\eta\dot{\gamma}$.

References

[1] O. Diat, D. Roux and F. Nallet, J. Phys. II (France) **3** (1993), 1427.
[2] F. Nettesheim, J. Zipfel, U. Olsson, F. Renth, P. Lindner and W. Richtering, Langmuir **19** (2003), 3603.
[3] P.-G. de Gennes, J. Prost, The Physics of Liquid Crystals (Clarendon Press, Oxford, 1993).

P038B

STRUCTURAL ANALYSIS OF MICROBIAL POLY(ε-LYSINE)/POLY(ACRYLIC ACID) BLEND BY USING SOLID-STATE NMR

Shiro Maeda*[1], Yasuhiro Fujiwara[1], Chizuru Sasaki[2], and Ko-Ki Kunimoto[3]

[1]*Division of Applied Chemistry and Biotechnology, Graduate School of Engineering, University of Fukui,* [2]*Department of Life System, Institute of Technology and Science, The University of Tokushima,* and [3]*Division of Applied Science, Graduate School of Natural Science and Technology, Kanazawa University*

Poly(ε-L-lysine) (ε-PL) is a product of a variant of *Streptomyces alubulus*, having amide linkage between ε-amino and α-carboxyl group. ε-PL is water-soluble and biodegradable, in addition to exhibiting antibacterial activities. We had reported molecular structure analysis of ε-PL and its derivatives in solid for the first time[1,2]. Figure 1 shows molecular structure of ε-PL. The blend films of ε-PL and poly(acrylic acid) (PAA) were made: ε-PL and PAA were separately dissolved in methanol. ε-PL and PAA solutions were mixed to make white precipitate. It was centrifuged and dried in vacuo at room temperature. Three kinds of blend films were made which have different compositions of ε-PL to PAA of 1/3, 1/1, and 3/1 in weight ratio.

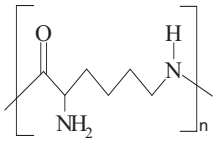

Figure1. poly(ε-L-lysine).

The molecular structure was studied by using FT-IR and high-resolution solid-state ^{13}C and ^{15}N NMR. ^{13}C NMR spectra of ε-PL, ε-PL/PAA blend films, and PAA are shown in Figure 2. ^{13}C and ^{15}N NMR measurements imply that ε-PL and PAA make poly-ionic complex and the conformation of ε-PL changes through complex formation.

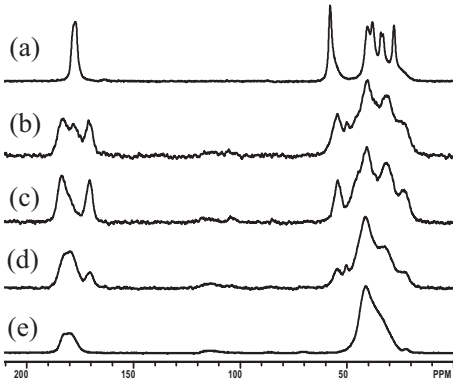

Figure2. ^{13}C CP/MAS NMR spectra of (a) ε-PL, (b) ε-PL/PAA (3/1), (c) ε -PL/PAA (1/1), (d) ε-PL/PAA (1/3) and (e) PAA.

References

1) S.Maeda, K.Kunimoto, C.Sasaki, A.Kuwae, K.Hanai, *J. Mol. Struct*., 655,149-267(2005)

2) S.Maeda, T.Mori, C.Sasaki, K.Kunimoto, A.Kuwae, K.Hanai, *Polym. Bull*., **53**,259-267(2005)

P039C

CHARACTERIZATION OF MICROBIAL POLY (ε-L-LYSINE) / CARBOXY METHYL CELLULOSE BLENDS BY IR AND SOLID STATE ^{13}C AND ^{15}N NMR SPECTROSCOPIES

Shiro Maeda*[1], Kumiko Kato[1], Chizuru Sasaki[2], and Ko-Ki Kunimoto[3]

[1]*Division of Applied Chemistry and Biotechnology, Graduate School of Engineering, University of Fukui,* [2]*Department of Life System, Institute of Technology and Science, The University of Tokushima,* and [3]*Division of Applied Science, Graduate School of Natural Science and Technology, Kanazawa University*

Poly(ε-L-lysine) (ε-PL) is a product of a variant of *Streptomyces alubulus*, having amide linkage between ε-amino and α-carboxyl group. ε-PL is water-soluble and biodegradable, in addition to exhibiting antibacterial activities. We had reported molecular structure analysis of ε-PL and its derivatives in solid for the first time[1,2]. Carboxymethyl cellulose (CMC) is also a biodegradable polymer made from natural cellulose. Figure 1 shows molecular structure of both homopolymers. The blend films of ε-PL and CMC were made: ε-PL and CMC were separately dissolved in water. ε-PL and CMC aqueous solutions were mixed and casted on a Teflon dish and dried at room temperature to make a film, then dried in vacuo. Three kinds of blend films were made which have different compositions of ε-PL to CMC of 1/2, 1/1, and 2/1 in each monomer units. These blend films were soft and transparent.

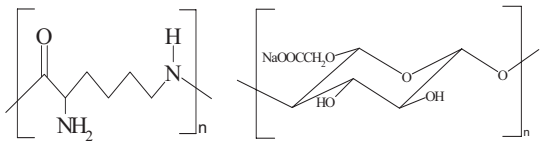

(a) (b)

Figure1. Chemical structure of (a) poly (ε-L-lysine) and (b) carboxy methyl cellulose, respectively

The molecular structure and the phase structure of the blend films were studied by using FT-IR and high-resolution solid-state ^{13}C and ^{15}N NMR spectroscopies. T1ρH measurements showed that ε-PL and CMC are miscible between a few nm and a few tens nm. Solid-state ^{15}N NMR spectrum of ε-PL/CMC blend film of 2/1 is shown in Figure 2. There appeared a new peak at 90 ppm assigned to α-NH_2. The formation mechanism of the complex is under investigation.

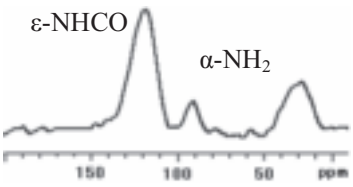

Figure2. ^{15}N CP/MAS NMR spectrum of a blend film of ε-PL/CMC=2/1

References

1) S.Maeda, K.Kunimoto, C.Sasaki, A.Kuwae, K.Hanai, *J. Mol. Struct.*, 655,149-267(2005)

2) S.Maeda, T.Mori, C.Sasaki, K.Kunimoto, A.Kuwae, K.Hanai, *Polym. Bull.*, **53**,259-267(2005)

P040A

IN SITU ANALYSIS *USING* FT-IR SPECTROSCOPY FOR POLYMERS-OZONE REACTION

Makoto Arisawa, Wingky Kurniawan and Takaomi Kobayashi*

Department of Chemistry, Nagaoka University of Technology,1603-1 Kamitomioka, Nagaoka, JAPAN 940-2188

Introduction

It is known that polymer treatment using ozone (O_3) is one of effective method due to the ability to improve chemical properties of polymer surface. Because O_3 decomposes into molecular oxygen and atomic oxygen, the formation of active radical introduces such hydrophilic functional group on hydrophobic polymer. In the present work, Polystyrene (PS), Polyethylene (PE), Polyethylene, Poly 4-Methylstyrene (P4MS) and Poly (α- Methylstyrene) (PαMS) were used to study O_3 effect on polymer surface. We focused O_3 treatment to different chemical structure of polymers.

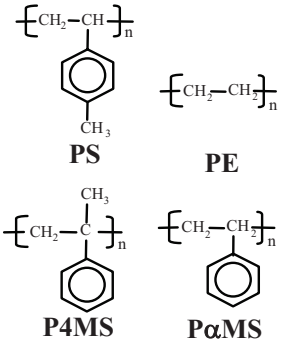

Scheme 1 Chemical structures of polymers

Experiments

O_3 gas was generated by aeration of pure O_2 gas using four silence discharge ozonizers to which the gas was controlled with the flow rate at 200ml/min. The polymer surface treated by gaseous O_3 (～3000ppm) was analyzed mainly by using *in-situ* FT-IR spectroscopy. FT-IR data containing information of the chemical structure were collected every 15minutes. In order to know the effect of temperature reaction, each spectrum also was measured at 0, 25, 50, and 70 ºC.

Results and discussion

The results of FT-IR measurement showed that O_3 oxidized all of polymers (PE, PS, P4MS and PαMS. In cases of PE, a new absorption of C=O band at 1719cm^{-1} was observed in the IR spectra (Fig.1(a)). The band on PE appeared more slowly with depending on the reaction temperature. However, the band appearance implied that for PS, O_3 directly and quickly oxidized polymer as shown in (b).

The presence of methyl group in aromatic ring (P4MS) had almost similar tendency with PS, while PαMS revealed relatively low oxidation as well as PE. Figure 2 indicates appearance of the C=O band at O_3 exposure time. Within about 15min the C=O band formed was saturated at 70 ºC. Apparently, the C=O band in PS was much highly formed relative to that in PαMS and PE. This meant that the methyl group on the polymer main chain inter fered the ozonation to PαMS. These indicated that increasing temperature was more effective to improve ozone treatment to these polymers. As results, the thermal

O_3-polymer treatment demonstrated as an effective method to modify polymers having phenyl group.

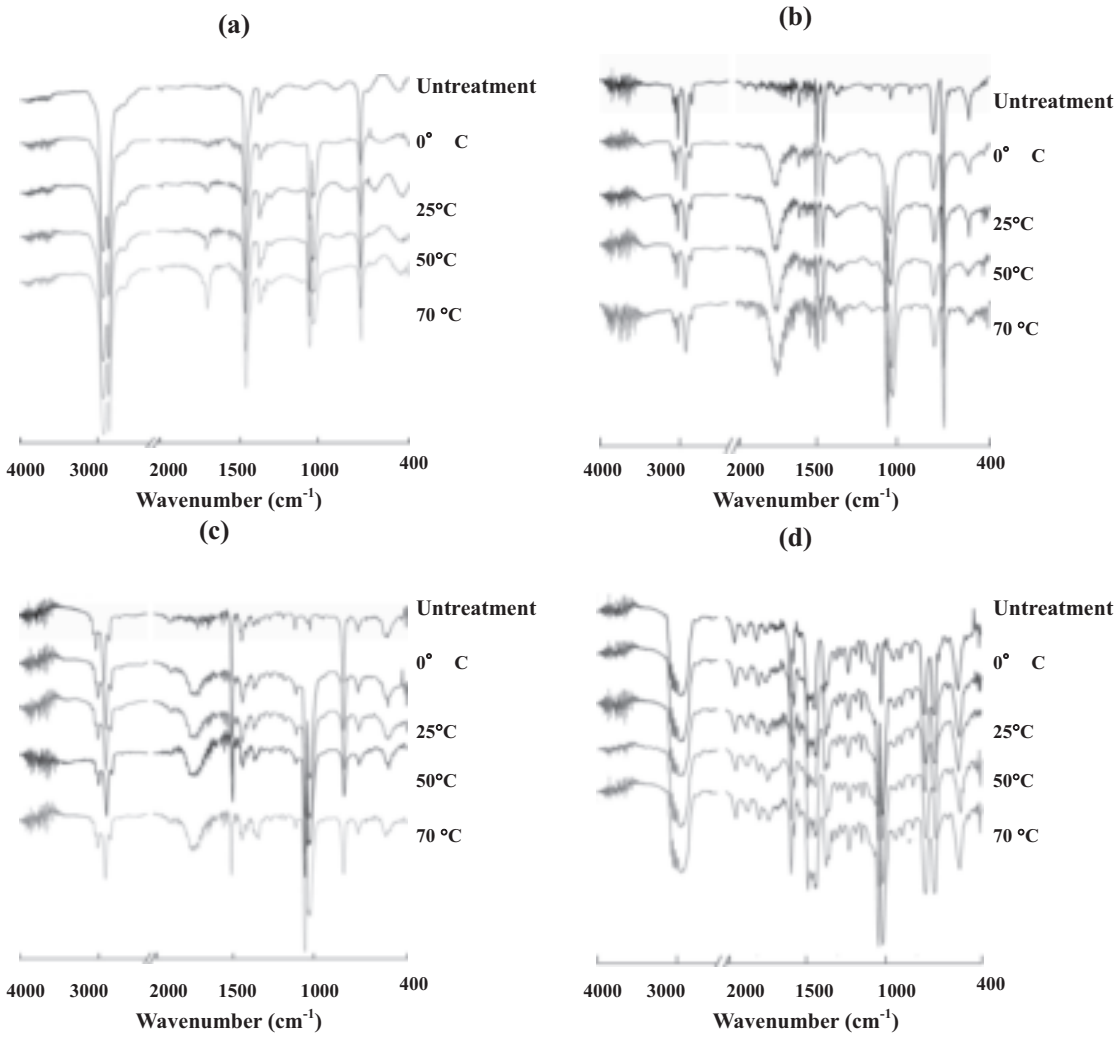

Figure 1 FT-IR spectra of PE (a), PS (b), P4MS(c), and PαMS(d) measured at different temperatures.

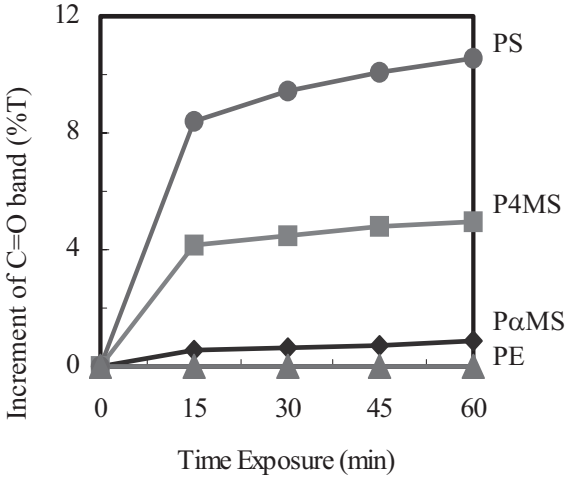

Figure 2 Time dependence of the increment of C=O band in obtained the treated polymers

P041B

PHASE STRUCTURE AND CRYSTALLIZATION OF ETHYLENE-ISOPRENE BLOCK COPOLYMERS AND THEIR BLENDS WITH CORRESPONDING HOMOPOLYMERS

Yuanji GAO, Yusuke TAKATA, Hiroki TAKESHITA,

Katsuhiko TAKENAKA, Tomoo SHIOMI*

Department of Materials Science and Technology, Nagaoka University of Technology
1603-1Kamitomioka, Nagaoka. Niigata 940-2188, Japan
tel: +81-258-47-9304, fax: +81-258-47-9300, e-mail: shiomi@vos.nagaokaut.ac.jp

INTRODUCTION

Phase structure and crystallization of block copolymers have attracted increasing interest in recent years. Structure development in semicrystalline block copolymers is controlled by two competing mechanisms: microphase separation and crystallization, i.e., the structure of block copolymers depends on the segregation strength in the melt and the kinetics in crystallization.

In this article, the structure formation in isothermal crystallization from melts studied mainly using a small-angle X-ray scattering(SAXS) will be presented for polyethylene-polyisoprene (EI) diblock copolymers and the blends (EI/PIp and EI/PE). Kinetic characteristic of crystallization will also be discussed.

EXPERIMENTS

Two kinds of EI diblocks copolymers, with different molecular weight, were prepared by catalytic hydrogenation of the precursor poly(1,4-butadiene)-block-poly(1,4-isoprene) with narrow-distribution of molecular weight. The characteristics of the samples are listed in Table 1 together with the corresponding homopolymers used for the preparation of the blend samples. Isothermal crystallization behavior was observed by DSC and SAXS after quenching from 140℃ to the desired crystallization temperatures. The SAXS measurements were performed at BL-10C, Photon Factory.

Table1 Characteristics of the samples

Sample	Mn		Composition	
	PIp	PE	PIp	PE
HEI	65.3	64.8	50	50
LEI	17.0	15.1	53	47
HPIp	12.0	-	100	
LPIp	25.0	-	100	
HPE		6.0		100
LPE		12.0		100

RESULTS AND DISCUSSION

Figure 1 and 2 depict the SAXS profiles of HEI and LEI crystallized at the indicated temperatures. For HEI, preexisted microphase-separated morphologies in the melt was kept at high and low crystallization temperature (T_c>=94℃ and T_c<60℃), while disrupted at intermediate T_c (60℃=<T_c<94℃). For lower T_c, the crystallization behavior is attributed to the competition between the crystallization and chain diffusion rates, while, for the higher T_c, the confined crystallization can be understood by the T_c dependence of crystallinity due to the ethyl branch of polyethylene (hydrogenated poly(butadiene)). On the other hand, although LEI does not have microphase separation structure in the melt (Figure 2) and the crystallization occurs from disordered state, lamellar structure is observed in the SAXS profiles of crystallized LEI. The lamellar structure is well-ordered and the domain size estimated form the peak position is almost independent of the crystallization temperature. This is because the structure is formed by the crystal lamellae of the PE, amorphous PE and PIp being left between PE, and the domain size is limited by the molecular size, not kinetics.

For the blends, peaks due to microphase separation can not be observed for HEI/PE and HEI/PIp in the molten state. For LEI/PE and LEI/PIp, crystallization also occurs from disordered molten state and well-ordered lamellar structure can be observed in crystallization just like the neat LEI. For the blend of HEI with PE and PIp, unlike LEI/PIp and LEI/PE, only a very broad peak from PE crystal lamellae was observed and no peak originating in the microphase separation was noted. This is because HEI and HEI blends have microphase separation structure enough large for PE blocks to crystallize without putting PIp between the crystal lamellae.

Crystallization behavior, in particular crystallization kinetics, was also investigated by DSC. Amrami exponents evaluated from DSC results for all samples were almost the same as those for PE homopolymers even when the crystallization was confined within the microdomain, which was quite different form the result in crystallization from a *frozen* microphase-separated melt reported previously.

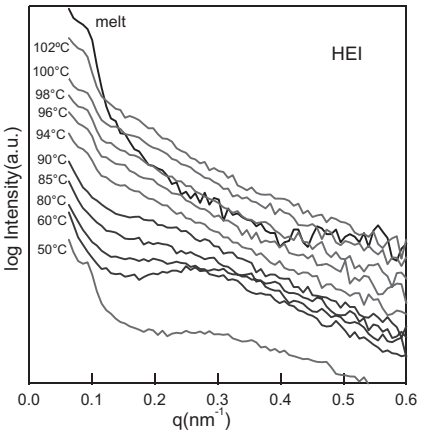

Figure1 SAXS profiles of HEI in the molten and crystalline states. The temperature in the molten state is 140℃. The samples were crystallized isothermally at the indicated temperatures after being rapidly quenched from 140℃

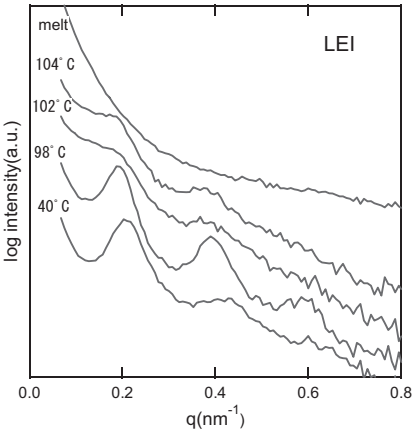

Figure2 SAXS profiles of LEI in the molten and crystalline states. The temperature in the molten state is 140℃. The samples were crystallized isothermally at the indicated temperatures after being rapidly quenched from 140℃

REFERENCES

1. I. W. Hamley, *The Physics of Block Copolymers,* Oxford, New York, 1998, Chapter 5.
2. T. Shiomi, H. Takeshita, H. Kawaguchi, N. Nagai, K. Takenaka, M. Miya, *Macromolecules*, **35**, 8056 (2002)
3. Takeshita, H.; Ishii, N.; Araki, C.; Shiomi, T.; *J. Poly. Scie. Part B,* **42**,4199(2004)
4. YenYu Huang.; Ching Hua Yang.; Willisa Liou.; *Macromolecules,* **37**, 486（2004）.
5. D. J. Quiram, R. A. Register, G. R. Marchand, A. J. Ryan, *Macromolecules*, **30**, 8338 (1997)

P042C

SYNTHESIS OF STYRENE-DIENE BLOCK COPOLYMER CONTAINING CHIRAL AMIDE FUNCTION AND ITS APPLICATION TO OPTICAL RESOLUTION OF AMINO ACIDS.

Shino Nakagawa, Masamitsu Miya, Hiroki Takeshita, Katsuhiko Takenaka*, and Tomoo Shiomi

Department of Material Science and Technology, Nagaoka University of Technology

Introduction

In the previous paper from our laboratory, we have reported the conventional free-radical[1)] and anionic[2)] polymerization behaviors of *N,N*-diethyl-2-methylene-3-buteneamide. In the anionic polymerization, polymerization condition such as kind of counter cation or polymerization temperature strongly affects the stability of propagating species. In this paper, we would like to discuss the synthesis of block copolymers containing chiral amide function using anionic initiator and the application of the resulting block copolymer to the optical resolution of amino acids.

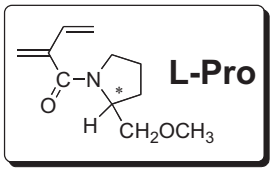

Experimental

Diene monomers containing chiral amide group(**L-Pro**) was prepared from L-proline according to the following scheme[1)]. Anionic polymerization was carried out in a sealed glass tube under high vacuum

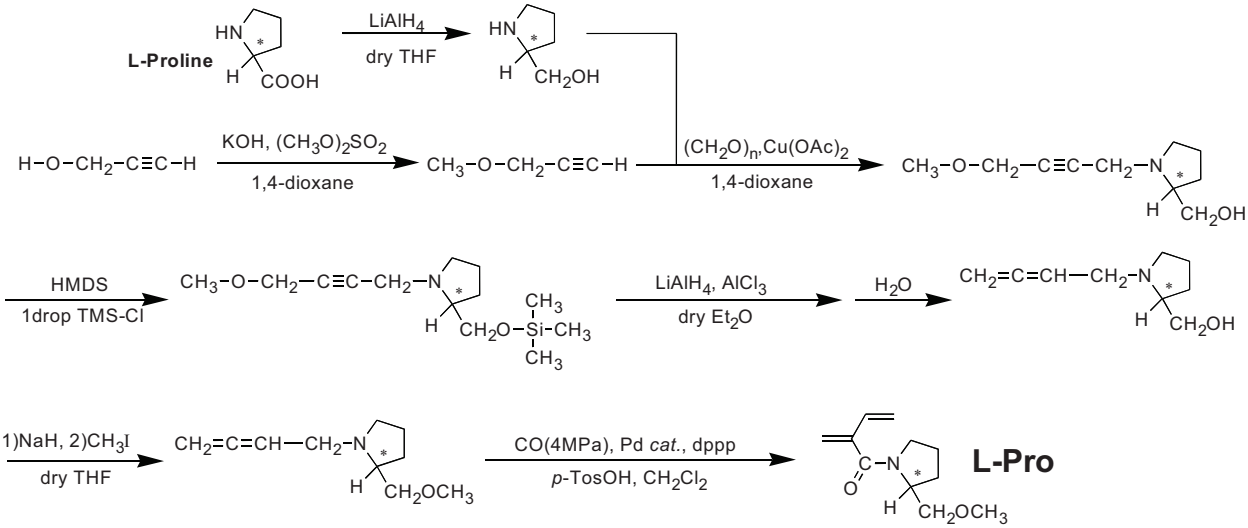

condition. Characterization of the block copolymer with styrene was carried out by NMR and SEC. Optical resolution of amino acid was performed by column chromatography using glass beads coated with block copolymer as a stationary phase and distilled water being mobile phase.

Results and Discussion

Anionic block copolymerization was carried out in THF. Styrene was allowed to react with sec-BuLi at -78 °C for 10 min. Then THF solution of LiCl ([LiCl]/[*sec*-BuLi] = 4) was introduced followed by L-Pro at 0 °C. The second stage polymerization was carried out at 0 °C for 60 h. Fig.1 shows the SEC chromatograms of poly(styrene-*b*-L-Pro) and its precursor polystyrene. As can be seen, small shoulder peak whose molecular weight was twice as large as that of the main peak was observed in the block copolymer. This indicates that some coupling or nucleophilic attack of carbanion to the amide group occurred at the rate stage of the polymerization. However, the main peak shifted to the higher molecular weight side, indicating block copolymerization underwent almost successively. Fig.2 shows ^{1}H-NMR spectrum of the block copolymer. The composition of the copolymer was determined by comparing the relative integrated intensity of aromatic protons and the methoxy protons around 4 ppm which can be assigned to poly(L-Pro) segment. Table 1 summarizes the result of block copolymerization. It is obvious that the molecular weight and copolymer composition were well-controlled.

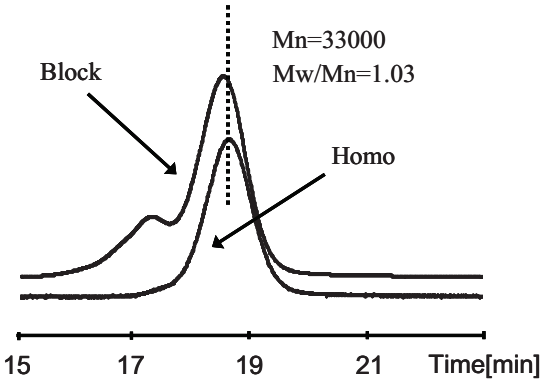

Fig.1 SEC chromatograms of poly(Styrene-*b*-L-Pro) and polystyrene

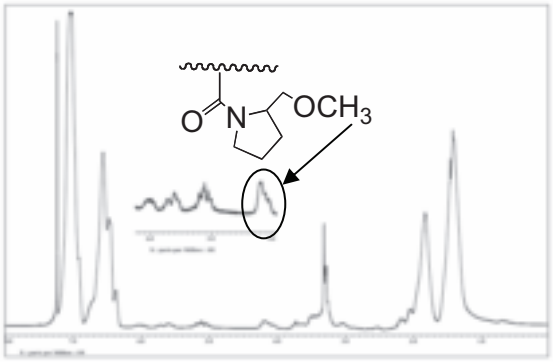

Fig.2 ^{1}H-NMR spectrum of the block copolymer

Table 1 Block Copolymerization of L-Pro with styrene

Molecular Weight						Mw/Mn	
calc			Obs				
St	L-Pro	Block	St	L-Pro	Block	PSt	Block
30100	5400	35500	29800	(3350)	33150	1.05	1.08
				(NMR)	31400	<-SEC	

Surface modification of glass beads with block copolymer was soaking the beads in the THF solution of the block copolymer. It was necessary to treat the glass beads with hexane solution of hexamethyldisilazane to make hydrophobic surface. Without this pretreatment, block copolymer was eluted out with amino acids in the chromatographic separation.

Reference

1) T. Yaegashi, S. Yodoya, M. Nakamura, H. Takeshita, K. Takenaka, T. Shiomi; *J. Polym.Sci. Part A: Polym.*,**42**, 999-1007 (2004)

2) Tsuchida *et al*. *Polymer Preprint, Japan*., **56**, 168 (2007)

P043A

Adhesive Bonding of Metal Nanowires

Takaaki Toriyama and Tsutomu Ishiwatari*

Department of Chemistry, Faculty of Textile Science and Technology, Shinshu University, 3-15-1 Tokida, Ueda, Nagano 386-8567, JAPAN

Self-assemblies of nano-particles have been extensively studied to draw meaningful arrays of nano-particles on a substrate[1, 2]. The next important subjects are how to fix the nano-particles to the substrate and how to keep the mutual contact among the meaningfully arranged nano-particles on the substrate. Piling the nano-particles up on a substrate can never be sufficient for the practical uses. On the other hand, bimetallic nano-wires could be expected as nano-diodes, nano-transistors or optical nano-tags. Adhesive bonding among nano-particles or nano-wires would then become a key technology especially in a future electric nano-circuit.

Here, we studied the adhesive bonding between metal nano-particles utilizing complex formation between metal salt and thiols. Yugang Sun, and Younan Xia[3] reported erosion-like substitution reaction of silver nano-wires with $HAuCl_4$. We tried to protect the surface of silver nano-wires from $HAuCl_4$ by binding dodecanethiol on the surface of silver nano-wires. After all, the protection did no work well. Instead, we observed an interesting phenomenon. The surface of the nano-wires was covered by a certain material containing many small particles. Some of them formed bridges between the separated nano-wires, and others formed solder-like joints between the contacted nano-wires. In order to fix the bridges or adhesive joint, the materials forming bridges or joints were reduced by adding a reducing agent or by heating. Metallization of the bridges and joints were confirmed. The interesting results might be applicable to a future nano-bonding method.

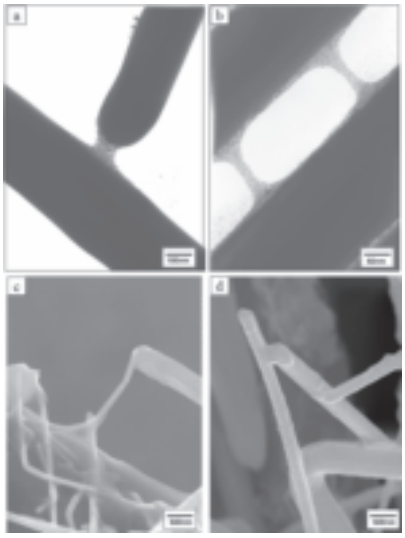

Fig.1 TEM and SEM images of bridges and joints formed between silver nanowires.

Reference(s)

1. Kanna Takagi and Tsutomu Ishiwatari, Chem. Lett., 2002, 990.
2. Ryo Takahashi and Tsutomu Ishiwatari, Chem. Commun., 2004, 1406.
3. Yugang Sun and Younan Xia, J. Am. Chem. Soc., **126**, 3892 (2004)

P044B

Construction of Cyclodextrin-Carbon Nanotube Hybrids

Tomoki Ogoshi[a], Tada-aki Yamagishi[a], Yoshiaki Nakamoto[a] and Akira Harada*[b]

[a]*Graduate School of Natural Science and Technology, Kanazawa University, Kakuma-machi, Kanazawa 920-1192, Japan*

[b]*Graduate School of Science, Osaka University, Toyonaka, Osaka 560-0043, Japan*

Single-walled carbon nanotubes (SWNTs) have received a great deal of interests because of their unique structural, electrical, and mechanical properties. However, their applications have been extremely limited due to their low solubility in solvents. Therefore, solubilization of SWNTs has been one of hot topics for the past few years. Soluble SWNTs in aqueous media are obtained using π–π interaction between pyrene having ionic groups and SWNTs. Herein, we report novel chemically-responsive supramolecular SWNT hydrogel by using soluble SWNTs functionalized cyclodextrin (CD) moieties on SWNT surface. Since CD shows high solubility in water, water-soluble SWNTs carrying CDs are obtained by using π–π interaction between pyrene modified *β*-CDs and SWNTs (Py-*β*-CD/SWNT hybrids) [1]. By utilizing host-guest interactions between poly(acrylic acid) carrying dodecyl groups (PAA2) and *β*-CDs of Py-*β*-CD/SWNT hybrids, nanocomposites of polymer and SWNTs were prepared. By mixing Py-*β*-CD/SWNT hybrids and PAA2 in aqueous media (Scheme 1a), a homogeneous SWNT hydrogel formed, indicating that host-guest complexes between *β*-CD moieties immobilized on the SWNT surface and dodecyl groups in PAA2 act as cross-links to form network structures which showed gel-like behavior. Furthermore, SWNT hydrogels composed of Py-*β*-CD/SWNT hybrids and PAA2 changed to sol by adding competitive guests or host compounds. When sodium adamantane carboxylate (AdCNa, 100 eq. to dodecyl moieties of PAA2) was added to the hydrogel as a competitive guest, gel to sol transition was observed (Scheme 1b). This result indicates dissociation of the host-guest complexes between *β*-CDs of Py-*β*-CD/SWNT hybrids and dodecyl groups of PAA2 because AdCNa strongly interacts with *β*-CD compared with dodecyl group. Upon addition of *α*-CD (100 eq. to dodecyl groups of PAA2) as a competitive host, the gel also changed to sol (Scheme 1c). It is because dodecyl moieties form complexes with *α*-CD more favorably than with *β*-CD.

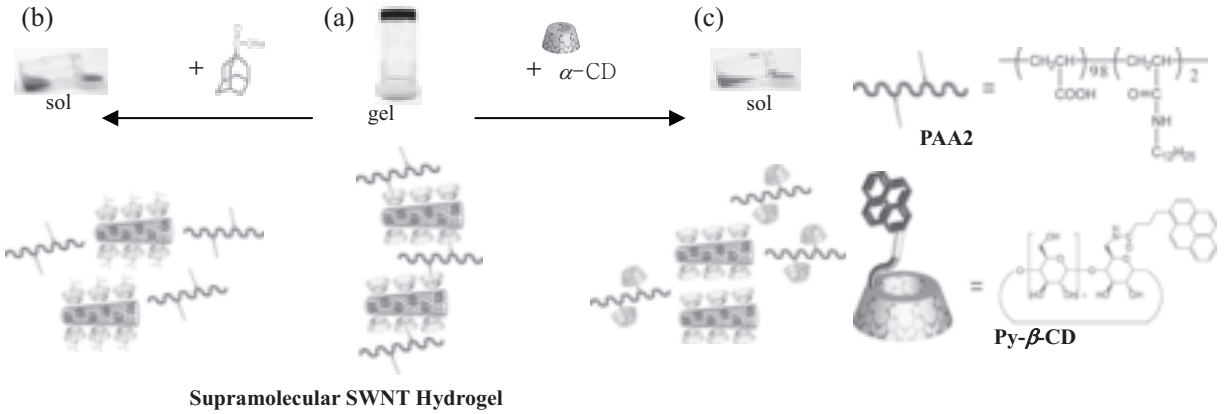

Scheme 1. Supramolecular SWNT Hydrogel Prepared from **Py-*β*-CD/SWNT Hybrids** and Guest Modified Polymer (**PAA2**).

Reference [1] T. Ogoshi et al. *J. Am. Chem. Soc.* **2007**, 129, 4878.

P045C

Postgraft Polymerization of Styrene from Poly (ethylene glycol)-grafted C_{60} Fullerene by Grafting-from Method

H. Wakai[1], T. Momoi[2], T. Shinno[1], T. Yamauchi,[1,3,4] N. Tsubokawa[2,3,4]*

[1]Graduate School of Science and Technology, Niigata University; [2]Faculty of Engineering,Niigata University; [3]Center for Transdisciplinary Research, Niigata University; [4]Center for Education and Research on Environmental Technology, Materials Engineering, and Nanochemistry, Niigata University

Introduction

We reported that the poly(ethylene glycol)(PEG) radicals formed by the thermal decomposition of macroazo-initiator, Azo-PEG, were successfully trapped by C_{60} fullerene to give the corresponding PEG-grafted C_{60} fullerene (C_{60}-$(PEG)_2$) by grafting-onto method [1]. In addition, we reported that the introduction of peroxyester (POE) groups on C_{60} fullerene and radical graft polymerization of vinyl monomers initiated by POE groups on C_{60} fullerene, by grafting-from method were successfully achieved. In the present paper, the introduction of POE groups on C_{60} fullerene cage of C_{60}-$(PEG)_2$ and postgraft polymerization of styrene (St) initiated by POE groups on C_{60} cage of C_{60}-$(PEG)_2$ were investigated as shown in Scheme 1.

Experimental

C_{60} fullerene used was obtained from Frontier Carbon Corporation Co., Ltd., Japan, which was used without further purification. 1,1-bis(*t*-butyldioxy) cyclohexane (Perhexa C) obtained from Nippon Oil and Fats CO., Ltd., Japan, was used without further purification. C_{60}-$(PEG)_2$ was prepared according to our previous report [1].

Result and Discussion

To introduce POE groups on C_{60} cage of C_{60}-$(PEG)_2$, C_{60}-$(PEG)_2$ was treated with Perhexa C in *o*-dichlorobenzene (*o*DCB) at 70°C for 10 h. The introduction of POE groups onto C_{60} cage of C_{60}-$(PEG)_2$ was identified by UV-vis spectra and iodometric titration.

Then, radical postgraft polymerization of St initiated by C_{60}-$(PEG)_2$(POE) in toluene at 100 °C was investigated. It was found that polymerization of St was initiated by POE groups on the C_{60}-$(PEG)_2$(POE) and PSt was postgrafted C_{60}-$(PEG)_2$: the PSt-grafted C_{60}-$(PEG)_2$ was confirmed by size exclusion chromatography. PSt-grafted C_{60}-$(PEG)_2$ having hydrophilic and hydrophobic grafted chains was slightly soluble in water and methanol, but soluble in THF and chloroform. Moreover, it was confirmed by thermogravimetric analysis that thermal stability of PSt and PEG were dramatically enhanced.

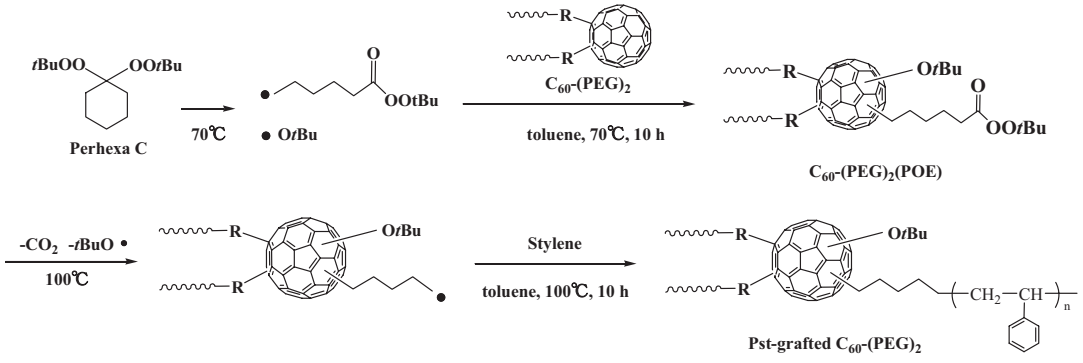

Scheme 1 Postgraft polymerization of styrene initiated from POE groups on C_{60}-$(PEG)_2$(POE)

1) H. Wakai et al., Polymer, 48, 1927 (2007).

P046A

Grafting of Polymers onto Carbon Microcoil by Use of Carboxyl Groups on the Surface and Dispersibility of the Polymer-Grafted Carbon Microcoil

Yuji Nishida,[1] Kazuhiro Hujiki,[2] Takeshi Yamauchi,[1,3,5] Norio Tsubokawa*,[3,4,5]
Kenji Kawabe,[6] Yukio Hishikawa,[6] and Seiji Motojima[7]

[1]Graduate School of Science and Technology, Niigata University, [2]Division of life and Health Science, Joetsu University of Education; [3]Center for Transdisciplinary Research, Niigata University, [4]Faculty of Engineering, Niigata University; [5]Center for Education and Research on Environmental Technology, Materials Engineering, and Nanochemistry, Niigata University; [6]CMC Technology Development Co. Ltd.; [7]Fuculty of Engineering, Gihu University

Introduction

Carbon microcoil (CMC) is a new class of carbon fiber with 3D-helical/spiral forms with diameter of μm orders, and a possible candidate for electromagnetic absorber, hydrogen absorber, and tactile sensor. However, it is difficult to disperse CMC in various solvents and polymer matrices uniformly because of unique morphology. In this work, to improve the dispersibility of CMC in solvents and polymer matrices, we investigated the grafting of polyester by the anionic ring-opening alternating copolymerization of cyclic anhydride with epoxide onto CMC surface. In addition, the dispersibility of the polyester-grafted CMC in solvent and polymer matrices will be discussed.

Experimental

CMC was supplied from CMC Technology Development Co., Ldt. Japan and dried before use. The introduction of COOH groups onto CMC was achieved by the treatment with nitric acid. Carboxyl group content was 1.34 mmol/g. The introduction of COOK groups onto CMC surface was carried out by the treatment of CMC-COOH with KOH. The grafting of polyester onto CMC was achieved by the anionic ring-opening copolymerization styrene oxide (SO) with phthalic anhydride (PAn) initiated by CMC-COOK as shown in Scheme 1.

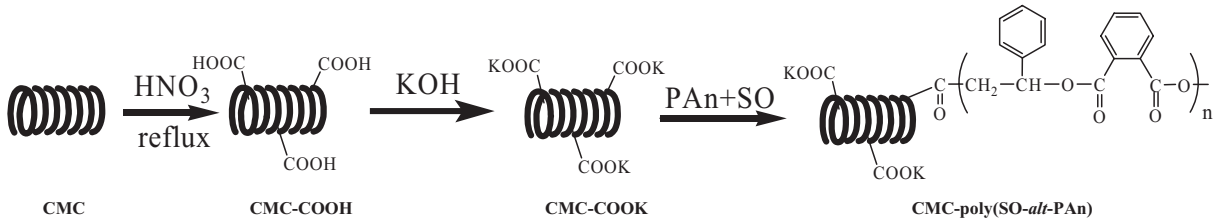

Scheme 1 Ring-opening alternating copolymerization of SO with PAn initiated by CMC-COOK

Result and discussion

In the presence of untreated CMC and CMC-COOH, the anionic copolymerization of SO with PAn was hardly initiated. On the contrary, the anionic ring-opening alternating copolymerization of PAn with SO was successfully initiated by CMC-COOK in nitrobenzene to give the corresponding polyester-grafted CMC: the percentage of polyester grafting reached to 15.7 % after 9 h. The grafting of polyester onto CMC surface was confirmed by FT-IR and thermal decomposition GC-MS.

By the grafting of polymers onto the CMC surface, the entanglement of CMC was effectively destroyed and polymer-grafted CMC uniformly dispersed in good solvents for grafted polymers, silicone rubber, as shown in Figure 1.

In addition, the grafting of polyurethane onto CMC by the polyaddition of diol and diisocyanate in the presence of CMC-COOH and the dispersibility of the polyurethane-grafted CMC in solvents and polyurethane were investigated.

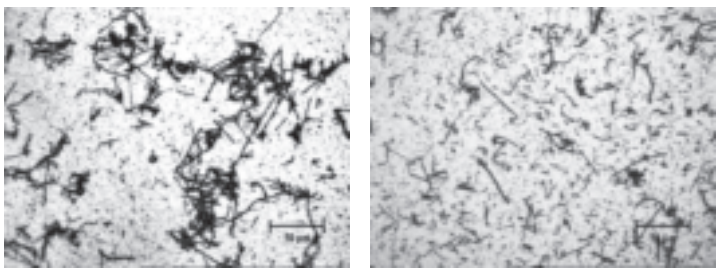

Untreated Poly(SO-*alt*-PAn)-grafted

Figure 1 Optical micrographs of untreated and CMC-poly(SO-*alt*-PAn) in silicone rubber
CMC/silicone rubber = 1.4/100 (wt/wt)

P047B

Immobilization of Capsaicin onto Hyperbranched Poly(amidoamine)-grafted Silica Nanoparticle and its Biorepellent Property

Tomoya Saito[1], Wei Gang[2], Kumi Shirai[3], Takeshi Yamauchi[1,4,5], Norio Tsubokawa[3,4,5,*]

[1]*Graduate School of Science and Technology, Niigata University;* [2]*Venture Business Laboratory, Niigata University;* [3]*Faculty of Engineering, Niigata University;* [4]*Center for Transdisciplinary Research, Niigata University;* [5]*Center for Education and Research on Environmental Technology, Materials Engineering, and Nanochemistry*

Introduction

We have reported the grafting of hyperbranched poly(amidoamine) (PAMAM) onto silica nanoparticle. Hyperbranched PAMAM-grafted silica nanoparticle have the potential to be utilized as a support for catalysts and enzymes due to their many terminal amino groups. On the other hand, marine fouling organisms, such as barnacles and mussels, cause serious problems by settling on ship hulls, fishing equipment, aquaculture cages, and cooling systems for power plants. It was pointed out that capsaicin shows antifouling activity against barnacle cyprids. However, low compatibility and low dispersibility of capsaicin in paints and polymer matrix limits applications of capsaicin in antifouling coatings. To improve these problems, the immobilization of capsaicin onto PAMAM-grafted silica nanoparticle was investigated. Moreover, the stimulus activity of capsaicin-immobilized silica property was discussed.

Experimental

Silica nanoparticle used was Aerosil 200, obtained from Nippon Aerosil Co., Ltd. The immobilization of capsaicin onto silica surface was identified by TGA and thermal decomposition GC-MS. The stimulus activity of capsaicin-immobilized silica was estimated by magnus test and paw lick test.

Results and discussion

The grafting of PAMAM onto silica surface was achieved by repeating reactions in a solvent-free dry-system: Michael addition of amino groups on the surface with methyl acrylate (MA) and amidation of terminal amino groups with ethylenediamine (EDA). The percentage of grafting of PAMAM onto silica was 50.7 % after repeating reaction cycled of 3-times.

The immobilization of capsaicin onto PAMAM-grafted silica nanoparticle was achieved by the reaction of hydroxyl groups of capsaicin with isocyanate groups on the silica, which were introduced by the reaction of hexamethylenediisocyanate (HMDI) with terminal amino groups of PAMAM-grafted silica nanoparticle as shown in Scheme 1.

Mass spectra of thermal decomposed gas of capsaicin-immobilized PAMAM-grafted silica nanoparticle were in agreement with that of capsaicin. The amount of capsaicin immobilized on silica was determined to be 0.10 mmol/g by TGA.

When PAMAM-grafted silica nanoparticle dispersed in Tyrode's solution was injected into mouse paws, no licking of paws was observed; however, when capsaicin-immobilized silica in Tyrode's solution and free capsaicin in Tyrode's solution were injected, the obtained paw-licking times were 57.0 sec/5min and 50.1 sec/5min, respectively. Based on the result, it was found that the capsaicin retained its stimulus activity even if immobilized onto PAMAM-grafted silica nanoparticle.

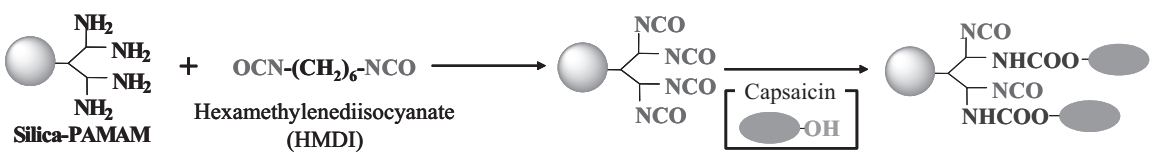

Scheme 1 Immobilization of capsaicin onto PAMAM-grafted silica nanoparticle

P048C

Preparation and Properties of Flame Retardant-immobilized Silica Nanoparticle

Akira Yuki[1], Takeshi Yamauchi[1,2,3], Norio Tsubokawa[2,3,4]*
[1]*Graduate School of Science and Technology, Niigata University;* [2]*Center for Transdisciplinary Research, Niigata University;* [3]*Center for Education and Research on Environmental Technology, Materials Engineering, and Nanochemistry,Niigata University;* [4]*Faculty of Engineering, Niigata University,*

Introduction

Several types of flame retardant additives are used to improve flame retarding properties to polymer materials. These flame retardants can be divided into halogen, inorganic, phosphorous, nitrogen and nitrogen-phosphorous flame retardant. However this flame retardant has a problem to bleeding phenomena. On the other hand, in our laboratory, it has been reported that successful surface grafting of various polymers onto silica nanoparticle by using previously introduced initiating groups on the surface.

In this paper, the immobilization of bromine flame retardants onto hyperbranched poly(amidoamine)-grafted silica nanoparticle (Silica-PAMAM) and phosphorous flame retardants onto silica nanoparticle was investigated. In addition, the flame retardant properties of the epoxy resins filled with flame retardant immobilized-silica were investigated.

Experimental

Silica nanoparticle used was Aerosil 200, obtained from Nippon Aerosil Co., Ltd. Amino groups was introduced onto silica surface by the treatment with silane coupling agent. In a solvent-free dry-system, the grafting of PAMAM onto silica surface was achieved by repeating reaction of Michael addition of amino groups on the surface with methyl acrylate (MA) and amidation of terminal amino groups with ethylenediamine (EDA). The flame retardant properties of the epoxy resin filled with modified silicas were estimated by the oxygen index method (JIS K7201).

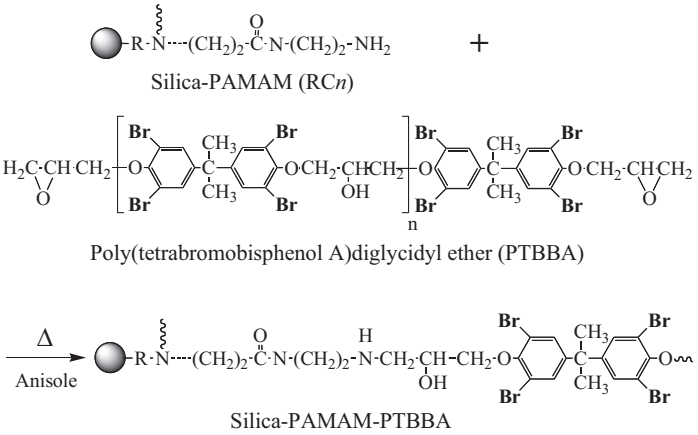

Scheme 1 Immobilization of PTBBA onto Silica-PAMAM surface

Results and discussion

The immobilization of flame retardant onto Silica-PAMAM (percentage of grafting=50.7%) was carried out by the reaction of terminal amino groups on the surface with epoxy groups of poly(tetrabromobisphenol A) diglycidyl ether (PTBBA) in anisole under N_2 as shown in Scheme 1. The immobilization of PTBBA onto silica-PAMAM was identified by FT-IR and thermal decomposition GC-MS of the flame retardant-immobilized silica. The amount of PTBBA immobilized onto Silica-PAMAM was determined to be 59.0% by TGA.

In addition, the immobilization of phosphorous flame retardant onto a silica nanoparticle surface was examined by the reaction of hexachlorocyclotriphosphazene moieties of silica surface with bis(4-aminophenoxy)phenyl phoshine oxide (BAPPO). It was found that by the above reaction, phosphorous flame retardant was successfully immobilized onto the silica surface. The immobilized cyclotriphosphazene and BAPPO onto silica (PH-BAPPO-silica) was also identified by thermal decomposition GC-MS of flame retardant-immobilized silica.

These flame retardant PTBBA- and PH-BAPPO-immobilized silicas were dispersed uniformly in epoxy resin and the mixtures were cured by hexamethylene diamine (HMDA) at 120℃ for 2 h. It was found that the oxygen index of cured epoxy resin filled with untreated silica, PTBBA and untreated silica, PTBBA-immobilized silica, and PH-BAPPO-immobilized silica was 20.3, 21.7, 23.4, and 25.9, respectively. The results indicate that the flame retardant properties of the epoxy resin were improved by addition of the PTBBA- and PH-BAPPO-immobilized -silica.

P049A

Grafting of Polybutadiene onto Silica Nanoparticle and Carbon Black Surface in the Presence of $Sc(OTf)_3$

Masaaki Takamura[1] , Takeshi Yamauchi[1,2,3], Norio Tsubokawa[2,3,4]*
[1]*Graduate School of Science and Technology, Niigata University;* [2]*Center for Transdisciplinary Research, Niigata University;* [3]*Center for Education and Research on Environmental Technology, Materials Engineering, and Nanochemistry,Niigata University ;* [4]*Faculty of Engineering, Niigata University,*

Introduction

We have reported that the grafting of functional polymers having amino and hydroxyl groups onto carbon black surface by direct condensation of carboxyl groups on the surface successfully proceeded in the presence of *N,N'*-dicyclohexylcarbodiimide (DCC).

It was reported that $Sc(OTf)_3$ catalyzed direct esterification of aliphatic alcohol with carboxylic acid at room temperature.

In this paper, the grafting of polybutadiene (polyBu-COOH) onto carbon black and silica nanoparticle by the reaction with hydroxyl groups of carbon black and amino groups on the silica were investigated using $Sc(OTf)_3$ as catalyst (Scheme 1).

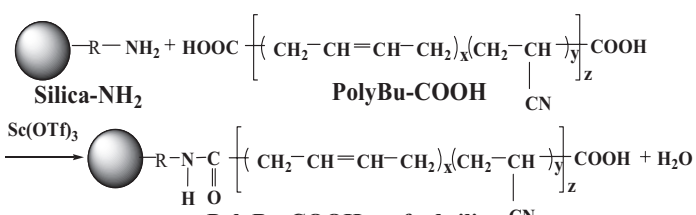

Scheme 1 Grafting of polyBu-COOH onto Silica-NH_2 surface in the presence of $Sc(OTf)_3$

Table 1 Effect of $Sc(OTf)_3$ on the grafting of polyBu-COOH onto nano particle

	Mn of PolyBu-COOH	$Sc(OTf)_3$ / g	Grafting / %
Silica-NH_2	3500	0	4.21
	3500	0.15	23.1
	4800	0	3.73
	4800	0.15	20.2
CB	3500	0	21.5
	3500	0,1	66.9
	4800	0	16.4
	4800	0,1	62.9

Experimental

Carbon black used was FW 200 obtained from Degussa AG. Silica nanoparticle used was Aerosil 200 obtained from Nippon Aerosil Co. Ltd. The specific surface area of carbon black and silica were 460 and 200 m^2/g, respectively. PolyBu-COOH obtained from Ube Ind. Co. Ltd. was used without further purification. $Sc(OTf)_3$ obtained from Aldrich was used without further purification.

Results and discussion

Table 1 shows the results of the grafting of polyBu-COOH onto carbon black and silica in the presence of $Sc(OTf)_3$. In the absence of $Sc(OTf)_3$, the grafting of polyBu-COOH onto CB and silica hardly proceeded. On the contrary, the grafting of polyBu-COOH with amino groups on silica and hydroxyl groups on CB successfully proceeded in the presence of $Sc(OTf)_3$.

The percentage of polyBu-COOH grafting onto carbon black and silica surface increased with increasing reaction time. It became apparent that the percentage of polyBu-COOH grafting onto silica nanoparticle surface was smaller than that onto carbon black. This may be due to the fact that the specific surface area of carbon black was higher than that of silica.

In addition, the effects of reaction temperature, the amount of polyBu-COOH, molecular weight of polyBu-COOH and the amount of $Sc(OTf)_3$ on the grafting reaction onto silica nanoparticle and carbon black were investigated.

After the reaction, the $Sc(OTf)_3$ was easily recovered by reprecipitation and successive extraction with water. The grafting of polyBu-COOH onto silica nanoparticle and onto carbon black surface in the presence of recycled $Sc(OTf)_3$ were also successfully achieved.

In addition, the crosslinking of polyBu-COOH by silica nanoparticle and carbon black in the presence of $Sc(OTf)_3$ was investigated in bulk. It was found that the crosslinking of polyBu-COOH by silica nanoparticle and carbon black in the presence of $Sc(OTf)_3$ were proceeded to give gels containing carbon black and silica.

P050B

Grafting of Antibacterial Polymers onto Silica Nanoparticle and Their Properties

Yoko Takeuchi [1], Wei Gang[2], Kumi Shirai[3], Takeshi Yamauchi[1,4,5], Norio Tsubokawa[*3,4,5]
[1]*Graduate School of Science and Technology, Niigata University;*
[2]*Venture Business Laboratory, Niigata University;* [3]*Faculty of Engineering, Niigata University;* [4]*Center for Education and Research on Environmental Technology, Materials Engineering, and Nanochemistry, Niigata University,*
[5]*Center for Transdisciplinary Research, Niigata University*

Introduction

We have reported the radical graft polymerization of vinyl monomers onto silica nanoparticle initiated by the system consisting of surface trichloroacetyl groups on the silica and $Mo(CO)_6$. Various kind of antibacterial polymers were reported. For example, polymers with quaternary phosphonium salt ($P^+(C_4H_9)_3Cl^-$) moieties show extremely strong antibacterial nature. In the present paper, the grafting of polymer with $P^+(C_4H_9)_3Cl^-$ moieties onto silica nanoparticle surface. The surface antibacterial activity of silicone rubber filled with the polymer-grafted silica will be discussed.

Experimental

Silica nanoparticle used was obtained from Nippon Aerosil Co., Ltd. Japan. The specific surface area and average particle size are 200 m^2/g and 12 nm, respectively. The introduction of trichloroacetyl groups onto silica nanoparticle was achieved by the reaction of trichloroacetyl isocyanate with amino groups on the surface. The antibacterial test of silicone rubber filled with the antibacterial polymer-grafted silica was carried out according to the method of JIS Z 2801. Bacterium used for the tests were *Staphylococcus aureus, Escherichia coli*, and *Pseudomonas aeruginosa.*

Result and discussion

The grafting of polymer having $P^+(C_4H_9)_3Cl^-$ moieties was achieved by two-step reactions as shown in Scheme 1.

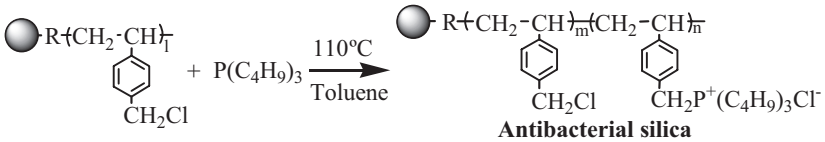

Scheme 1 Synthesis of antibacterial polymer grafted silica

In the first step, poly(vinylbenzylchloride) (poly(St-CH_2Cl)) was successfully grafted onto silica surface by the graft polymerization of the corresponding monomer initiated by the system consisting of trichloroacetyl groups on the surface and $Mo(CO)_6$; the percentage of grafting was 50%. In the second step, the poly(St-CH_2Cl)-grafted silica was treated with tributhylphosphine ($P(C_4H_9)_3$) to convert the CH_2Cl groups to alkyl phosphonium salt, $P^+(C_4H_9)_3Cl^-$. The grafting of polymer with $P^+(C_4H_9)_3Cl^-$ onto silica surface was confirmed by ^{13}C-CP/MAS-NMR and GC-MS. The content of $P^+(C_4H_9)_3Cl^-$ moieties of grafted chains on the silica was determined to be 1.5mmol/g.

Figure 1 shows antibacterial activity of surface of silicone rubber filled with untreated and antibacterial polymer-grafted silica to *Escherichia coli*. It was found that cells of *Escherichia coli* increased from 1.0×10^5 to 5.6×10^6 colony forming unit (CFU) par mL on the silicone rubber filled with untreated silica. On the contrary, it was found that the silicone rubber filled with the antibacterial polymer-grafted silica shows strong antibacterial activity to *Escherichia coli*. Moreover, the silicone rubber filled with the antibacterial polymer-grafted silica shows strong antibacterial activity to both of *Staphylococcus aureus* and *Pseudomonas aeruginosa.* Therefore, the composites from antibacterial polymer-grafted silica have potential use as sanitary goods, toilet seats, medical polymer tubes, and paints.

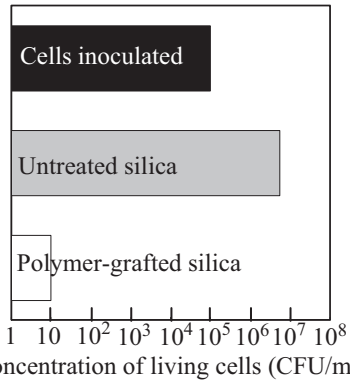

Figure 1 Antimicrobial activity of silicone rubber filled with silica to *Echerichia coli*

P051C

Surface Grafting of Poly(amidoamine) onto Silica Nanoparticles in Solvent-Free Dry-System

Norio Tsubokawa,[1,2,3] Jun Ueda,[4] Takeshi Yamauchi,[2,3,4]
[1]Faculty of Engineering, Niigata University; [2]Center for Transdisciplinary Research, Niigata University; [3]Center for Education and Research on Environmental Technology, Materials Engineering, and Nanochemistry, Niigata University; [4]Graduate School of Science and Technology, Niigata University

Introduction

We pointed out that polymer grafting onto nanoparticle surfaces is of interest for designing new functional organic-inorganic hybrid materials, which have excellent properties of both nanoparticles and grafted polymers, including photosensitivity, curing ability, bioactivity, and pharmacological activity. However, scaled-up synthesis of polymer-grafted nanoparticles is difficult to achieve, because complicated reaction processes, such as centrifugation, filtration, and solvent extraction, are required for the synthesis of polymer-grafted nanoparticles, and large amounts of waste solvent are obtained (Figure 1).

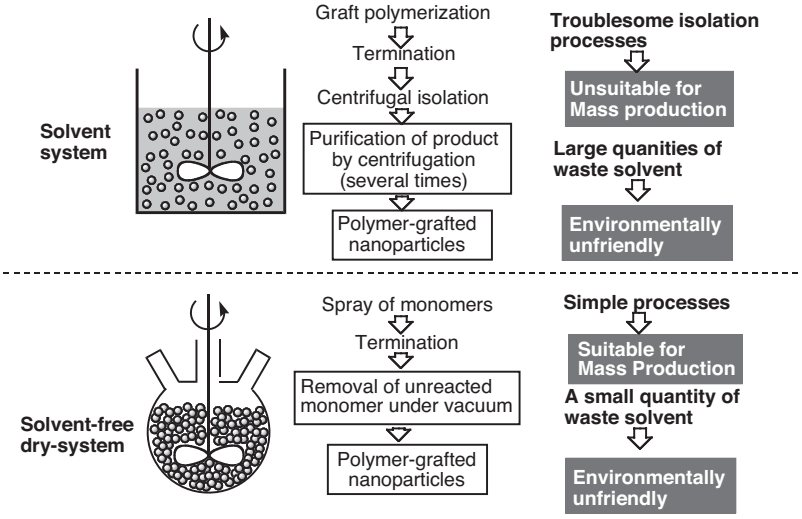

Figure 1. Graft polymerization of polymers onto the nanoparticle surface in a solvent system vs. in solvent-free dry-system.

In this paper, for the prevention of environmental pollution and simplification of reactions, the scale-up synthesis of hyperbranched poly(amidoamine) (PAMAM)-grafted silica nanoparticles in a solvent-free dry-system was investigated.

Experimental

Materials

Silica nanoparticle used was Aerosil 200 obtained from Nippon Aerosil Co., Ltd., Japan. The specific surface area and particle size were 200 m^2/g and 12 nm, respectively. The silica was dried in vacuo at 110 °C for 48 h before use. The silanol group content was determined to be 1.38 mmol/g by volumetrically measuring the amount of ethane evolved by reaction with triethylaluminum.

Introduction of Amino Groups onto Silica Surface

The introduction of amino groups onto the silica was also achieved by the treatment of surface silanol groups with γ-aminopropyltriethoxysilane in a solvent-free dry-system.

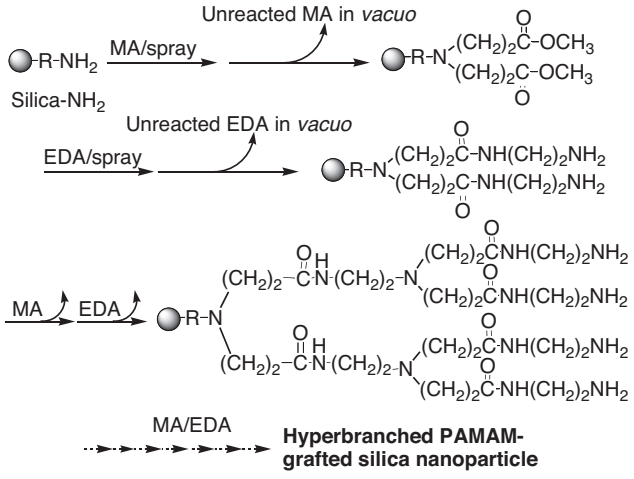

Scheme 1

Grafting of PAMAM onto Silica Surface in a Solvent-free Dry-system

Into a 500-mL four-necked flask, containing 15.0 g of Silica-NH_2, 3.0 g of MA (34.8 mmol; excess of surface amino groups) were sprayed and the silica was agitated at 300 rpm at 50 °C under argon gas. After the reaction for 21 h, unreacted MA was removed under high vacuum at 50 °C. Without isolation of the resulting silica, 3.0 g of EDA (50 mmol; excess of surface ester group) were sprayed into the flask, and the reaction was conducted at 50 °C with agitation. After 21 h, unreacted EDA and methanol formed was also removed under vacuum at 50 °C, and MA were sprayed again without isolation of the silica. Michael addition and amidation reactions were repeated to grow PAMAM from the silica surface as shown in Scheme 1.

Result and discussion

Grafting of PAMAM onto silica surface in a solvent-free dry-system

Amino group content of silica nanoparticle and PAMAM grafting onto silica nanoparticle surface (wt% of grafted polymer on silica) after the grafting reaction is shown in Table I. The amino group content and PAMAM grafting of the resulting silica nanoparticle increased with repeated reaction cycles. With untreated silica nanoparticles, no increase of surface amino group and no grafting of PAMAM onto the surface were observed even after repeated reaction cycles of 8-times.

Table I. Grafting of PAMAM onto silica nanoparticle surface in a solvent-free dry-system[a]

Cycles of reperated reaction	Amino group (mmol/g)		Grafting (%)		
	Experimental	Calcd.	Experimental	Calcd.	R [b]
2-times	1.7	1.3	14.5	22.6	0.64
4-times	4.0	5.3	69.2	112.9	0.61
6-times	7.6	21.1	129.4	474.0	0.27
8-times	8.8	84.5	141.0	1918.6	0.07

[a]Amino group content of initiator site, 0.33 mmol/g.
[b]R=Experimental value / Calculated value.

However, the obtained values for PAMAM grafting and amino group content were considerably smaller than the calculated values. The ratio of experimental value to calculated value, R, decreased as the number of reaction cycles increased. The same tendency was observed for grafting of PAMAM onto silica nanoparticles in a methanol solvent system.

During the grafting reaction, a small amount of ungrafted polymer was formed: the major part, which was methanol-soluble, was hyperbranched PAMAM, while the minor part, which was soluble in THF, was a mixture of polyMA and unknown viscous materials. This indicates that removal of the unreacted monomer in each step was incomplete, probably due to strong adsorption of the monomers on the silica nanoparticle surface.

Table II. Effects of amino group content of grafting site on silica nanoparticles on PAMAM grafting in a solvent-free dry-system

Amino group content (mmol/g)	Grafting[a] (%)	R [b]
0.12	7.2	0.88
0.19	9.6	0.74
0.33	14.5	0.64
0.45	19.8	0.64
0.62	23.2	0.55

[a]After 2 reaction cycles.
[b]R=Experimental value / Calculated value.

Table II shows the effects of amino group content on the grafting of the hyperbranched PAMAM onto silica nanoparticle surface. The percentage of grafting with repeated reaction cycles of 2-times increased with initial amino group content on the surface. However, R (experimental value/theoretical value) decreased with increasing amino group content on the surface as the grafting site. This may be due to the fact that the steric hindrance to surface amino groups increased with increasing density of surface amino groups.

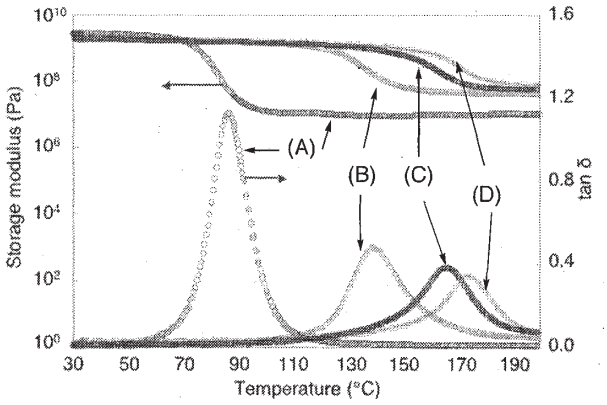

Figure 2. DMA curves of epoxy resin cured by (A) EDA in the presence of untreated silica nanoparticle, (B) Silica-PAMAM:BF_3 (10 wt%), (C) Silica-PAMAM:BF_3 (20 Wt%), and Silica-PAMAM:BF_3 (30 wt%).

Curing of epoxy resin by hyperbranched PAMAM-grafted silica

We have reported that hyperbranched PAMAM-grafted silica containing BF_3-amine complex groups (Silica-PAMAM:BF_3) acts as effective curing agent for epoxy resins. BF_3 complexation of terminal amino groups of PAMAM-grafted silica was achieved by treatment of PAMAM-grafted silica with a boron trifluoride diethylether complex.

The temperature dependence of the dynamic mechanical properties of the epoxy resin/silica nanocomposite prepared from PAMAM-grafted silica (repeated reaction cycles of 3-times) containing BF_3-amine complex groups is shown in Figure 2. It is interesting to note that the glass transition temperature of the epoxy resin/silica nanocomposite increased with increasing Silica-PAMAM:BF_3 content; the glass transition temperature of resin/silica nanocomposites containing 30 wt% Silica-PAMAM:BF_3 exceeded 170 °C. In addition, the storage modulus of these resin/silica nanocomposites was maintained at high values even in high-temperature region. These results suggest that the micro-Brownian motion of the epoxy network is strongly restricted, and the heat resistance of the cured epoxy resin is significantly improved by hybridization with the Silica-PAMAM:BF_3 in epoxy resin.

P052A

Preparation of polymer gels with ionic liquids as solvent and its functional evaluation

Yoshihide ITO[1], Takeshi YAMAUCHI[1,3,4,*], and Norio TSUBOKAWA[2,3,4]

[1]Graduate School of Science and Technology, Niigata University, [2]Faculty of Engineering, Niigata University, [3]Center for Transdisciplinary Research, Niigata University, [4]Center for Education and Research on Environmental Technology, Materials Engineering, and Nanochemistry

〔Introduction〕

Recently, there has been various kind of research work about hydro-polymer gels to develop smart materials such as biomedical devices, sensors, and actuators. For the high-grade soft materials, it has required that new polymer gels using functional solvent. An ionic liquid have high viscosity at the room temperature, nonvolatile, high ionic conduction, and flame resistance. In this study, we have prepared polymer gels with ionic liquids as a solvent by photo-polymerization and mechanical characteristic of the polymer gels were examined.

〔Experimental〕

Polymer gels were prepared by photo-polymerization with irradiation of ultraviolet light. 1.0 M of Monomer (*N*-isopropylacrylamide (NIPAM), Acrylamide, 2-acrylamide-2-methylpropanesulfonic acid, 2-Hydroxyethyl methacrylate) and 30.0 mM of *N,N'*-Methylenebis (acrylamide) in 1.0 ml of ionic liquid (imidazole system). In addition, 10.0 mM of α-Ketoglutaric acid was added to in this solution and deoxidized for 30 minutes. Photo-polymerization was carried out was irradiation of ultraviolet light (wavelength ; 365 nm) at room temperature for 1 hour. Synthesized polymer gels were allowed to stand for 5 hours at the room temperature. The mechanical characteristic was examined by the compression test with a digital push-pull gauge. Thermo-sensitivity of PNIPAM gels were evaluated by relationship between temperature and volume alteration modulus, and phase transition temperature was identified from differential scanning calorimetry (DSC)

〔Results and Discussion〕

A white colored PNIPAM gel was synthesized by this method using ionic liquid as a solvent. The PNIPAM gel was maintained its weight in air at room temperature to stand for 5 hours. These results indicated that nonvolatile gel was synthesized by using the ionic liquid as a solvent. Ratio of ionic liquid and water as solvent was significantly related with color of PNIPAM gels. The PNIPAM gels contained water as a solvent was colorless and transparent, and white colored PNIPAM gels were obtained containing more than 60 % of ionic liquid in water solvent. Thermo-sensitivity of PNIPAM gels were also depended on the ratio of ionic liquid and water. Increased with the ratio of water against ionic liquid in the gels, the gels changed their volume with temperature as same as normal PNIPAM gel and showed phase transition temperature at 35 ^{o}C.

P053B

Electrical properties of polypyrrole/calcium alginate composite gel

Shotaro KON[1], Takeshi YAMAUCHI[1, 3]*, and Norio TSUBOKAWA[2, 3]

[1]Graduate School of Science and Technology, Niigata University, [2]Faculty of Engineering, Niigata University, [3]Center for Transdisciplinary Research, Niigata University, [4]Center for Education and Research on Environmental Technology, Materials Engineering, and Nanochemistry

〔Introduction〕

Conducting polymers are new electrochemical materials with high conductivity, excellent processing and electrochromic characteristic that is known as that the materials changed their color with electrical stimulus. The conducting polymers have actively researched on the application to displays, sensors, and actuators in various fields. In general, a main chain of the conducting polymers have rigid structure and it is difficult to use these stiff materials for soft electrochemical devices. For the high-grade electrochemical devices, it has required that new conducting material which composed conducting polymers and a soft material such as gels.

Alginic acid is a polysaccharide of electrolyte that has carboxyl groups and it can be easily prepared polymer gel by the ionic bond with the Ca^{2+}. The calcium alginate gel changed its volume to contraction by applied voltages, on account of alginate gal is ionic gel. The composite materials of alginic acid and conducting polymer would have multi functional characteristics with a simultaneous change in the color and the volume.

In this research work, we developed polymerization of conducting polymer composite gel, and the electric characteristics of the conducting polymer composite gel was investigated.

〔Experimental〕

The calcium alginate gel was prepared from 1 wt% sodium alginate solution that was added dropwise to $CaCl_2$ solution, and it was allowed to stand for 24 hours. The calcium alginate gel was contained the pyrrole to immerse the gel in 1M pyrrole solution for 24 hours. I_2 and KI mixture solution was used as oxidant. The polypyrrole/calcium alginate composite gel was prepared by oxidation polymerization of pyrrole in calcium alginate gel immersed in iodine mixture solution.

A part of composite gel was immersed in the electrolyte solution and the constant potential was applied, the change in the color and the volume of composite gel was observed as an evaluation of electrical properties. The electrolyte solution was used KCl solution or $CaCl_2$ solution. The volume alteration was evaluated to measure diameter of composite particles gel by changing the voltage and concentration of Ca^{2+} in the electrolyte solution.

〔Results and Discussion〕

Calcium alginate gels were gradually changed their color into the black from surface, polypyrrole/calcium alginate composite gel was prepared within 24 hours. The surface structure of composite gel was observed with the Scanning Electron Microscope (SEM). The surface structure of composite gel was alternated into rough surface after polymerization.

The composite gel which immersed in the iodine solution for five minutes showed electrochromism by applied the voltage in the electrolyte solution. The result of the applied 1.5 V, the color of the composite gel changed its color from a yellowish black into a bluish black. The composite gel was arbitrary contracted under applied voltage. The gel contracted about 15 % of total volume within 20min by applying voltage. It was appeared that the concentration of I^- and Ca^{2+}ion were related with the electrochromic characteristics and volume change of polypyrrole/calcium alginate composite gel.

P054C

Preparation of high molecular weight phenolic resins

Wang Pengfei, Tada-Aki Yamagishi*, Tomoki Ogoshi, and Yoshiaki Nakamoto

Graduate School of Natural Science and Technology, Kanazawa University

Introduction

Phenol resin is a typical thermosetting resin and widely used in engineering fields because of its heat-stability, electric insulation, and cost effectiveness. The resin, however, has serious shortcomings like brittleness and weak thermo-oxidative stability, which have limited the application to other fields. In order to improve these properties, some modifications are needed and a copolymerization with long chain alkyl phenols and a blend of phenolic resins with elastomers have been attempted.Recently, high molecular weight phenolic resins have been prepared in good yield.[1)] The advantages of high molecular weight polymers are 1) the increase of intermolecular interaction, 2) the increase of entanglement, and 3) the expansion of chain by exclusion volume effect. These effects will make the heat-stability and flexibility of polymer higher. Therefore, linear type of phenolic resins with higher molecular weight will have the same heat-stability as phenolic resin with network structure. In this report, we attempt to prepare high molecular weight and also soluble phenolic resins from *o*-cresol as monomer in organic solvents and the thermal properties are investgated.

Preparation of high molecular weight novolak :

o-Cresol (1 mol) and a 95 % paraformaldehyde (1 mol as formaldehyde component) were dissolved in 250 mL of acetic acid. Conc. H_2SO_4 (0.05 mol) was added dropwise and the reaction mixture was stirred at 80 °C for 1 h. The reaction mixture was poured into a large amount of water to obtain the resin. The resin was purified by repetition of dissolution in THF and precipitation in water twice.

Results and Discussion

1) Effect of solvent on molecular weight of resin

The effect of solvent on the molecular weight of resins was investigated. It was expected that the molecular weight of resins will increase by the polycondensation in good solvents for resins. THF is a good solvent for phenolic resins. However, the molecular weight of resin obtained in THF was smaller than that in others. It was found that acetic acid was a reactive solvent for the preparation of high molecular weight phenolic resins (Table 1).

Table 1 . Molecular weights of polymers prepared in different solvents

Run	Solvent	Temp/℃	Time	Mw/10^4	Mn/10^3	Mw/Mn
1	THF20%	80	4h	6.2	3.8	16.0
2	Dioxane 20%	80	3h	4.3	4.0	10.6
3	Methanol 50%	80	18h	0.2	1.4	1.5
4	Methanol 20%	80	6h	13.8	5.3	25.9
5	Acetic acid 100%	80	1h	17.4	5.5	31.5

Catalyst: sulfuric acid. Molar ratio: o-cresol/formaldehyde=1/1.

Solvent: acetic acid + another solvent.

2) Thermal properties of resin

The thermal properties were investigated by the differential scanning calorimetry (DSC) and the thermogravimetric analysis (TGA) measurements. The effect of molecular weight of resins on the thermal properties was shown in Figure 2. Higher molecular weight resin (sample a) showed high heat-stability. The thermal property of high molecular weight *o*-cresol resin was comparable to that of phenolic resins cross-linked by hexamethylene tetramine. On the other hand, a lower molecular weight resin (sample d) showed low heat-stability. Sample c was a mixture composed of high molecular weight resin and low molecular weight one. Even though the weight average molecular weight of sample c was higher than that of sample b, the heat-stability of sample c was lower. The lower molecular weight component might play role as a decomposing stimulator. It was found that the molecular weight strongly influenced the thermal properties of phenolic resin.

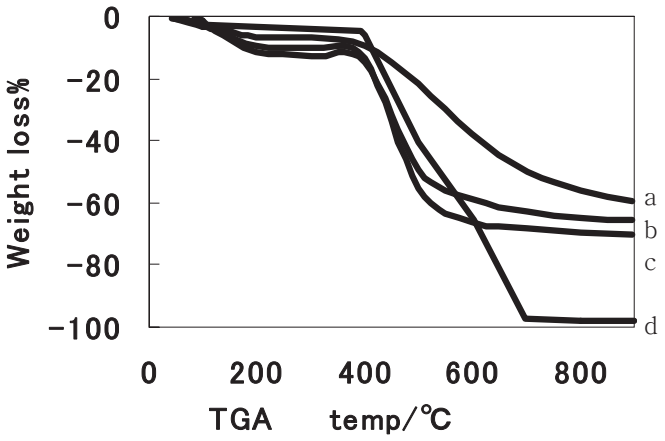

Figure2. Weight loss of o-cresol resins.
a: Mw=1.3×10^6, Mw/Mn=3.4; b: Mw=1.5×10^4, Mw/Mn=2.5
c: Mw=1.74×10^5, Mw/Mn=31; d: Mw=0.2×10^3, Mw/Mn=1.9

3) Molecular structure

The molecular structure of resins was determined by ^{1}H and ^{13}CNMR measurements. The typical ^{13}C NMR spectra of resins with Mw=1.1×10^4 and 7.8×10^5 are shown in Figure 3. The methylene carbon of *ortho-ortho*', *ortho-para*', and *para-para'* linkages give peaks in the range from δ = 30.8 to δ = 41.0 ppm.[2] In this work, the structure of the high molecular weight resin was estimated by the fractions of three kinds of methylene linkages. In high molecular weight *o*-cresol resin, the fractions of *ortho-ortho*', *ortho-para*', and *ortho-para*' linkages were close to 25%, 50%, and 25%, respectively, as the molecular weight became higher. This indicated that the reactivity of *ortho* position was equal to that of *para* position in *o*-cresol ring. In the previous report, the reactivity of *ortho* position was lower than that of *para* position under acidic conditions for the preparation of random novolak resin.[3] The difference in reactivity between *ortho* and *para* positions became small under this reaction condition. In the spectrum of resin with Mw=7.8×10^5 new signals were observed at δ = 35 and 33 ppm. The assignment was not clear, but the signals were expected to be corresponding to new methylene linkages to form gels.

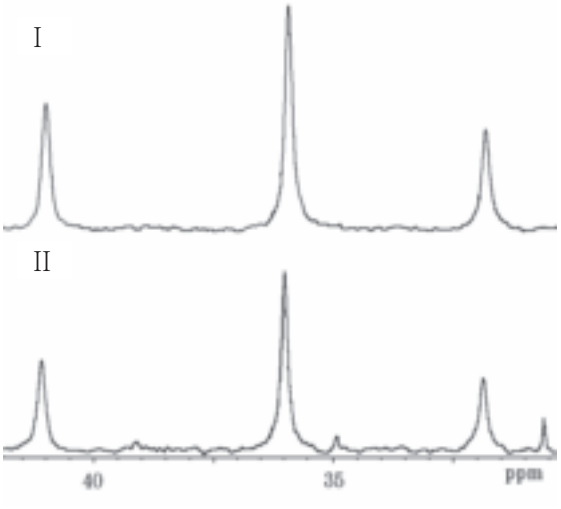

Figure 3. ^{13}CNMR spectra of o-cresol resins.
Ⅰ : Mw=1.1×10^4; Ⅱ : Mw=7.8×10^5.

References

1) T.Yamagishi, M.Nomoto, S.Ito, S.Ishida, and Y.Nakamoto, *Polym. Bull.*(Berlin),**32**,501 (1994)
2) S. A. Sojka, R. A. Wolfe, E. A. Dietz, Jr., B. F. Dannels, *Macromolecules*,**12**, 767 (1979)
3) T.Yamagishi, T.Nakatogawa, M.Ikuji, Y.Nakamoto, S.Ishida, *Angew. Makromol.Chem.* **240**, 181 (1996)

P055A

PREPARATION OF POLY(ARYLENEMETHYLENE)S DERIVED FROM MULTI-SUBSTITUTED AROMATIC SERIES AND EVALUATION OF THEIR PROPERTIES.

Tadamasa NEMOTO, Ataru KOBAYASHI, Gen-ichi KONISHI*

Department of Organic and Polymeric Materials, Graduate School of Science & Engineering, Tokyo Institute of Technology, Ookayama, Meguro-ku, Tokyo, 152-8552, JAPAN

Aromatic, especially phenolic resins, and related polymers are a very important class of common organic polymers with significant material applications, such as thermosetting resins, adhesives, photoresists and polymer composites. These materials show good thermal stability and mechanical properties, however the solubility in organic solvents is very poor. We have previously discussed the design of a new high performance aromatic polymer,[1] especially, alkoxylated phenol-based phenolic resins, such as anisole, phenethol, diphenyl ether, and so on. These polymers have good solubility in organic solvents and are more stable to heat and oxidation than the conventional phenolic resins. In this presentation, we report the synthesis of the organo-soluble and well-defined substituted benzene or naphthalene-formaldehyde copolymers *via* addition-condensation. The thermal and solution properties of the obtained polymers are also described.[2]

The acid-catalyzed polymerization of 1,3,5-trimethylbenzene (**1**), 1,2,4-trimethylbenzene (**3**) or 2,6-dimethylnaphthalene (**5**) with formaldehyde were carried out. The results of the polymerization of **1**, **3**, or **5** with formaldehyde under various conditions are summarized in Table 1. From FT-IR spectrum, ^{1}H and ^{13}C NMR spectra, the polymer derived from run2 in Table 1 (**2**) had the methylene bridge. This result indicated that polymer **2** consisted of the phenylenemethylene backbone. For the 1,2,4-trimethylbenzene (**3**), the polymerization proceeded, but the number-average molecular weights (M_n) of the obtained polymer was lower than that of polymer **2**. Organo-soluble naphthalene-based polymer (**6**) was also obtained in only a 33% yield because of the many reactive sites. The T_{10} (10% loss in weight) of polymer **2** and **6** were 243 and 377 ^{o}C, respectively. From the light scatting method, polymer **2** had a spherical structure with a densely branched three-dimensional topology in dilute THF solution.

Table 1 Polymerization of substituted benzene and naphthalene.[a]

Run	Substrate	Solvent (mL)	Yield (%)	M_n[b]	M_w/M_n[b]
1	1	AcOH (20)	>99	1400	1.3
2	1	AcOH (5) / $CHCl_3$ (15)	>99	3200	3.2
3[c]	1	AcOH (5) / $CHCl_3$ (15)	84	2800	13.0
4	3	AcOH (20)	>99	2100	1.4
5	3	AcOH (5) / $CHCl_3$ (15)	91	1300	1.6
6	3	AcOH (10) / DCB[d] (10)	87	1500	5.9
7[e]	5	AcOH (40)	33[f]	580	1.05

a: substrate:formaldehyde = 10:20 mmol, catalyst: H_2SO_4, 60 ^{o}C, 2 h.
b: Determined by GPC using THF as an eluent with polystyrene standards.
c: reaction time: 7 h. d: DCB = o-dichlorobenzene.
e: substrate: formaldehyde = 10:10 mmol. f: A soluble part in chloroform.

References
1) Kimura, T.; Nakamoto, Y.; Konishi, G. *Polym. J.* **2006**, *38*, 606.
2) Nemoto, T.; Ueno, T.; Nishi, M.; Shin, D.-M.; Nakamoto, Y.; Konishi, G.; *Polym. J.* **2006**, *38*, 1278.

P056B

COPOLYMERIZATION OF VINYL ETHER WITH A TRICYCLODECANE UNIT AND *n*-BUTYL VINYL ETHER: SYNTHESIS OF NEW POLYMERIC MATERIALS CONSISTING OF POLY(VINYL ETHER) BACKBONES

Takeshi Namikoshi,[1,2] Tamotsu Hashimoto[3*]

[1]Venture Business Laboratory, [2]Center for Transdisciplinary Research, Niigata University, Ikarashi 2-8050, Nishi-ku, Niigata 950-2181, Japan
[3]Graduate School of Engineering, University of Fukui, Bunkyo 3-9-1, Fukui 910-8507, Japan

To develop new plastic materials and thermoplastic elastomers consisting totally of poly(vinyl ether) backbones, cationic copolymerizations of TCDVE (tricyclodecane unit-containing vinyl ether) with n-butyl vinyl ether (NBVE) as a linear alkyl vinyl ether were carried out in toluene solvent with various cationic initiators. The random copolymers showed similar transparency to those of polymethyl methacrylate (PMMA) and polycarbonate (PC), which are conventional optical plastics, and even lower specific gravity and water absorption than PMMA and PC. On the other hand, the A-B-A type triblock copolymers [poly(TCDVE-b-NBVE-b-TCDVE)] were prepared by living cationic polymerization method. Although only one glass transition temperature was observed for the random copolymer of TCDVE and NBVE, the two glass transition temperatures were observed for the triblock copolymers. These results indicate that the triblock polymer forms microphase-separated structure.

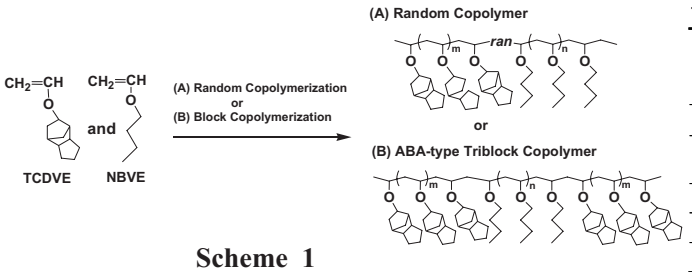

Scheme 1

Table 1. Properties of Poly(TCDVE) and Poly(TCDVE-*ran*-NBVE)

	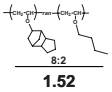 8:2	PMMA	PC
Refractive Index	1.52	1.49	1.59
Light Transmission Factor (%)	93	93	90
Specific Gravity	1.07	1.19	1.19
Water Absorption(%)	0.05	2.0	0.4
T_g	76	105	140

References

1) T. Namikoshi, T. Hashimoto, T. Kodaira *J. Polym. Sci., Part A*, **42**, 3649 (2004)

2) T. Namikoshi, T. Hashimoto, M. Urushisaki *J. Polym. Sci.*, *Part A,* **45**, (in press)

P057C

PREPARATION of $(A)_f$-*star*-$(B)_1$ STAR BLOCK COPOLYMERS *via* ANIONIC LIVING POLYMERIZATION of MACROMONOMERS

Teppei Yamazaki, Yasunari Hayashino and Kazunori Se*

Faculty of Engineering, Fukui University
Bunkyo 3-9-1, Fukui 910-8507, Japan
Phone: 0776-27-8957 Facsimile: 0776-27-8767 e-mail: se@matse.fukui-u.ac.jp

(4-Vinylbenzyl)polystyrene macromonomer (PStM, M_n= 5.4_5x10^3, M_w/M_n=1.0_3) was living-anionically polymerized by *sec*-BuLi to produce the $(PSt)_n^-$ star polymer under high vacuum at room temperature. Then, isoprene (Is) was sequentially copolymerized by $(PSt)_n^-$ to yield the $(PSt)_{6.1}$-*s*-$(PIs)_1$ star block copolymer (M_n = 6.3_9x10^4, M_w/M_n=1.0_4) having a narrow PIs composition distribution as shown in Figure 1. Similarly, the $(PIs)_{6.6}$-*s*-$(PSt)_1$ star block copolymer (M_n=$10._8$x10^4, M_w/M_n=1.0_4) was prepared using (4-vinylbenzyl)polyisoprene macromonomer (PIsM, M_n=5.1_9x10^3, M_w/M_n=1.0_4). The resultant star polymers and star block copolymers were characterized by a special analysis using GPC-LALLS.

The living mechanism of the macromonomers polymerization was discussed from a viewpoint of initiation efficiency. On the other hand, first each distribution ($N_{f,i}$) in a degree of polymerization (i) of $(PSt)_f$, ($i \sim N_{f,i}$) was calculated using $N_{f,i} = \Sigma_{i=j+k}$ ($N_{(f-1),j}$ $N_{1,k}$) and ($i \sim N_{1,i}$) of the PStM, and then the distribution in a degree of polymerization of $(PSt)_{<f>}$, ($i \sim N_{<f>,i}$)^{cal} was calculated by $N_{<f>,i}^{cal} = \Sigma_f n_f N_{f,i}$, where $<f>$ and n_f are an average number of arms and a number fraction (n_f) of number of arms, respectively. By comparing ($i \sim N_{<f>,i}$)^{cal} with ($i \sim N_{<f>,i}$)^{obs}, each distribution in number of arms ($f \sim n_f$) of the $(PSt)_f$ star polymers was determined (Figure 2). From polymerization time dependence of the resultant ($f \sim n_f$), a non-linear polymerization rate constant of PStM was discussed.

The asymmetric architecture of the resultant $(A)_f$-*star*-$(B)_1$ star block copolymers was discussed based on a relationship between molecular weights and molecular dimensions using a model of regular comb-shaped polymers. Two films of the samples showed a clear microphase-separated structure as observed by transmission electron microscopy. As shown in Figure 3, their morphologies shifted to the higher star polymer content side of the morphological transition line for linear block copolymers. This interesting gap in the morphology between the star block copolymers and linear ones was quantitatively explained by a volume fraction (Φ_{PSt}) and an asymmetric factor (ε).

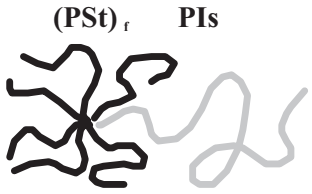

Figure 1 Molecular structure of $(PSt)_f$-*star*-$(PIs)_1$ hetero-arm star block copolymers.

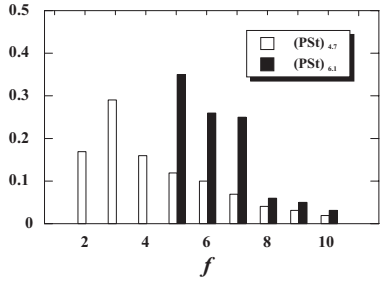

Figure 2 Distribution in number of arms for $(PSt)_f$ star polymers.

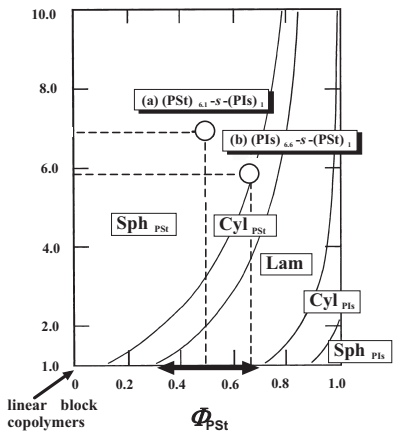

Figure 3 Phase diagram of $(PSt)_f$-*star*-$(PIs)_1$ calculated by Milner.

P058A

RAFT POLYMERIZATION OF *N,N*-DIETHYL-2-METHYLENE-3-BUTENAMIDE

Masahito Matsui, Masamitsu Miya, Hiroki Takeshita, Katsuhiko Takenaka*, and Tomoo Shiomi

Department of Material Science and Technology, Nagaoka University of Technology

Introduction

In the previous paper from our laboratory, we have reported the conventional free-radical[1)] and anionic[2)] polymerization behaviors of *N,N*-diethyl-2-methylene-3-buteneamide [**DEA**]. In the former case, polymer of high molecular weight with broad molecular weight distributions having high 1,4-structure was obtained. In the latter case, 1,2- as well as 1,4- structure was incorporated in the polymer chain although the MWD was narrow. In this paper, the reversible addition fragmentation chain-transfer [RAFT] polymerization of **DEA** will be described.

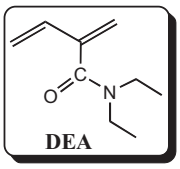

DEA

Experimental

Preparation of DEA was described elswhere[1)]. Benzyl dithiobenzoate was chosen as chain-transfer agent. 4,4'-Azobis(isobutyronitrile) [AIBN] for initiator and chlorobenzene for polymerization solvent were purified according to the ordinary procedure. RAFT polymerization was carried out in a sealed glass tube under high vacuum condition. Conversion was determined by ^{1}H-NMR spectrum of the polymerization mixture by comparing the relative integrated intensity of olefinic methyne proton of the monomer and that of methyl protons in the monomer and the polymer. Molecular weight and its distributions were estimated by SEC based on the polystyrene calibration. MALDI-ToF-MS was obtained with 2,5-dihydroxybenzoic acid as matrix and sodium iodide as ionization enhancer.

Results and Discussion

Table 1 summarizes the result of RAFT polymerization of **DEA**. The number average molecular weight estimated by SEC was always slightly smaller but close to the calculated one based on the amount of the monomer consumed and the amount of initiator on assumption that two polymer chains were formed from one AIBN molecule. As can be seen, the molecular weight increased proportionally with the increase of conversion, indicating that the number of active chain-end does not change during the course of polymerization. Figure 1 shows the SEC chromatograms of the polymers at different polymerization time. It is obvious that the

Table 1 RAFT polymerization of **DEA** at 70 °C in chlorobenzene

time [hr]	DEA/AIBN	conv. [%]	Mn[×10^{-3}] calc.	Mn[×10^{-3}] obs.	Mw/Mn
1	100	20	1.5	1.3	1.16
2	100	30	2.2	2.0	1.18
5	100	52	4.2	3.1	1.17
10	100	74	5.9	4.6	1.17
15	100	85	6.7	4.9	1.18
20	100	94	7.3	5.8	1.18
15	50	96	3.9	4.1	1.19
15	100	85	6.7	4.9	1.18
15	150	82	9.6	7.9	1.15
15	200	80	12.5	9.1	1.2

[BDB]:[AIBN] = 2 : 1

curves moved to the higher molecular weight side with time, keeping its distribution narrow. These indicate that the radical polymerization **DEA** was well controlled by the addition of BDB. Figure 2 shows MALDI-ToF-Mass spectrum of poly**DEA**. One series of signals were observed in 153 Da intervals, which corresponds to the molecular weight of the **DEA** unit. The absolute m/z value of each signals agreed well with the molecular weight of the polymer molecules having a pair of BDB fragments. For example, signal with * mark (m/z=4093) corresponds to the Na^+ adduct of 25-mer having one BDB unit (m/z calc = 4094).

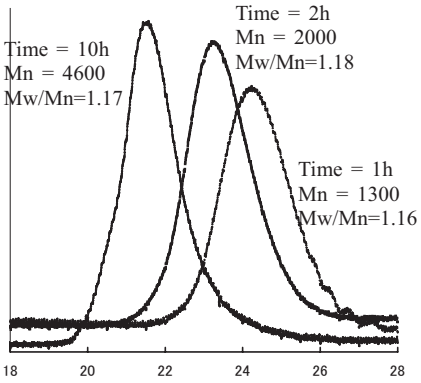

Figure 1 SEC chromatograms of polyDEA at different polymerization time. [BDB]:[AIBN]:[DEA]=2:1:100, 70 °C

Through the study of diene polymerization, the control of the microstructure is important because the physical property of the polydienes strongly depends on the microstructure. Figure 3 shows ^{1}H-NMR spectra of poly**DEA** prepared by anionic, conventional free-radical, and RAFT polymerizations. As previously reported, 1,4-E and Z was the main structure of polyDEA prepared by radical polymerization whereas 1,2-structure was also incorporated when polymerized by anionic initiators. As can be seen, polymers by RAFT process has similar microstructure to the one obtained by usual radical process. Table 2 summarizes the microstructure of poly**DEA** obtained by different polymerization condition. No significant difference was observed between conventional radical and RAFT polymerization.

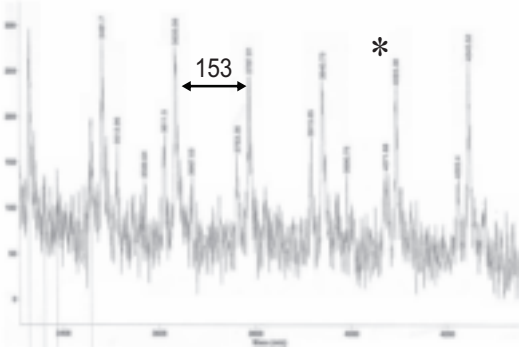

Fig.2 MALDI-ToF-MS of Poly**DEA**

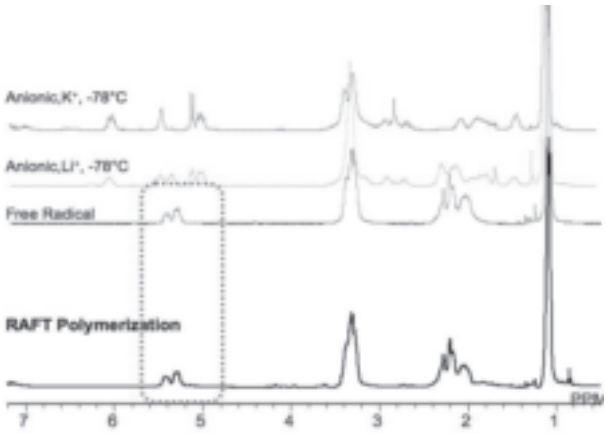

Figure 3 1H-NMR spectra of polyDEA repared by anionic, free-radical, and RAFT polymerization

Conclusion

Poly**DEA** of narrow MWD with high 1,4-structure was obtained by RAFT polymerization.

References

1) T. Yaegashi, S. Yodoya, M. Nakamura, H. Takeshita, K. Takenaka, T. Shiomi; *J. Polym.Sci. Part A: Polym. Chem*., **42**, 999-1007 (2004)
2) Tsuchida *et al*. *Polymer Preprint, Japan*., **56**, 168 (2007)

Table 2 Microstructure of poly**DEA** prepared under various conditions

Condition		1,4-		1,2-
		E-	Z-	
Anionic	K^+	49%	<1%	50%
	Li^+	35%	30%	35%
Free Radical		45%	50%	<5%
RAFT		38%	60%	<2%

P059B

Phase Structure of Block Copolymers Consisting of Two Liquid Crystalline Components

Shin-ichi Taniguchi, Takebumi Abe, Masamitsu Miya, Hiroki Takeshita, Katsuhiko Takenaka and Tomoo Shiomi*

(Dept. of Materials Sci. and Technol., Nagaoka Univ. of Technol., 1603-1 Kamitomioka, Nagaoka, Niigata 940-2188, Japan)Tel: +81-258-47-9304, Fax: +81-258-47-9300 e-mail: shiomi@vos.nagaokaut.ac.jp

Introduction

Diblock copolymers composed of incompatible block segments form various morphologies such as sphere, cylinder and lamella in nano-order depending on the copolymer composition. In liquid crystallization within small droplets and narrow channels, nano-scale surroundings greatly affect the LC structure. For LC-LC block copolymers, in addition, it is expected that hierarchy structure consisting of microdomains containing two kinds of liquid crystalline phases is formed. In this report, we will present formation of phase structure by interplay of liquid crystallization and microphase separation for liquid crystalline block copolymers consisting of two liquid crystalline components.

Experiment

Diblock copolymers (PCB-PCh) composed of cyanobiphenyl and cholesteryl side chain liquid crystalline components were prepared via atomic transfer polymerization (Fig.1, Table.1). The samples were annealed at temperature above the both LC transition temperatures and then were liquid crystallized in cooling. The structures of microphase separation and LC were observed by time-resolved SAXS measurements at beam line 10C of Photon Factory, KEK, Japan. DSC and POM were also used for observation of LC transition.

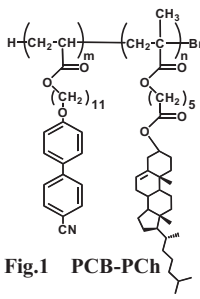

Fig.1 PCB-PCh

Table 1 Characteristics of samples

Samples	M_n (kg/mol)		Degr.Polym.		Φ_{PCh} [b]	M_w/M_n [a]
	PCB [a]	PCh [b]	m [a]	n [b]		
PCB12-PCh03	12.0	3.6	28	6	0.25	1.10
PCB12-PCh09	12.0	9.6	28	16	0.46	1.09
PCB12-PCh28	12.0	28.9	28	50	0.71	1.06
PCB12-PCh65	12.0	65.0	28	114	0.84	1.09

a) Determined by GPC measurement relative to polystyrene standards.
b) Determined by ^{1}H-NMR measurement.

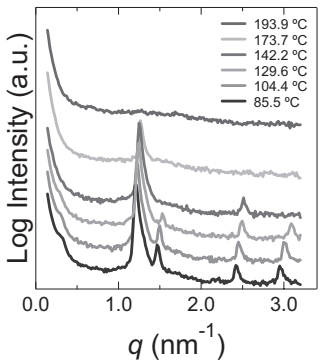

Fig.2 SAXS profiles for PCB12-PCh03 in cooling process

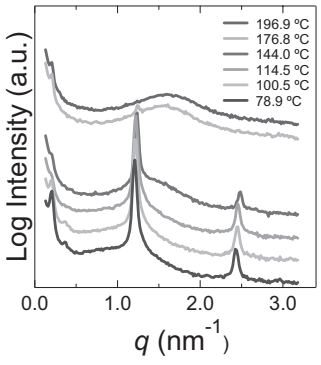

Fig.3 SAXS profiles for PCB12-PCh65 in cooling process

Results and Discussion

Both PCB and PCh homopolymers showed smectic structure (Sm). As shown in Fig. 2, PBA12-PCh03 had no microphase separation structure in the isotropic state, and then a SAXS peak due to microphase structure appeared with liquid crystallization. The liquid crystalline structure was Sm for both PCB and PCh phases (their 1st-order peaks: q=1.4nm^{-1} and 1.2nm^{-1}, respectively). In PCB12-PCh65, as shown in Fig. 3, PCB12-PCh65 formed the microphase separation structure (PCB sphere) in the isotropic state, and in addition the peaks due to Sm layer also appeared below the LC transition temperature. These peaks due to Sm are for PCh but not for PCB, in spite of an appearance of LC transition for both PCB and PCh in DSC observation. This suggests that the LC structure in the spherical domain is not Sm but any other one.

P060C

Phase Structure of Liquid Crystalline Block Copolymers Having a Rubbery Amorphous Component.

Noriaki OKUMURA, Shin-ichi TANIGUCHI, Masamitsu MIYA, Hiroki TAKESHITA, Katsuhiko TAKENAKA and Tomoo SHIOMI*
Dept. of Materials Sci. and Technol., Nagaoka Univ. of Technol., 1603-1 Kamitomioka, Nagaoka, Niigata 940-2188, Japan
Tel: +81-258-47-9304, Fax: +81-258-47-9300, e-mail: shiomi@vos.nagaokaut.ac.jp

Introduction

Block copolymers tend to self-assembles into ordered micr ophase-separated domains with dimensions of several nanometers. The microphase separation has various domain structure such as sphere, cylinder, and lamellar depending on the copolymer c omposition. When block copolymers contain a liquid crystallin e (LC) component, the phase structure is governed by the com plex interplay between LC phase transition and microphase sepa ration. It is expected that LC ordering is grealty affected by the nano-scale confinement due to the microphase separation. In this study, phase structure and its transition behavior of sid e-chain LC-amorphous block copolymers composed of poly(buty l acrylate) (PBA) and poly((S)-(-)-methyl-butyl 4'-(11-acryloylo xy-undecyloxy)- biphenyl-4-carboxylate) (P11OCMB) (Fig. 1) was investigated by using differential scanning calorimetr y (DSC), polarized light microscopy, and small-angle X-ray scattering (SAXS).

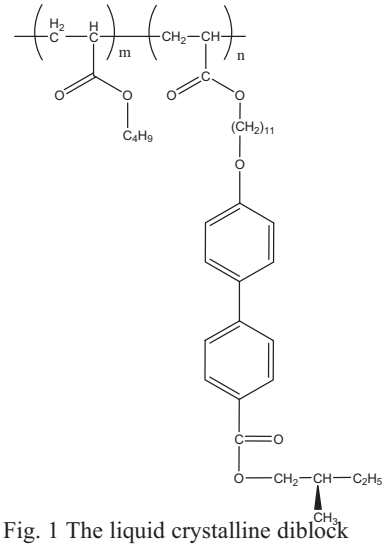

Fig. 1 The liquid crystalline diblock copolymer.

Experiment

The LC-amorphous diblock copolymers were prepared via successive atom transfer radical polymerization of butyl acryl ate and (S)-(-)-methyl-butyl 4'-(11-acryloyloxy- undecyloxy)biphenyl-4-carboxylate. Molecular wei ght and composition of the sample are listed in Table 1. The samples were annealed at a temp erature above the LC transition temperatures and then liquid crystallized by cooling. The structu res of microphase separation and LC are observed by time-resolved SAXS measurements at beam line 10C of Photon Factory, KEK, Japan. DSC and POM observation were also performed.

Table.1 Molecular weight and composition of the diblock copolymer

	Mn(kg/mol)		Degree of Polymerization		ΦP11OCMB[b)]	Mw/Mn[a)]
	PBA[a)]	P11OCMB[b)]	PBA[a)]	P11OCMB[b)]		
PBA7.6-b-P11OCMB16	7600	16800	60	33	0.68	1.08

a) Determined by GPC measurement relative to polystyrene standards. b)Determined by ^{1}H NMR measurement.

Result and Discussion

Fig. 2 shows the temperature dependence of the SAXS profile of PBA-P11OCMB. As cooling, a pea k due to the smectic ordering of the LC block appea rs at around q=1.8 nm^{-1} below 100 °C, which corres ponds to the LC transition temperature, T_{iso}, estimate d by DSC. At the same temperature with the LC tr ansition, a peak due to microphase separation also ap pears at around q=0.5 nm^{-1}, while at higher temperat ures, only a diffuse peak can be observed. This me ans that the order-disorder transition is induced by L C phase transition, or vice versa. Because T_{iso} for th e block copolymers is almost the same as that for th e LC homopolymer, order-disorder transition may be induced by liquid crystallization.

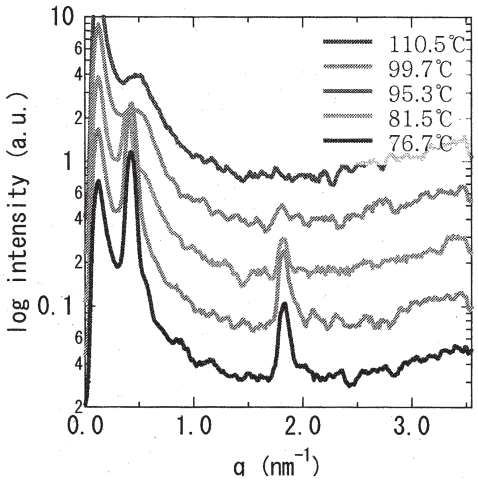

Fig. 2 SAXS profile for the PBA7.6-P11OCMB during a cooling ramp from 140 to 70℃.

P061A

ASYMMETRIC INDUCED COPOLYMERIZATION OF ACHIRAL PHENYLACETYLENE WITH A CHIRAL AMINO GROUP

Mohammed Hoda,[1] Masahiro Teraguchi,[1,2,3] ,Masayuki Sato,[1] Takeshi Namikoshi,[3,4] Edy Marwanta,[3,4,] Takashi Kaneko,[2,3] and Toshiki Aoki[1,2,3,4*]

[1] Graduate School of Science and Technology, [2]Center for Education and Research on Environmental Technology, Materials Engineering, and Nanochemistry, [3]Center for Transdisciplinary Research, [4]Venture Business Laboratory, Niigata University, Ikarashi 2-8050, Nishi-ku, Niigata 950-2181, Japan

A novel chiral phenylacetylene monomer with chiral phenylethylamine residue ((R)-PEAPA) was synthesized. Using a rhodium complex this monomer copolymerized with different ratios of an achiral trimethylsilylphenylacetylene (SPA) at room temperature to give an optically active chiral helical copolymers with molecular weights (M_w) of around 2-5x10^5 and molecular weight distributions (M_w / M_n) of around 2. The chemical structures of these copolymers were confirmed by FT-IR and ^{1}H NMR. The FT-IR spectra of the copolymers did not show absorption at 2119 and 3293 cm^{-1} indicating the absence of C≡C-H bond the corresponding monomers have. CD spectroscopic studies revealed that the copolymer backbone took predominantly one-handed helical conformation because strong Cotton effects were observed at wavelengths around 300-500 nm.

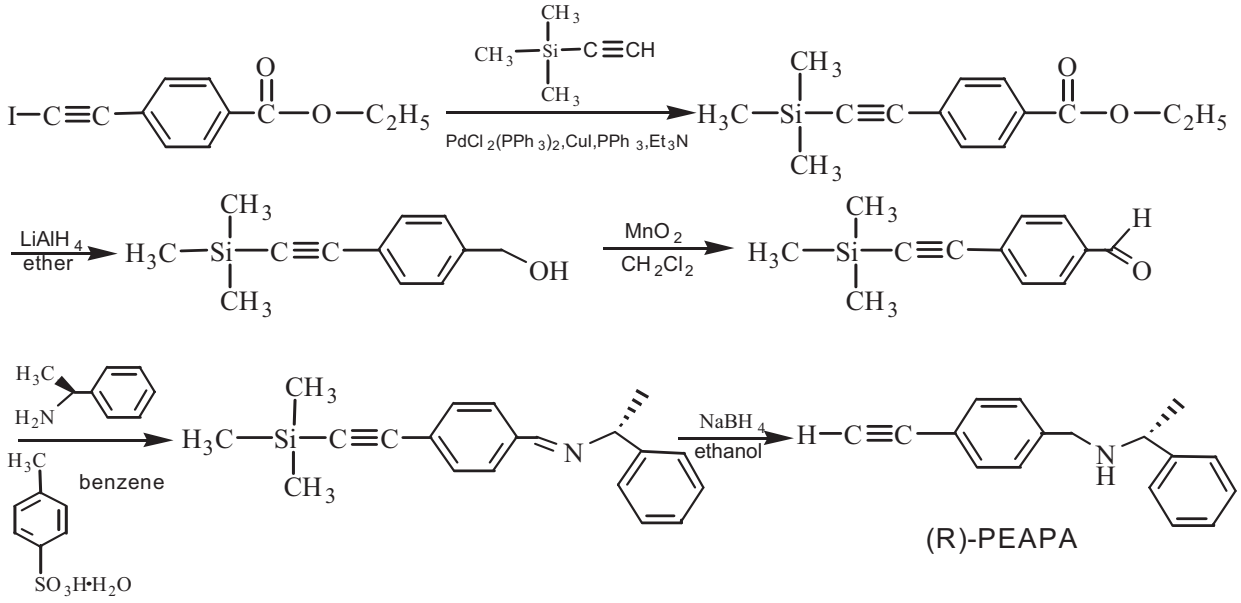

Scheme 1. Synthetic route of a chiral phenylacetylene monomer ((R)-PEAPA).

Table 1. Preparation of copoly ((R)-PEAPA/SPA) [a)]

No.	SPA (mol%)	PEAPA (mol%)	Yield (%)	M_w [b)] ($x10^5$)	M_w / M_n [b)]
1	100	0	58.06	4.26	2.46
2	90	10	37.7	5.90	2.48
3	70	30	58.6	5.15	2.68
4	50	50	54.6	2.01	2.83
5	30	70	9.46	3.15	2.20

a) Polymerized for 3h at room temperature. b) Determined by GPC (eluent = THF; polystyrene standard).

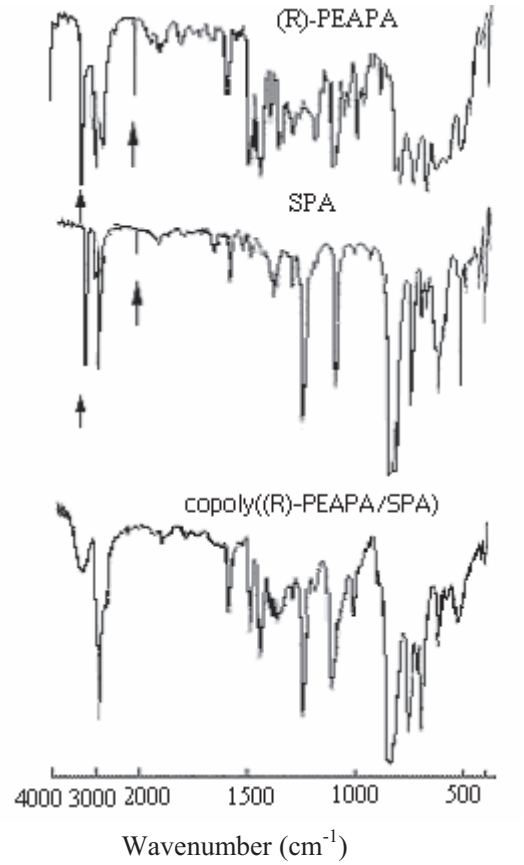

Fig. 1. IR spectra of (R)-PEAPA, SPA (NaCl), and copoly ((R)-PEAPA/SPA) (KBr, sample from Table 1. No.3).

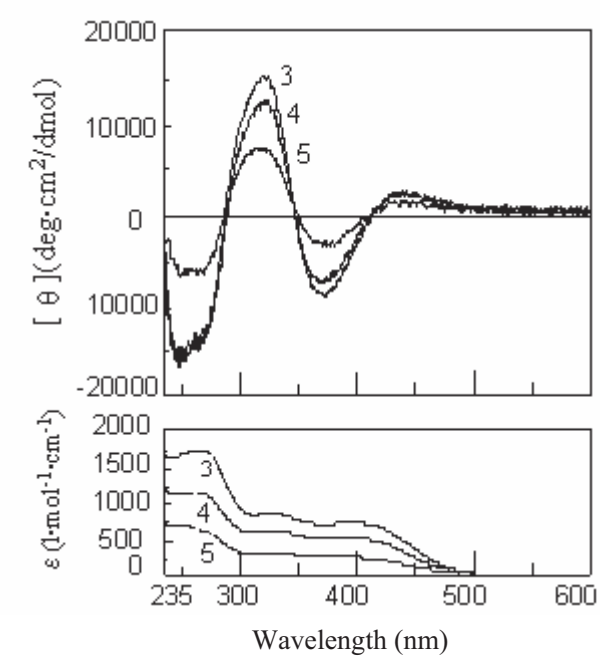

Fig. 2. CD and UV spectra of copoly ((R)-PEAPA/SPA) in $CHCl_3$ at 20°C,for the codes, see Table 1.

P062B

APPLICATION OF CHIRAL HELICAL POLY(PHENYLACETYLENE)S FOR OPTICAL RESOLUTION

S. Hadano [1, †], M. Teraguchi [2, 3], T. Kaneko [3], and T. Aoki* [1-3]

[1] *Venture Business Laboratory, Niigata University, Ikarashi 2-8050, Niigata 950-2181, Japan*

[2] *Graduate School of Science and Technology, Niigata University, Ikarashi 2-8050, Niigata 950-2181, Japan*

[3] *Center for Transdisciplinary Research, Niigata University, Ikarashi 2-8050, Niigata 950-2181, Japan*

[†] *Graduate School of Engineering, Kyoto University, Katsura, Nishikyo-ku, Kyoto 615-8510, Japan (From April 2007)*

In our previous study, we succeeded to obtain chiral helical poly(phenylacetylene) (Figure 1) from achiral 4-dodecyloxy-3,5-bis(hydroxymethyl)phenylacetylene (DoDHPA) by helix-sense-selective polymerization using a chiral catalytic system consists of $[Rh(nbd)Cl]_2$ and (*R*)-phenylethylamine.[1] When methanol was added to poly(DoDHPA)-THF solution, the polymer was precipitated with maintaining the chiral helicity.[2] On the basis of the result, we developed new optical resolution method called "enantioselectively adsorbed precipitation".

In this study, we carried out enantioselectively adsorbed precipitation with combinations of two kinds of chiral helical poly(phenylacetylene) and nine kinds of racemates (Figure 2, Scheme 1).

To optimize a proportion of [monomer unit] / racemate, enantioselectively adsorbed precipitation using DL-phenylalanine and poly(DoDHPA) was performed under several conditions. As shown in Table 1, enantioselectivity was observed in [DoDHPA unit] / [DL-phenylalanine] = 16 and 32. It is desirable that the proportion of polymer and racemate is as small as possible. Therefore, the condition of [DoDHPA unit] / [DL-phenylalanine] = 16 was used in the subsequent experiments.

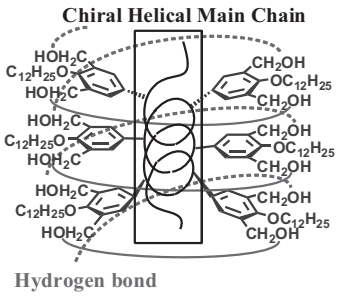

Figure 1. Structure of chiral helical poly(DoDHPA)

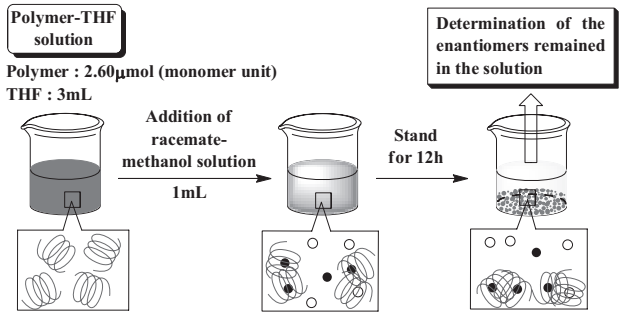

Figure 2. Schematic procedure of enantioselectively adsorbed precipitation.

Table 1. Enantioselectively adsorbed precipitation in combination of poly(DoDHPA) and DL-phenylalanine

[DoDHPA unit] / [DL-Phenylalanine]	4 / 1	8 / 1	16 / 1	32 / 1	32 / 1[b)]
α in supernatant solution[a)]	1.00	1.00	1.15 (D)	1.00	1.31 (D)

a) Separation factor (= [major enantiomer] / [minor enantiomer]. b) The concentration of polymer-THF solution was twice those in the other tests.

Results of enantioselectively adsorbed precipitation are summarized in Table 2. Poly(DoDHPA) and poly(PSPA) exhibited enantioselectivity to six and three racemates, respectively. Since poly(DoDHPA) has two hydroxyl groups in monomer unit, poly(DoDHPA) can interact with racemates by hydrogen bond. This is one of the reasons why poly(DoDHPA) could be recognized enantiomers better than poly(PSPA). In spite of high amount of adsorption, both polymers exhibited low enantioselectivity to flavanone. This suggests that strong interaction is not necessary for good resolution.

In addition, when conventional adsorption was carried out under condition of [DoDHPA unit] / [DL-phenylalanine] = 16, no enantioselectivity was observed. This result indicates that "enantioselectively adsorbed precipitation" is superior to conventional adsorption method.

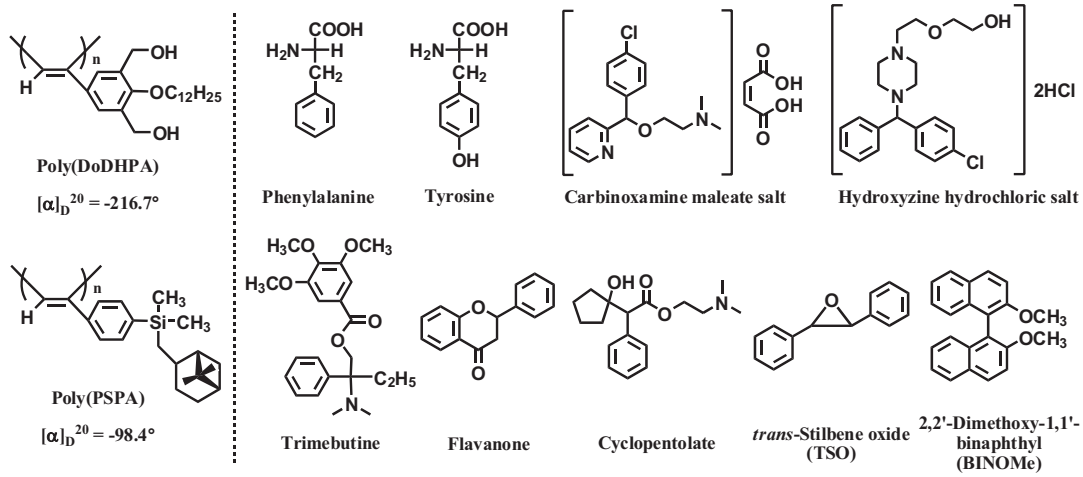

Scheme 1. Structures of chiral helical poly(phenylacetylene)s and racemates.

Table 2. Summary of enantioselectively adsorbed precipitation

Racemate	α in supernatant solution [a)]		α adsorbed in polymer [a), b)]		Amount of adsorption (%)	
	Poly(DoDHPA)	Poly(PSPA)	Poly(DoDHPA)	Poly(PSPA)	Poly(DoDHPA)	Poly(PSPA)
Phenylalanine	1.15 (D)	1.01 (L)	1.10 (L)	1.02 (D)	59.3	30.6
Tyrosine	5.07 (D)	2.57 (D)	1.85 (L)	1.21 (L)	69.3	81.8
Carbinoxamine	1.34 (-)	1.14 (+)	1.06 (+)	1.05 (-)	83.7	71.9
Hydroxyzine	1.17 (+)	1.38 (+)	1.09 (-)	1.15 (-)	65.0	70.0
Flavanone	1.02 (*S*)	1.02 (*S*)	1.01 (*R*)	1.01 (*R*)	84.3	86.9
Trimebutine	1.06 (-)	1.00	3.03 (+)	1.00	7.75	0
Cyclopentolate	1.55 (2nd)	1.03 (2nd)	1.84 (1st)	1.04 (1st)	42.5	45.6
BINOMe	1.03 (-)	1.08 (+)	1.38 (+)	13.0 (-)	8.64	4.24
TSO	3.65 (*R,R*)	—[c)]	—[c)]	—[c)]	—[c)]	—[c)]

a) Configulation (D or L, *R* or *S*) or optical rotation (+ or -) or the order of elution of the major enantiomer were shown in the parentheses. b) Calculated from the analytical results in supernatant solution. c) Not measured.

References

1) T. Aoki et al., *J. Am. Chem. Soc.*, **125**, 6346-6347 (2003).

2) S. Hadano et al., *Polym. Prepr. Jpn.*, **54 (1)**, 251 (2005).

P063C

SYNTHESIS AND ATTEMPTS OF HELIX-SENSE-SELESTIVE POLYMERIZATION OF ACHIRAL PHENYLACETYLENES HAVING TWO ALKYLAMIDO GROUPS

Chen Chen Liu,[1] Masahiro Teraguchi,[1,2,3] Takeshi Namikoshi,[3,4] Edy Marwanta,[3,4] Takashi Kaneko,[2,3] and Toshiki Aoki[1,2,3,4*]

[1] Graduate School of Science and Technology, [2]Center for Education and Research on Environmental Technology, Materials Engineering, and Nanochemistry

[3]Center for Transdisciplinary Research, [4]Venture Business Laboratory,

Niigata University, Ikarashi 2-8050, Nishi-ku, Niigata 950-2181, Japan

In this laboratory, an achiral phenylacetylene having two hydroxyl groups[1)] or two amide groups[2)] were polymerized using a chiral catalytic system((R)-phenethylamine(PEA) and $[Rh(nbd)Cl]_2$(nbd=norbornadene)) to give a chiral structure only arised from its one-handed helical main chain **HSSP**(helix-sense-selestive polymerization).The helical structure of this polymer was stabilized by hydrogen bonds in the molecule. However, monomer structures suitable for **HSSP** were limited. In this study, we synthesized several new monomers (See scheme) having two alkylamide groups, which can make hydrogen bonds and tried **HSSP** of them **(Figure. 1)**.

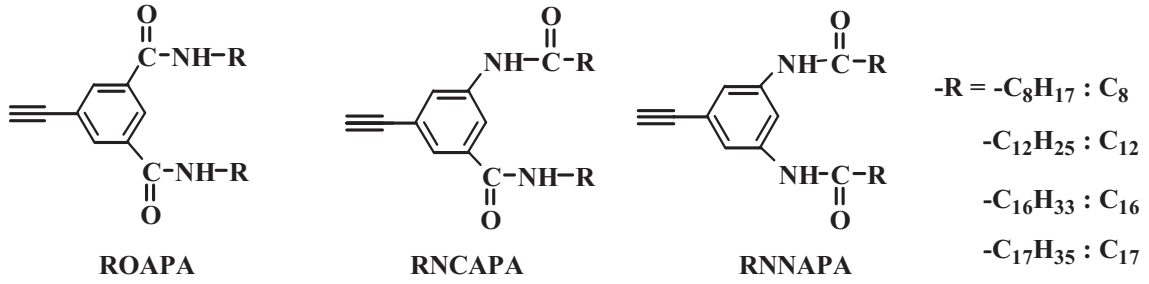

Scheme. Chemical structures of OAPA,NCAPA, and NNAPA

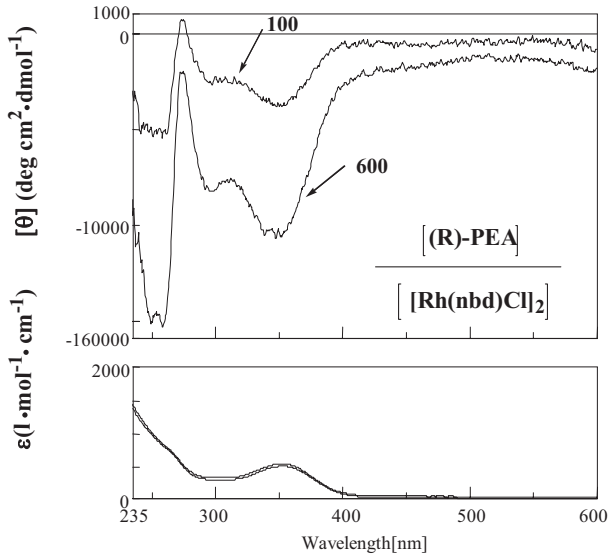

Fig. 1 CD and UV-vis spectra of poly(C_8OAPA) polymerized by $[Rh(nbd)Cl]_2$-(R)-PEA.

Refererces :

1) T. Aoki, T. Kaneko, N. Maruyama, A. Sumi, M. Takahashi, T. Sato, and M. Teraguchi, *J. Am. Chem. Soc.*, **125**, 6346(2003).
2) M. Teraguchi, D. Tanioka, T. Kaneko, T. Aoki, *Polym. Prepr. Jpn.*, **52**,203 (2003).
3) T. Aoki, T. Kaneko, and M.Teraguchi, *Polymer,* **47***,* 4867(2006).

P064A

THE CONTROL OF THE HELIX SENSE IN THE CO-POLYMERIZATION OF (4-ETHYNYLPHENYL)GALVINOXYL BY THE COMPOSITION OF CO-MONOMER

Yasuhiro Umeda,[1] Takashi Kaneko,[2,3*] Takeshi Namikoshi,[3,4] Edy Marwanta,[3,4] Masahiro Teraguchi,[1,2,3] and Toshiki Aoki[1,2,3,4]

[1] Graduate School of Science and Technology, [2]Center for Education and Research on Environmental Technology, Materials Engineering, and Nanochemistry, [3]Center for Transdisciplinary Research, [4]Venture Business Laboratory, Niigata University, Ikarashi 2-8050, Nishi-ku, Niigata 950-2181, Japan

Recently, we have succeeded in the helix-sense-selective polymerization of achiral phenylacetylene monomers bearing galvinoxyl moiety using the catalyst $[Rh(nbd)Cl]_2$ in the presence of chiral 1-phenylethylamine.[1-2)] In the present study, we polymerized chiral monomer **1** with achiral monomer **2a** or **3**, and discussed the helix-sense-selectivity in the copolymerization and the chiroptical and magnetic properties of the obtained copolymers. The copolymers poly(**1**-co-**2a**) and poly(**1**-co-**3**) were obtained in a good yield, and the compositions of the copolymers were almost the same as the feed compositions of monomers. The CD spectra of the copolymers were difficult from that of the mixture of homopolymers, indicating the excess of one-handed helical polyacetylene backbone of all copolymers. The sign of the CD signal depend on the composition of monomers in poly(**1**-co-**2a**)s. This result indicates that the helix sense can be controlled by the feed of chiral comonomer in the copolymerization of **1** with **2a**. In the CD spectrum of polyradical containing 30 mol% of **1**, Cotton effects was observed in the absorption region of the galvinoxyl and backbone chromophore. This result indicated the maintenance of the excess of one-handed helix even after the oxidation reaction, and the successful synthesis of an optically active polyradical. The static magnetic susceptibility of the powdered polyradicals was measured with a SQUID magnetometer at 2-300K. The observed negative Weiss temperature indicated antiferromagnetic interaction between unpaired electrons.

Chart 1. Monomer structures

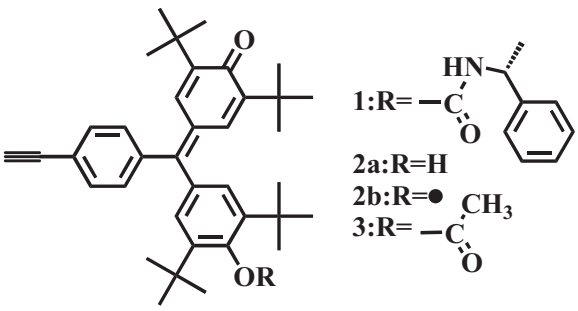

References

1) Y. Umeda, T. Kaneko, M. Teraguchi, and T. Aoki, *Chem.Lett*, **34**, 854(2005)

2) T. Kaneko, Y. Umeda, T. Yamamoto, M. Teraguchi, and T. Aoki, *Macromolecules,* **38**, 9420(2005)

P065B

SYNTHESIS OF ONE-HANDED HELICAL POLYPHENYLACETYLENES STABLE IN SOLUTION BY REMOVING THE CHIRAL GROUPS FROM POLY(PHENYLACETYLENE HAVING CHIRAL GROUPS) IN MEMBRANE STATE

Yunosuke Abe[1], Masahiro Teraguchi,[1,2,3] Takeshi Namikoshi,[3,4] Edy Marwanta,[3,4] Takashi Kaneko[2,3], and Toshiki Aoki,[1,2,3,4*]

[1] Graduate School of Science and Technology, [2]Center for Education and Research on Environmental Technology, Materials Engineering, and Nanochemistry, [3]Center for Transdisciplinary Research, [4]Venture Business Laboratory, Niigata University, Ikarashi 2-8050, Nishi-ku, Niigata 950-2181, Japan

We already reported that the asymmetric induced polymerization of chiral phenylactylenes having two hydroxyl groups using an achiral catalytic system, $[Rh(nbd)Cl]_2$-Et_3N gave stable helical polymers.[1)] In addition, the one-handed helical structure was also maintained after removal of the chiral groups in membrane state[1)]. However, after the removal of the chiral groups, the polymer membrane became insoluble in any organic solvent[1)].

In this study, we synthesized and copolymerized a new monomer, **MDHPA** with **DoDHPA** (Scheme 1). The copolymers showed CD signals and specific rotations, and these values increased with increasing the content of **MDHPA** (Fig. 1,2).

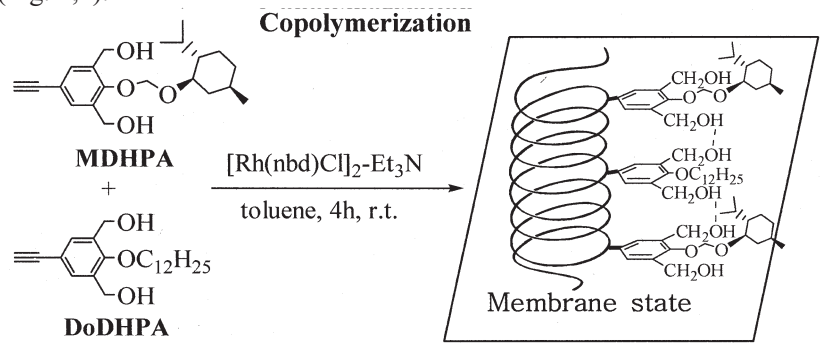

Scheme1. Copolymerization of MDHPA and DoDHPA.

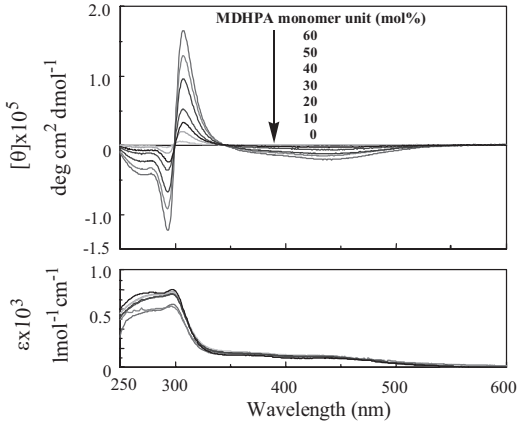

Figure 1. CD and UV-vis spectra of poly(**MDHPA**-*co*-**DoDHPA**) **;** before removal of the menthoxy groups in chloroform (*c* 0.001 mol / l) at room temperature**.**

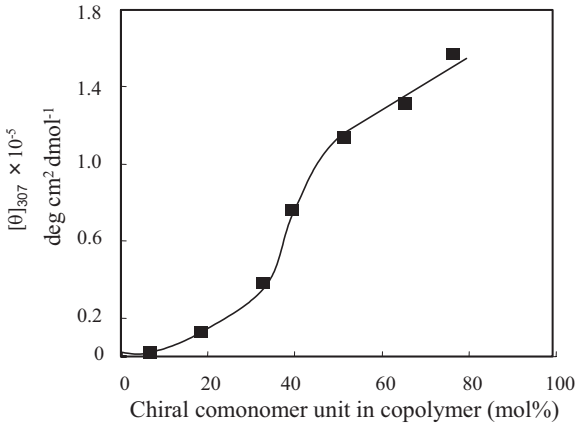

Figure 2. Plots of [θ] versus **MDHPA**unit ratio in co-polymer.